DEVELOPMENT OF A COST ESTIMATION MODEL FOR SLA PROTOTYPING BASED ON VOLUMETRIC INFORMATION

JACQUES COMBRINCK

Dissertation submitted in fulfillment of the requirements of the Degree

MAGISTER TECHNOLOGIAE: ENGINEERING: MECHANICAL

in the

School of Mechanical Engineering and Applied Mathematics
Faculty of Engineering Information and Communication Technology

at the

Central University of Technology, Free State

Supervisor: Prof. DJ de Beer (D Tech. Mech. Eng.)
Co-Supervisor: Mr. LJ Barnard (M Tech. Mech. Eng.)

Bloemfontein
February 2005

DECLARATION

I, JACQUES COMBRINCK, do hereby declare that this research project submitted to the Central University of Technology, Free State for the degree MAGISTER TECHNOLOGIAE: ENGINEERING MECHANICAL, is my own independent work that has not been submitted before to any institution by myself or any other person in fulfillment of the requirements for the attainment of any qualification.

J COMBRINCK

Student

07/04/2015

Date

ACKNOWLEDGEMENTS

I wish to acknowledge some persons and institutions for their contributions whilst I was working on this project:

Dr DJ de Beer and Mr. LJ Barnard for their guidance and supervision for the duration of this project

Mr. GJ Booysen from the Centre for Rapid Prototyping and Manufacturing, for the use of their equipment and the assistance I received during the project.

The owners of Nu-Era Tool and Die, for the encouragement and motivation I received from them to finish the project

To my family – for all the encouragement I received from them during the project

Lastly, this project would not have been possible without the grace of God

UITTREKSEL

Die Stereolitografie proses is 'n welbekende proses in Suid Afrika en reg oor die wêreld. Ontwerpers en uitvinders vra daagliks kwotasies aan om 'n prototipe van hul ontwerp of uitvindsel te groei.

Nie alle uitvinders en ontwerpers het toegang tot Rekenaar Gesteunde Ontwerp programme om hulle ontwerp na 'n 3-Dimensionele soliede model om te skakel nie. Hulle kan dus nie 'n .STL lêer na 'n snelprototipiëring dienssentrum vir 'n akkurate kwotasie stuur nie, en moet op 'n 2D-skets vir hulle kwotasie staat maak.

Hierdie studie bied 'n metode aan om die boutyd akkuraat binne 10 % van die werklike waarde te voorspel. 'n Model, soortgelyk aan die 2D-skets, word uit basiese volumetriese vorms soos byvoorbeeld silinders, kegels ensovoorts, opgebou. Die boutyd van hierdie model word dan met behulp van modelle wat in TK Solver geskep is, bereken.

SYNOPSIS

The Stereolithography process is a well-known process in South Africa and around the world. Quotations for designers and inventors are issued daily for the growing of a prototype of his/her invention or design.

Not all the inventors and designers have access to CAD software to transform their design or invention into a solid model. Because of this they cannot submit an .STL file to a Rapid Prototyping service bureau for a quotation. They can only submit a 2D-sketch to the Rapid Prototyping service bureau for a quotation.

This study presents a method of calculating build time estimations within a limit of 10% of the actual build time of a prototype. This is achieved by using basic volumetric shapes, such as cylinders and cones, added together to represent the model in the 2D-sketch. By using this information the build time of the product is then calculated with the aid of models created in TK Solver.

Contents

LIST OF TABLES

LIST OF FIGURES

CHAPTER 1

COST ESTIMATION FOR STEREOLITHOGRAPHY PROTOTYPING

1.1 INTRODUCTION TO RAPID PROTOTYPING

Rapid Prototyping (RP) is a group of new manufacturing technologies that build prototype models primarily on a layer-by-layer basis. By using these technologies the building time of prototype models, of any complexity, is shortened in comparison to conventional model building methods. Hence the term Rapid Prototyping.

3D Systems Inc presented the first commercial RP process in Detroit in November 1987. Since then, more than 30 processes have been developed and the model dimensional accuracy has been improved significantly. The range of building materials has also been extended to make provision for operational prototypes.

1.1.1 Rapid Prototyping in Manufacturing

In the competitive industry product lifetimes become shorter, forcing designers to develop new products in a shorter time. The time to the market therefore becomes the critical key factor for profitability – thus the development time, and not the cost becomes critical for production [13]; [21]; [26]; [24]; [25].

By using Rapid Prototyping in Manufacturing, the following practical applications may be noted:

- **Visualisation:** No matter how proficient one may be at reading blueprints and Computer Aided Design (CAD), images of a complex object may be very difficult to visualise precisely in terms of exact appearance. Blind holes, complex interior passageways, compound curved surfaces etc., often lead to difficulties in interpretation.
- **Verification:** A prototype can be generated speedily, so that the process of pinpointing desired and undesired features is made easier. For certain high-risk products, design verification has been a practice for many years. The conventional methods used have been both manual, and NC machining [23]. Disadvantages however, include accuracy and time to implement design changes.
- **Optimisation:** Since prototypes can be generated rapidly, a range of test models can be completed in weeks. This gives the designer the opportunity to attempt to optimise the design.
- **Fabrication:** This is done either by using material with appropriate properties in the RP process itself, or by using the prototype as a pattern or a mould for following a process. Once an optimised prototype has been manufactured, it is important to fabricate a functional test model. Until such a model has been fabricated or tested, it is not known if it will pass functional test requirements. There are a number of techniques that have been successfully used to go from a RP prototype to a fully functional test model in a relatively rapid and cost-effective manner. These processes include Room Temperature Vulcanising (RTV), Vacuum casting, Spin casting, Investment casting and Epoxy tool moulding.

1.1.2 Typical RP Processes Available

The majority of RP processes require 3-Dimensional CAD models in the Stereolithography (.STL) file format as data input. The .STL model is then sliced into layers by specialised software. These layers are then used by the RP system to build the model by consecutive layer addition.

Presently the processes available in South Africa are:

- Stereolithography (SLA)
- Selective Laser Sintering (SLS)
- Sanders 3D Printing
- Fused Deposition Modeling
- Laminated Object Manufacturing
- *Z* –Corp 3D Printing
- JP Systems 5
- Thermojet

Of the above–mentioned processes, the SLA and the SLS processes have the largest industrial application. These two processes may be summarised as follows:

- ***Stereolithography***

  An elevator is located in a vat at a distance from the surface of the photopolymer, equal to the thickness of the first, bottom-most layer. An ultra-violet (UV) laser beam scans the surface of the polymer, following the contours of the slice. The interior of the contour is then hatched using a hatch pattern. The photopolymer solidifies and cures

when it is exposed to the laser beam. The elevator is moved downwards, and the subsequent layers are produced. Finally, the part is removed from the vat, and the liquid that is still trapped in the interior is usually cured in a special UV enclosure.

Because the part is built in a liquid environment, it is necessary to add supporting structures to increase the rigidity of the part and to avoid overhangs from sinking to the bottom of the platform or from floating freely in the vat. The support structures are usually removed manually after the part is taken away from the platform.

Scanning time depends on the geometry of the contours, hatching patterns, the speed of the laser, and the re-coating time, *i.e.* the time taken to place a layer of photopolymer over the last solidified layer [8]; [13]; [29].

- ***Selective Laser Sintering***

Powders of different materials are spread over a platform by a roller. A laser sinters selected areas causing the particles to melt and then solidify. In sintering there are two phase transitions: from solid to fluid and back to solid. Processes that behave in this way are generally known as selective laser sintering (SLS) processes. In the SLS process there is no need for support structures, since the surrounding powder supports the parts being built [6].

1.1.3 Comparison between the SLA and the SLS Processes

Important issues to take into consideration when selecting a particular prototype process are time, cost, functionality, accuracy, material, geometry, and size. Table 1.1 presents a short summary of the differences between these two processes [6].

Table 1.1 Comparison between the SLA and the SLS processes for the SLA 250 and SLS 2000 machines

Process	SLA 250	SLS 2000
Company	3D Systems Inc.	DTM Corp. (Now also 3D Systems Inc.)
Layer thickness (mm)	0.1 – 0.9	0.07 - 0.14
Speed (vertical)	Part geometry dependent Machine dependent (vertical repositioning of platform after the resin has settle in the vat)	Part geometry dependent Machine dependent (vertical repositioning of platform after a layer of powder had been deposited)
Accuracy	0.2 mm	0.05 – 0.25 mm
Materials	Photo curable resins	Thermoplastics, wax, sand and metal powders

1.2 PROBLEM STATEMENT

If a designer needs a prototype of a product, a 3-Dimensional CAD model is delivered to the Rapid Prototype (RP) manufacturer in the Stereolithography (.STL) file format. Once the RP manufacturer receives the model, time estimations can be calculated with specialised software. Sometimes the .STL can be corrupted by various anomalies – often caused by file conversions. The RP manufacturer must then attempt to correct these anomalies. This is a time consuming process, and a corrupted .STL file is seldom recoverable, necessitating file recreation. The result is wasted time and increased cost for the client, who only requires a quotation for the building of the prototype required for project planning or budgetary issues.

A major disadvantage of the cost estimation process, where .STL files are required, is that data obtained from 2-Dimensional drawings or sketches needs to be converted into 3-Dimensional models adding additional time to the cost estimation process. Currently, generating quotes from 2-Dimensional drawings or sketches where .STL files are not available, results in "guestimates" being made with a low degree of accuracy. Disadvantages are however, that since the manufacturing of the prototypes is a costly operation, prospective orders could be lost as a result of high quotes, or financial loss to the Service Bureau could arise, if time estimates are too low. Thus, more accurate data is essential for project planning.

1.3 AIM OF STUDY

To implement RP as a strategic development tool, reasonable cost estimates must be made without requiring the time-consuming creation of a 3-Dimensional CAD model and an .STL file. Thus, a procedure is required where costing can be done using dimensional data from engineering drawings or even design sketches. This procedure can be incorporated in software such as Microsoft Excel or TK Solver™ [I], which make use of the rule-based programming language.

1.4 HYPOTHESIS

A simple, though accurate procedure can be developed for determining the cost of prototypes built on the Stereolithography machine without requiring .STL files. This procedure can be implemented through software such as Microsoft Excel or TK Solver™.

1.5 SCOPE OF STUDY

For the purpose of this study a costing procedure will be developed for the SLA process, since it is the most widely implemented process [24]; [27]. Model data will be obtained from the Centre for Rapid Prototyping and Manufacturing's database. Estimated building data obtained from commercial software presents model volumes and surfaces with building times related to laser output power. The actual building data obtained merely presents the job starting and ending times, from which the total duration can be derived.

[I] TK Solver™ is an industry-oriented mathematical equation solver software [9]; [28].

This data will be analysed and compared to obtain a statistical accuracy of the predictions given by the commercial software using .STL files. The accuracy obtained will be used as benchmarks for the software program development.

The software program will make use primarily of standard volumetric shape substitution and also consider support generation, scanning speed of the laser and the operations between layers such as, for example, the time taken by the sweeper blade. The software will be tested by predicting building times of volumetric shapes of practical geometries and comparing this to actual building times from which accuracy will be derived. The accuracy will be compared to the benchmarks. Revisions to the software program will be made to obtain an acceptable level of accuracy.

CHAPTER 2

CAD PROCESS

2.1 CAD DESIGN

The entire process begins with an object design. The design must be converted into a three dimensional, surface or solid model, Computer Aided Manufacturing (CAM) or Computer Aided Engineering (CAE) system. The subsequent computer model must represent a clearly defined, enclosed volume.

2.1.1 Solid Modelers

Solid modelers, by definition, allow the user to create only unambiguous objects. This requires that the design be complete and have continuity. One method of creating a solid is by manipulating a number of solid primitives, such as spheres and cylinders, which can be joined and subtracted from each other. Another method is to sweep a predefined cross-section through another predefined curvature in space.

2.1.2 Surface Modelers

A design is created with a surface modeler by building a number of mathematical patches or surfaces that, when joined together, form the desired object. Because there is no defined association between these surfaces, it is possible to have gaps or discontinuance, or even find surfaces completely missing in an object. However the object must be designed as a closed

surface that unambiguously defines an enclosed volume. That is, the model data must specify the inside, outside and boundary of the object.

2.1.3 CAD Resolution

CAD systems internally approximate curved surfaces (cylinders, spheres) by polygons or facets in order to reduce display times. The larger the number of polygons, the more closely the surface is approximated. This results in a smoother curve on the final part. When faceted data is used to direct the SLA, these approximations are reflected in the final part. To minimise this effect, the number of polygons used should be increased. However, as the number of polygons or facets increase, so does the file size [7].

2.1.4 Wall Thickness/Feature Size

Wall thickness and feature size, which can be built reliably, are resin dependent. However, the minimum recommended wall thickness or feature size is 0.5 mm. The absolute minimum wall thickness or feature size is the width of the laser beam diameter.

2.2 CAD INTERFACE

The CAD model must be converted from the CAD internal format to a planar faceted representation or contoured surface representation for use by SLA software. CAD vendors have written interfaces to convert their surfaces or solid models into readable formats for Stereolithography. This format is known as Stereolithography files (.STL).

2.2.1 Classification of .STL Files

The .STL format is a faceted representation of the CAD model. It is comprised of many triangles, connected at the vertices. The .STL file basically consists of the *x*, *y* and *z*-coordinates of the three vertices of each surface triangle, as well as an index that describes the orientation of the surface normal. The surface normal is a line perpendicular to the triangle.

The latter feature is necessary to ensure that a clear distinction is made between the inner and outer surface. The orientation of the facets is specified in two ways that must be consistent. First, the direction of the normal is outward, and secondly the vertices are listed in a counterclockwise order when looking at the object from the outside (right hand rule). The right hand rule states that the vertices of each facet must be ordered so that when the fingers of the right hand pass from point one through point two to point three, the thumb will point away from the solid object. This is illustrated in Figure 2.1 where the un-shaded triangle represents an exterior surface.

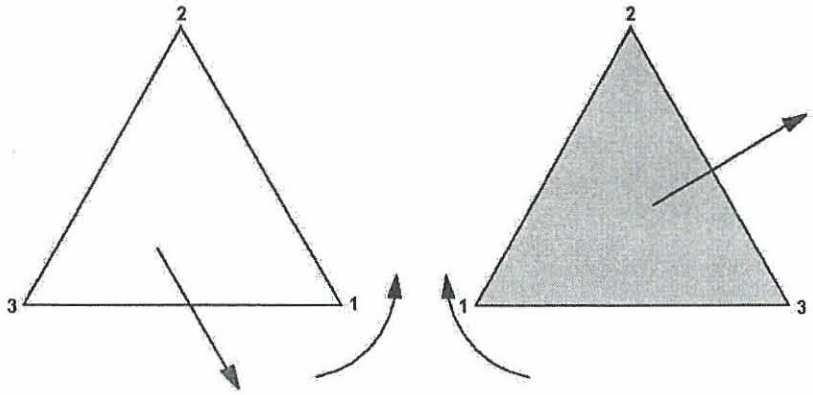

Figure 2.1 Illustration of the right-hand rule used to identify interior or exterior surfaces

In order to create a valid .STL file, each facet must have three vertices and every facet edge must connect with two vertices on the edge of neighboring facets until all facets are accounted for, and no open edges remain. In order to create a proper .STL file the CAD model has to be a single volume closed surface or solid model. Closed means that all surfaces must be trimmed back to intersections with adjoining surfaces [21]. Each triangle within the .STL file must meet all adjacent triangles along common edges, as shown in Figure 2.2.

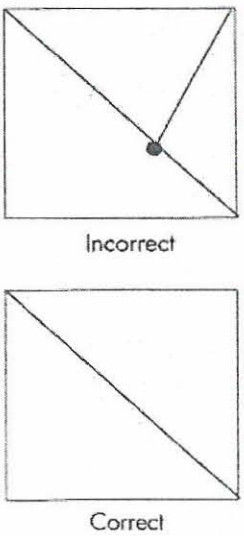

Figure 2.2 Vertex-to-vertex rule applicable to .STL files

Every triangle must share exactly two common vertices with each adjacent triangle. A triangle vertex may not intersect with the side of an adjacent triangle.

When CAD models with missing surfaces or gaps are translated to the slicer, the resulting intersection curves will not be closed, making it impossible for the slicer to calculate the area and ultimately the vector file necessary for scanning. Therefore it is absolutely crucial to the effectiveness of the process that CAD models used in conjunction with Rapid Prototyping processes are closed and contain a single volume [21]. The .STL file can be either ASCII or Binary format. Binary is preferred for disk space and performance considerations [29].

CHAPTER 3

LASER CONCEPTS

3.1 INTRODUCTION

The word LASER is an acronym for Light Amplification by Stimulated Emission of Radiation. The laser makes use of processes that increase or amplify light signals after those signals have been generated by other means. These processes include: (i) stimulated emission, a natural effect that was deducted by considerations relating to thermodynamic equilibrium, and (ii) optical feedback that is usually provided by mirrors. In its simplest form, a laser consists of a gain or amplifying medium (where stimulated emission occurs), and a set of mirrors to feed the light back into the amplifier for continued growth of the developing beam. A laser is a device that amplifies light and produces a highly directional, high intensity beam that most often has a very pure frequency or wavelength. The power of a laser can range from 10^{-9} to 10^{20} W, and wavelengths can range from the microwave to the soft-X-ray spectral regions with corresponding frequencies from 10^{11} to 10^{17} Hz [1].

3.2 COMMERCIAL LASERS

There are many possible reasons why certain lasers do not find their way onto the market. Some require unusual operating conditions or laser media, such as high temperatures or highly reactive metal vapours, and some can only emit feeble powers. Others have only limited applications, particularly lasers emitting low power in the far infrared, or in parts in

the infrared where the atmosphere is opaque. Table 3.1 lists a summary of lasers that are commercially available [10].

Table 3.1 Commercially available lasers

Type	Wave Length	Power output
Helium Neon	632.8 – 543.5 nm	0.5 – 100 mW
Argon Ion	488 – 514.5 nm	100 mW – 50 W
Helium Cadmium	441.6; 353.6; 325 nm	10 – 200 mW
Copper Vapour	510.5; 578.2 nm	1 MW/pulse, 20 kHz repeat rate
Carbon Dioxide	10.6 –9.4 μm	1 – 10 000 W
Excimer	XeF : 351 nm XeCl : 308 nm KrF : 248 nm ArF : 193 nm	1 J/pulse at 100 Hz = 100 W
Far infrared	28 transitions ranging from 99 to 373 μm	1 kW (pulsed), and up to 100 Mw
X – ray	3.56 – 46.9 μm	1 – 2 MW
Free – electron	248 – 8 nm	1 GW (pulsed) up to 10 W

3.3 LASERS IN THE SLA ENVIRONMENT

The SLA uses an Ultraviolet (UV) laser to draw vectors on photo-curable resin, thereby forming hard plastic parts. Although UV light is invisible to the human eye, many materials including the resin, fluoresce when struck by UV light. The fluorescence can be seen where the laser beam intersects the resin surface.

3.3.1 HeCd Laser

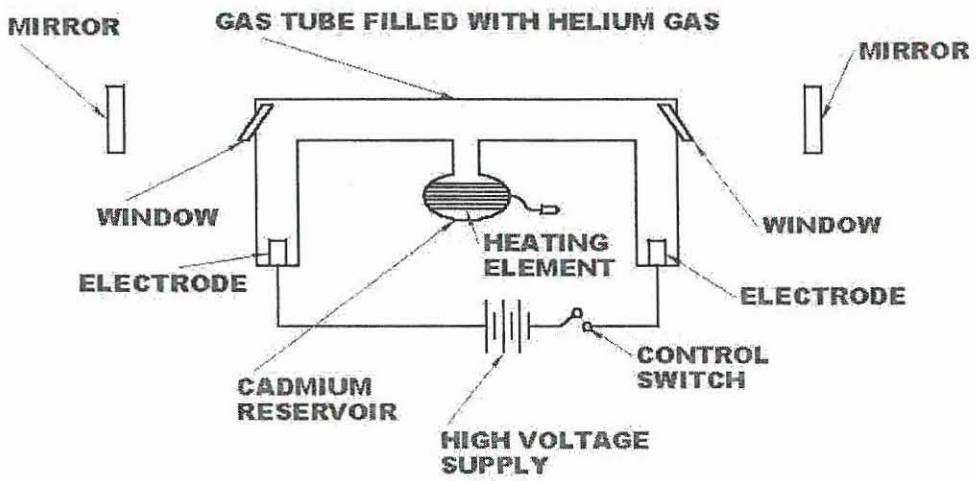

Figure 3.1 Diagram of a HeCd laser used in a SLA-250 machine

The laser consists of a U-shape glass plasma discharge tube with an electrode at both ends and an optical window at either end of the straight section, as illustrated in Figure 3.1. The plasma tube is filled with helium gas at low pressure and has an attached reservoir of solid cadmium.

The cadmium reservoir is heated to vapourise cadmium that mixes with the helium gas. A high voltage potential applied across the plasma tube electrodes creates a powerful electric field, which ionises this gaseous mixture. Free electrons, accelerated by the field, strike and transfer energy to the cadmium atoms. This energy causes the cadmium atoms to enter a long-lived upper energy state. The excited atoms can give up their excess energy and return to an unexcited, stable state. The excess energy is often emitted in the form of photons, at precise wavelengths, characteristic of cadmium.

The device described is a weak plasma discharge lamp. To make a laser, aligned, parallel mirrors are added to either end of the plasma tube. These mirrors define an "optical resonator" and are designed to reflect photons at one of the characteristic wavelengths of cadmium (325 nanometers) while transmitting all others.

Photons that are travelling parallel to the resonator are reflected through the plasma tube by the resonator mirrors. When one of the reflected photons strikes an already excited cadmium atom, it stimulates the atom to release its excess energy in the form of another photon – a photon that is identical to the reflected photon in wavelength, phase and direction of travel. Since the first photon is not exhausted by this interaction, both of the identical photons travel through the plasma tube, reflecting back and forth between the mirrors, creating an increasing number of identical photons.

The resonator mirror located at the output end of the laser transmits a few percent of these coherent photons while reflecting the rest. It is these transmitted photons, which the SLA uses to cure resin [29].

3.3.2 Important Factors for Part Building with a Laser on a Stereolithography Machine

The irradiance (power per unit area) of the laser beam on the surface is of prime importance. Maximum irradiance is obtained at the focal point of a lens, where the beam is at its smallest diameter [3]; [22].

- ***Laser Beam Characteristics***

  The beam profile can be characterised by its transverse electromagnetic mode (TEM). TEM modes are normally written in the form of TEM_{nm}. The subscripts n and m denote the number of nodes in directions orthogonal to the beam propagation, such as for example, TEM_{00} or TEM_{01}. Figure 3.2 shows that the cross-sectional intensity distribution of a typical laser beam may consist of a single beam called a Gaussian or TEM_{00} beam, or a collection of sub-beams closely spaced together or concentric with each other and usually overlapping.

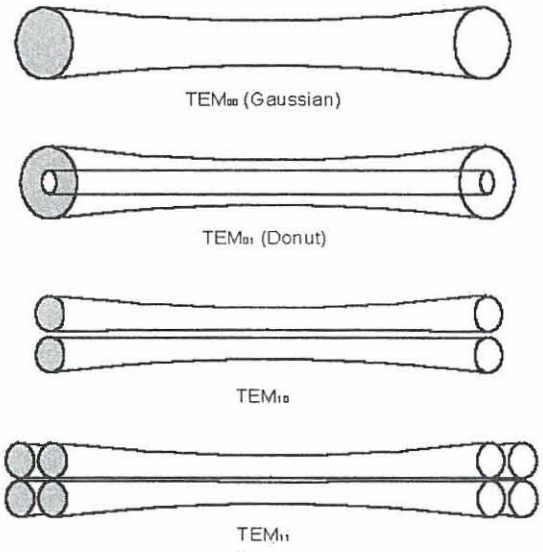

Figure 3.2 Different laser beam profiles (TEM_{nm} modes)

TEM_{00} has a Gaussian spatial distribution and is considered the best mode for laser machining, because the phase front is uniform and there is a smooth drop off of irradiance from the beam center. This minimises diffraction effects during focusing and allows the generation of small spot sizes.

An unaltered Gaussian beam always has a minimum beam waist, Wo, at one location in space. The coordinate axis z that is used to define the propagation direction of the beam can be defined to have a value of z = o at the location of the minimum beam waist. Thus a beam having a Gaussian spatial distribution at the mirrors implies that a Gaussian beam profile exists at all other locations of that beam as it propagates between and beyond the mirrors.

The general equation for the radius, Wo, of a beam focussed by a lens with focal length f is given by equation 3.1:

$$Wo = \Phi \times f \tag{3.1}$$

Where:

Φ = Angle of divergence of the laser beam (Figure 3.3) [20].

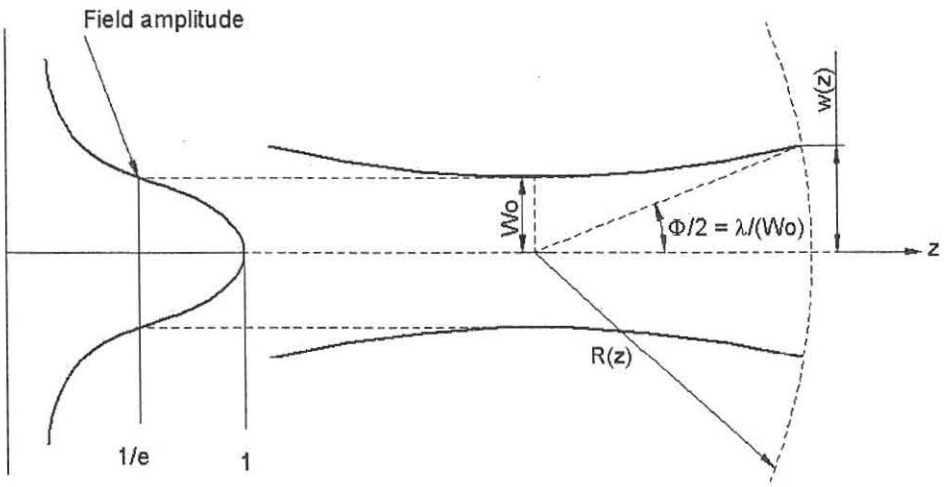

Figure 3.3 Gaussian beam parameters associated with angular divergence

A Gaussian shaped beam (TEM_{00} mode) is often referred to as diffraction limited beam because it can be focused to the smallest spot size. Higher order modes are not Gaussian shaped, therefore real laser beams operating multi-mode beams, are not perfect Gaussian beams. A parameter has been developed that describes how close a real laser beam is to that of an ideal Gaussian beam. A real laser beam has both a waist and divergence that are bigger than that of an ideal Gaussian beam. The factor M^2 describes the relationship of the real beam to that of a Gaussian beam.

The value of M^2 is given by equation 3.2:

$$M^2 = \pi \Phi W /(2\lambda) \quad (3.2)$$

Where:

W = the primary waist of the beam before the lens

λ = wave length of the beam

For a perfect Gaussian beam, $M^2 = 1$. Values of M^2 greater than one represent laser beams with higher order modes than the TEM_{00} Gaussian mode [20].

From equation 3.2 Φ can be derived as:

$$\Phi = 2 M^2 \lambda / (W \pi) \quad (3.3)$$

Substituting equation 3.3 into equation 3.1 results in:

$$W_0 = 2 f M^2 \lambda / (W \pi) \quad (3.4)$$

The initial diameter of the laser beam is reduced in size by focusing optics in order to control the width of a cured line of resin, and to enable imaging of reasonably small features. When using a fixed focal length optical system, the diameter of the focused laser beam, or spot, is a function of the distance from the focusing elements to the resin surface. Thus, the spot's shape and size, incident on the resin surface, changes as the surface is displaced up or down.

As the spot size varies, the irradiance distribution changes. It is this irradiance distribution that determines the photopolymer curing characteristics, such as how deeply

the resin is cured, the width of a cured layer and how strongly a given layer attaches to the one below.

- ***Depth of Focus***

The resin surface defines a horisontal plane, while the motion of the focused laser spot defines that of a sphere, as shown in Figure 3.4.

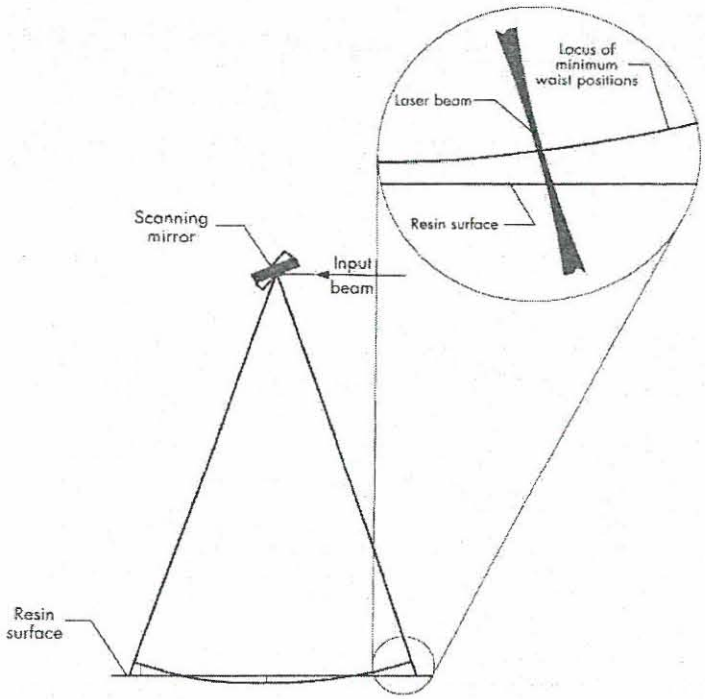

Figure 3.4 Spherical sweep of a focused laser beam over a flat resin plane

The best point of focus does not intersect the resin surface over the entire image area. Keeping the laser spot a consistent size and shape throughout the working envelope can be achieved by taking advantage of depth of focus. Significant depth of focus is possible due to the non-linear Raleigh propagation of a focused Gaussian laser beam.

The resin is positioned in such a way that the free resin plane bisects the spherical surface of theoretical optimum laser focus. If the resin is placed above or below this expected

level, the system begins to operate outside the range of acceptable focus, and the beam shape is different across the resin surface. Displacement of the resin surface relative to its ideal position results in varying cured line width and depths across the working envelope [23].

3.4 SLA-250 LASER SPECIFICATION

The specification of the laser used inside the Stereolithography machine, at the time of the project is summarised in Table 3.2 [15].

Table 3.2 Summary of the SLA-250 laser's specifications

Manufacturer	Kimmon Electric Co. , Ltd
Wavelength	325 nm
Power	51 Mw
Mode	Multi
Beam diameter	1.59 mm
Warm up time (90% power)	10 minutes
Polarisation	Linear
Power stability (at constant temperature)	1.5 %
Noise	4.7 %
Optimised Condition: **Tube voltage**	 2810 V
Tube Current	85 mA
Beam divergence	0.72 mrad

CHAPTER 4

POLYMERISATION PROCESS

4.1 POLYMERISATION

Various types of liquid photo-polymers can be solidified by exposure to electromagnetic radiance over a wide range of wavelengths including, gamma rays and x-rays, ultraviolet (UV) and visible. Electron-beam and UV curing of polymers are the most established and widespread commercial process [23].

Stereolithography is made possible by a process called photo-polymerisation in which a liquid resin is converted into a solid polymer upon exposure to UV light. The degree at which polymerisation occurs, and thus the level of solidification of the material is dependent on the total absorbed actinic radiation.

4.2 PHOTO-POLYMERS

The photo-polymers used in Stereolithography are composed of two basic materials. The first is a photo-initiator, which absorbs the laser energy and forms reactive radical or cationic species, which initiates the polymerisation process. The photo-polymers also contain acrylic or epoxy functionalised monomers and oligomers, which polymerise upon exposure to either a free radical or cationic species.

The photo-initiators and monomers used in Stereolithography systems have excellent thermal stability at room temperature. However, if the resin is exposed to excessive heat in the liquid state, it can polymerise uncontrollably. The UV cured resin, in solid state, will not polymerise uncontrollably even with the application of heat [29].

4.3 PHOTO-POLYMERISATION PROCESS

Figure 4.1 illustrates the photo-polymerisation process, used to create a solid polymer from liquid resin.

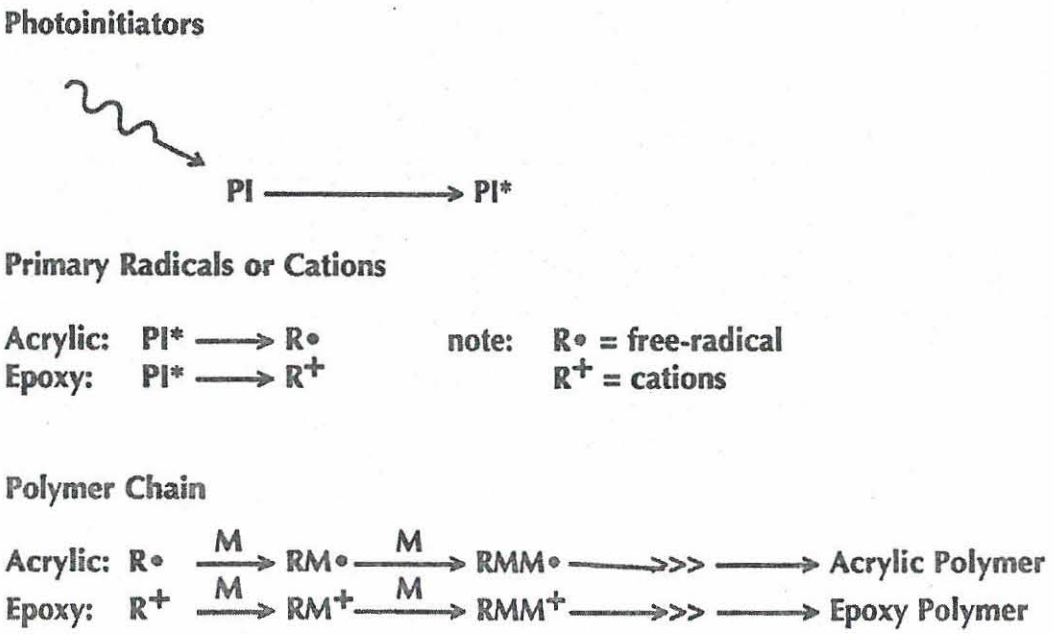

Figure 4.1 Photo-polymerisation process of polymers used in the Stereolithography process

4.3.1 Photoinitiators

Photoinitiator (PI) molecules absorb actinic UV radiation from the laser and are converted to an excited state PI*. This short-lived high-energy species quickly relaxes to a lower energy excited state.

4.3.2 Primary Radicals or Cations

The excited PI* molecules catalyse formation of one or more highly reactive species called primary radicals (R•) or cations (R^+) with the formation reaction and number dependant on the specific photoinitiator used.

4.3.3 Polymer Chain

The primary radical or cation then reacts with an acrylic or epoxy monomer (M) to form a new reactive species (RM• or RM^+). This starts a chain propagation process (polymerisation) in which the reaction is repeated over and over again to form a polymer chain involving many monomers.

4.3.4 Solidification

The polymer quickly increases in molecular weight until the viscosity increases to the point where the material is effectively a solid. The polymerisation process in the exposed region slows down and eventually stops when the monomer concentration decreases in that specific region. However, the polymerisation reaction within the irradiated region continues for a prolonged period for epoxy resins. For acrylate resins, the reaction almost stops immediately

after the actinic exposure is terminated. The irradiance of the laser beam and the period of exposure, control the overall dimensions of the solid polymer, formed when an UV laser is focused on the surface of a photopolymer. A longer exposure or increased laser power increases the depth and width of the solidified region.

Both epoxy and acrylate resins for Stereolithography are designed such that the polymerisation, and thus solidification, stays localised. This polymerisation does not extend substantially beyond areas that are exposed with actinic laser photons. This characteristic property allows the generation of parts with extremely high definition and resolution.

4.3.5 Influencing Factors

A relatively small change in temperature can cause a large change in the viscosity, volume of resin, and resin curing characteristics. Higher temperatures and reduced viscosity result in thinner liquid that settles faster during dipping and drain faster during post processing. However, higher temperatures also result in more voids or dimples, increased swelling and decreased green strength. The best results are obtained working within the temperature range specified for a given resin.

For epoxy resins, small amounts of naturally occurring impurities inhibit the sustained photo-polymerisation. These effects create a threshold of minimum exposure, known as critical exposure, which is needed to support photo-polymerisation required to generate a solid polymer.

4.4 CREATING SOLID PLASTIC

4.4.1 Bullets

During the build process, a stationary UV laser beam focussed on the surface of the photopolymer solidifies a small volume of liquid into the shape of a bullet, as shown in Figure 4.2.

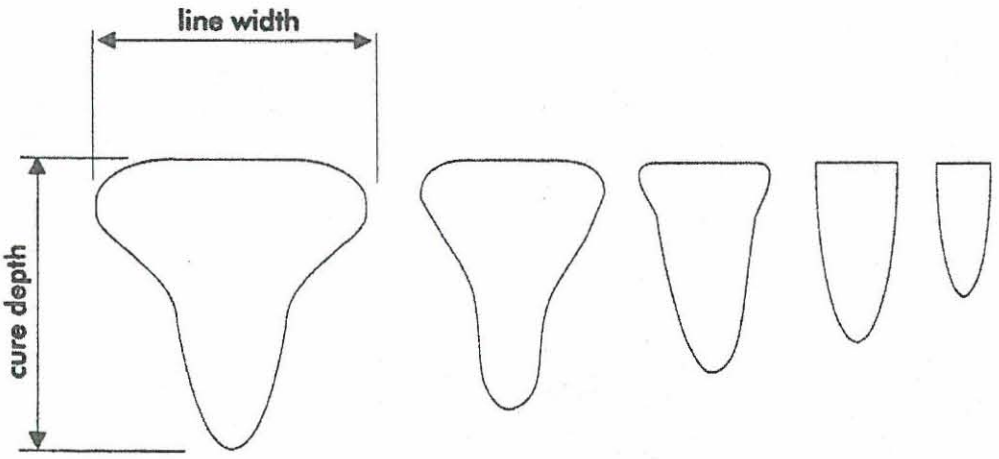

Figure 4.2 Typical bullet shapes created during the build process

The intensity profile of the laser beam varies from point to point with the maximum intensity near the center of the beam. As the laser beam strikes the surface, a quantity of light is absorbed (polymerising the liquid) while a portion is transmitted to the liquid below it. The overall dimensions of the plastic bullets are determined by how much laser energy enters the liquid. This quantity of laser energy is the exposure. The bullet is the basic building block for Stereolithography part building.

Since the degree of polymerisation is proportional to the amount of light absorbed, the surface area of the resin is the most solid, and the area below the surface hardens in proportion to the amount of actinic radiation absorbed.

4.4.2 Cure Depth

The depth of the cured plastic increases as the exposure to actinic radiation increases. This exposure varies across the width of the laser beam since the laser beam cross-section is not uniform. The center of the beam cures to the greatest depth because it is the area of highest intensity. The maximum solid depth achieved after laser exposure is known as the cure depth. If a part is built with no overcure, the layers would just be touching and there would be almost no adhesion between the layers. Useful parts require adhesion and overcure to avoid delamination. Stereolithography uses two values when defining cure depth: layer thickness and over-cure. Over-cure is the amount of cure applied over or under the layer thickness.

4.4.3 Vectors

As the laser beam moves across the surface of the liquid resin, interconnecting bullets of cured resin called vectors are formed. Stereolithography utilises three types of vectors to create a solid part: border, hatch and fill. Each of the vectors has a specific purpose.

- Border vectors form the highly accurate exterior of the part. This is the base for all other resin curing.
- Hatch vectors form the internal structure of the part and with the border vectors, provides a means of bonding each layer of vectors to the previous.

- The cure depth of fill vectors is independent of layer thickness. Skin fills are used to fill in flat or horizontal surfaces. They are not used to bond layers together.

4.4.4 Bonding and Overlap

To adhere or bond a layer with the previous one below, the cure depth must be greater than the slice thickness by a layer overlap or over-cure factor as illustrated in Figure 4.3.

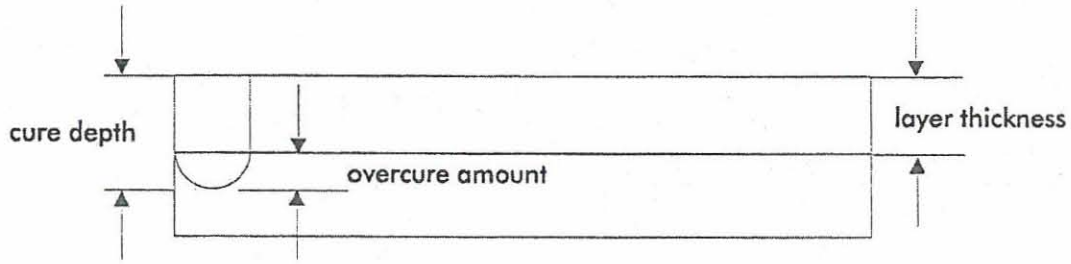

Figure 4.3 Illustration of the layer over-cure factor for proper bonding

Layer-to-layer bonding occurs when the UV light of the laser, curing the current layer, penetrates down to the previous layer to form a chemical bond between the lower level and the newly formed top layer. Strong layer-to-layer bonding, created by the required overlap, is needed to build strong parts. Excessive overlap, however, may cause internal part stress and curl.

4.4.5 Critical Exposure

For photopolymer resins when exposure is less than the critical value, the resin remains a liquid. If the exposure is more than the critical value, the resin undergoes at least partial polymerisation. However, if the exposure is equal to the critical exposure, the resin is at the so-called "gel point" corresponding to the transition from the liquid to the solid phase.

Critical exposure can be defined as radiant energy per unit area; it is proportional to the laser power and inversely proportional to the product of the laser beam width at the liquid surface and the laser scan speed. Each resin has its own critical exposure value [13].

4.4.6 Penetration Depth

Penetration depth can be defined as that depth of resin which will reduce the irradiance to 1/e of the surface resin, where e = 2.7182818..., the base of natural logarithms. Each resin has its own penetration depth [13].

4.5 PHOTO-POLYMER SHRINKAGE AND PART ACCURACY

Stereolithography photo-polymers must be capable of generating parts with excellent dimensional accuracy to satisfy the tolerance requirements for various applications. Accuracy generally requires photo-polymers with minimal shrinkage during building, and also during the post-curing process.

4.5.1 Curl Distortion

Curl distortion is characteristic of objects built in multiple layers. If the laminates undergo shrinkage or expansion when an additional layer is applied over a cured layer, the object will distort. This distortion may be instantaneous or delayed.

4.5.2 Volumetric Shrinkage

The Ciba-Geigy epoxy resin SL5170 shrinks about 6-7 % by volume when the liquid resin is completely post-cured to the solid state. The effective linear shrinkage is 0.05% for this specific resin.

4.5.3 Cantilever Curl

Cantilever curl is one of the inherent tendencies for the resin to undergo warpage during the building process, when the part is not properly supported. When cantilever sections are properly supported, curl distortion can be minimised or even effectively eliminated.

4.5.4 Part Accuracy

Accuracy in the *z*-direction depends on the formation of the layers and cure depth control. This involves laser scanning velocity, as well as liquid leveling. For Stereolithography the *x-y* dimensional accuracy depends strongly on the shrinkage of the resin and the positioning accuracy of the laser scanning system. User-part accuracy is established from the error values associated with the coordinate measuring machine measurements. The root-mean-square error (RMS) is calculated from at least 170 measurements. With increased measurements, the statistical significance of the results improves. The latest results for user parts built with SL 5170 on a SLA 250 is 45 microns RMS error. This RMS value is based on 10 user parts (1700 measurements) built on the same machine over a period of three months.

4.6 RESIN SPECIFICATION

Resins used during this study where the Ciba-Geigy Cibatool® SL 5170 and the Somos® 9110 Epoxy Photopolymer. The typical properties of these resins are summarised in Table 4.1 [4]; [5].

Table 4.1 Typical properties of the Cibatool® SL 5170 and the Somos® 9110 Epoxy Photopolymer resins

	Cibatool® SL 5170	**Somos® 9110**
Appearance	Clear	Transparent amber
Density	1.14 g/cm^3 (25°C)	1.13 g/cm^3 (25°C)
Viscosity	165 – 195 cP (30°C)	450 cP (30°C)
Penetration depth (D_p)	4.8 mils	5.2 mils
Critical exposure	13.5 mJ/cm^2	8 mJ/cm^2
Tensile strength	59 – 60 N/mm^2	31 N/mm^2
Tensile modulus	2400 –2500 N/mm^2	1590 N/mm^2
Elongation at break	8 – 14 % (ISO R 527)	15 – 21 %
Flexural strength	107-108 N/mm^2	44 N/mm^2
Impact strength	27 – 30 kJ/m^2 (initially)	
	80-90 kJ/m^2 (3 weeks)	
Hardness	85 Shore D	83 Shore D

CHAPTER 5

STEREOLITHOGRAPHY BUILD PROCESS

5.1 INTRODUCTION

The Stereolithography process contains six major components; .STL verification, orientation, support creation, preparation, building and post processing. The first step is verification of the .STL file. Verification involves verifying the compatibility of the .STL file created during the CAD design step. The second step concentrates on the orientation of the part and involves the proper placement of the part in which supports will be placed for the best results. Supports are then created for the part. The next step, preparation, involves the selection of build and re-coating styles, slicing, creation of build files, and the selection of resin shrinkage and the number of copies to build. The following step is the actual build followed by post processing.

5.2 VERIFICATION

This allows one to verify and fix .STL files to make them acceptable for the preparation process. Flaws that are identified and fixed include the following: gaps between triangles, overlapping triangles, redundant triangles and incorrect normal direction.

5.3 ORIENTATION

Object orientation for an SLA build should follow the following guidelines:

- Each object must reside entirely in the positive *x, y, z* Octant of CAD space

- The part must be at least 6.5 mm above the platform for efficient draining.
- Optimisation of part draining by reducing the number of areas (trapped volumes) that can hold resin after the part is completed.
- Ensure that the part or parts fit in the build envelope. If the part is large, it may be sectioned, built in several runs, and assembled during post processing.

5.4 SUPPORT CREATION

During the build process it is essential that the position of the part be maintained. This is the function of the support structure, without which part build-up becomes an impossible task.

Support structure design is a necessary link in the process of creating a prototype on a Stereolithography machine. The support structure is needed for the following reasons:

- It is needed to prevent sagging and delamination during the build process.
- Support structures should prevent sections from becoming free-floating and moving out of their correct position.
- Without a support structure it is nearly impossible to attain reasonably accurate prototype parts.

Since the support structure is built along with the part, it requires a certain amount of polymer liquid and laser power to build it. Both of these are expensive, so minimising the volume of the support structure will help to minimise the cost of building Rapid Prototype models.

It also takes time to remove the support structure from the part. This must be done manually, and the difficulty of doing it is proportional to the size of the support structure, the area of the intersection between the support structure and the required surface finish of the part over that area [2].

5.5 PREPARATION

This step at the build station involves the selection of build parameters, slicing, selection of re-coat parameters, merging, and selecting the resin shrink factors.

5.6 SLICING

Slicing is the process by which the CAD model is divided into successive cross-sectional layers. It transforms the solid CAD model into vector data, which the imaging system ultimately draws on the surface of the resin. Slicing can be a very time-consuming and process-intensive task, depending on the slice thickness and the complexity of the CAD model. As layer thickness is decreased, the object generated is better suited to the design intent, and surface quality is correspondingly improved [23].

5.7 BUILDING

The build phase is where the three-dimensional part is actually produced. This is done entirely on the SLA using the control computer. Prior to building, the platform is installed, the laser is turned on, and the build options are selected. The control computer uses data from the build station preparation to maintain the machine operation during the build. The

form of this data is in four build files; .L (which stands for layer), .PRM (which stands for parameter), .R (which stands for range) and .V (which stands for vector). SLA hardware and software are automatically initialized in the first step of the build process.

Before the build takes place, software on the control computer will verify the resin level. If the resin level is too low it is adjusted by manually adding more resin, if too high, resin is manually removed from the vat. When the resin is near the correct level, an automatic leveling system takes over to perform fine adjustment. Next, the laser power and beam position is verified to establish the speed at which the laser beam movement will occur during the build. The speed affects the depth and width of the resin solidification.

The laser draws the first support cross-section that adheres to the platform. After each layer is drawn, the elevator dips the hardened cross-section below the surface, coating the cross-section with a layer of resin. After drawing a number of support layers, the first part layer is solidified. The laser then draws the second part layer. As the second layer is drawn, it becomes firmly attached to the first. This process is repeated until all layers have been drawn to form the 3-Dimensional object.

The SLA is designed for continuous operation and can be left unattended while in operation. When the last layer has been drawn, the completed part is raised up out of the vat. The building time is logged into a history file (build.log) and the laser is automatically powered off.

5.7.2 ACES Build Style Parameters

Tables 5.1 and 5.2 show the ACES build style parameters used to create parts and support structures on the SLA-250 machine.

Table 5.1 ACES part build style parameters (SL5170AP15)

Layer thickness	0.15 mm
Hatch type	Box
Hatch spacing	0.1 mm
Stagger weave	On
Alternate Sequence	On
Retraction start point	0.00 mm
End point	0.025 mm
Fill type	*x* , *y*
Fill spacing	0.1 mm
Border overcure	0.175 mm
Fill cure depth	0.225 mm
Hatch overcure	- 0.075 mm

Table 5.2 ACES support build style parameters (SL5170AS15)

Layer thickness	0.15 mm
Hatch type	Box
Fill type	No fill
Border overcure	0.15 mm
Fill cure depth	0.0 mm
Hatch overcure	0.0 mm

5.8 RE-COATING PROCESS

The resin surface preparation in all Stereolithography machines is important for the following reasons:

- The resin surface must be maintained at the focal plane of the imaging system.
- The resin surface must be uniformly flat, level, and free of extraneous features.
- The resin surface must be a controlled distance above the previously drawn cross-section of the part, typically in the range of 0.10 mm to 0.25 mm.

The re-coating process is a combination of elevator and re-coating blade movements. These movements add a precise and level layer of liquid resin to the top of the most recently completed layer. This establishes the thickness of the new layer to be solidified.

The re-coating steps during the part building process on the Stereolithography machine are outlined in the Figure 5.1.

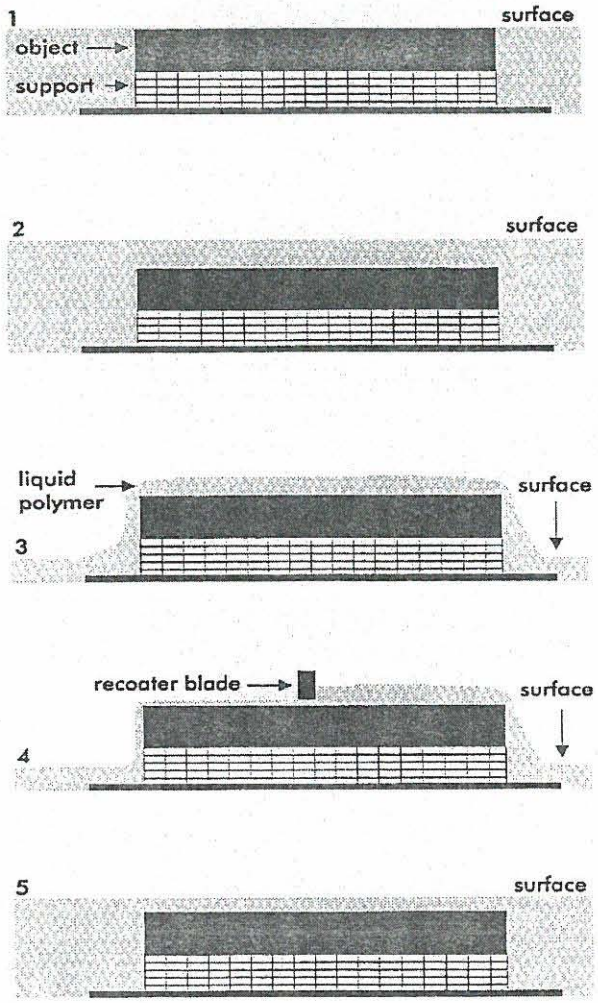

Figure 5.1 Steps involved during the re-coating process

1. The top of the newly cured resin is level with the surface of the surrounding liquid resin after a layer is first solidified. Resin level adjustments are made and then the elevator lowers to position (2).
2. The elevator is lowered to completely cover the newly solidified layer with resin.
3. The platform is raised until the gap between the top surface of the solidified layer and bottom edge of the re-coating blade is equal to the next desired layer thickness. Excess resin covers the part due to surface tension and resin viscosity.
4. The re-coating blade removes excess resin to establish the precise liquid layer thickness.
5. The platform is lowered until the top surface of the cured part is at the desired layer thickness below the resin surface [29].

5.9 POST PROCESSING

After the part has been built it requires post processing. This includes cleaning, UV curing, and final finishing.

5.9.1 Cleaning

First, the liquid resin is allowed to drain off the part and platform, back into the resin vat. The platform, with the part still attached, is then removed from the SLA process chamber and the remaining excess liquid is removed by various cleaning methods.

5.9.2 UV curing

The part is removed from the platform, and the support structure is removed from the part before UV curing. UV curing solidifies liquid resin in and around the part. This is accomplished by placing the cleaned part in a Post Curing Apparatus.

5.9.3 Finishing

Final finishing may include sanding, sandblasting, polishing, buffing and painting.

CHAPTER 6

SLA-250 BUILD STATION

6.1 INTRODUCTION

The Stereolithography part is built on the SLA build station as shown in Figure 6.1.

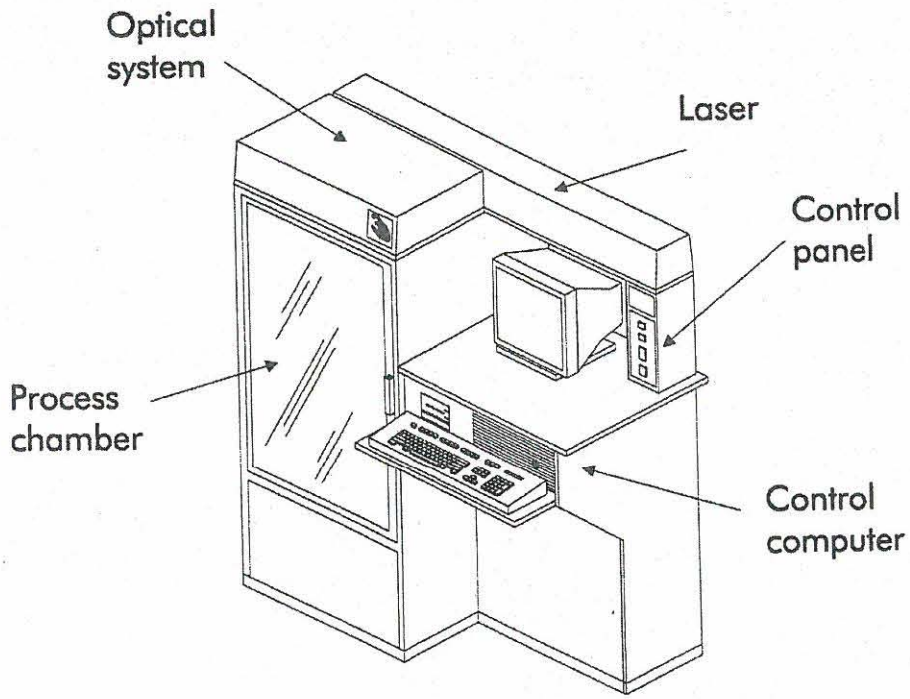

Figure 6.1 SLA-250 Build station

The major components of a SLA-250 include the laser, process chamber, control panel, re-coating system, optical system and the control computer.

6.2 LASER

The UV laser used in the SLA-250 build station to cure the resin, is a HeCd laser. This specific laser has a characteristic wavelength of 325 nm. For a detailed discussion of the laser refer to Chapter 3.

6.3 OPTICAL SYSTEM

Optical elements are used to fold the laser beam path, helping to keep overall machine size as compact as possible, and providing an appropriately sized laser spot on the surface of the resin. The optics are coated to either reflect or transmit the wavelength in use.

Positioned at the head of the laser is the optics platform, which contains the focusing and steering devices, needed to direct the laser beam. The optical system in the SLA consists of a mechanical safety shutter, three beam turning mirrors, a beam expander, and *x-y* dynamic mirrors mounted on an optics table above the process chamber as shown in Figure 6.2. An optical window isolates optical components from the chamber environment, while allowing the laser beam to enter the process chamber.

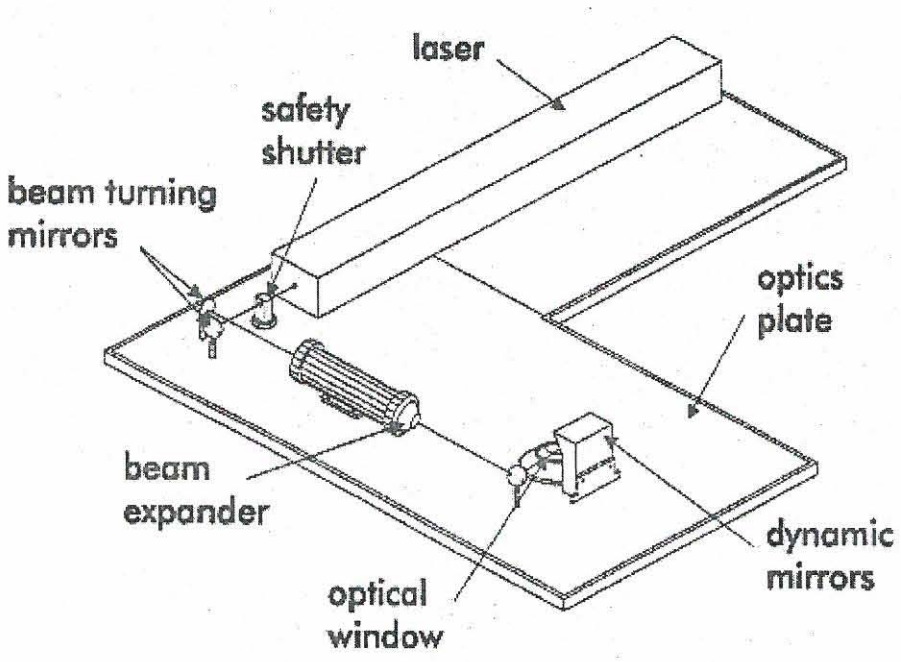

Figure 6.2 Layout of the optics plate

6.3 OPTICAL SYSTEM

Optical elements are used to fold the laser beam path, helping to keep overall machine size as compact as possible, and providing an appropriately sized laser spot on the surface of the resin. The optics are coated to either reflect or transmit the wavelength in use.

Positioned at the head of the laser is the optics platform, which contains the focusing and steering devices, needed to direct the laser beam. The optical system in the SLA consists of a mechanical safety shutter, three beam turning mirrors, a beam expander, and *x-y* dynamic mirrors mounted on an optics table above the process chamber as shown in Figure 6.2. An optical window isolates optical components from the chamber environment, while allowing the laser beam to enter the process chamber.

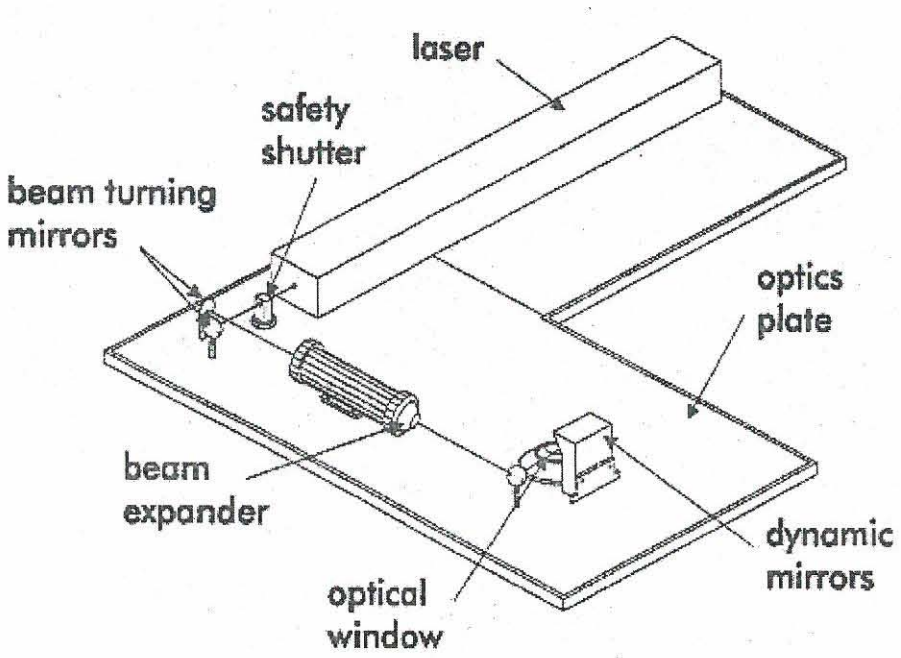

Figure 6.2 Layout of the optics plate

6.3.1 Safety Shutter

After the beam exits the laser, it passes through the safety shutter. A solenoid-actuated shutter operates to block the laser beam when an interlock switch on the chamber is activated, or when directed to open or close by the control computer.

6.3.2 Beam Expander

The beam expander expands the diverging laser beam diameter, and then focuses it so that the beam converges to a small spot on the surface of the resin. Since the laser determines the smallest feature that the system can generate, a highly focussed beam is desirable for Stereolithography. A small focussed beam spot has a higher power density and cures resin faster, resulting in higher resolution.

6.3.3 Turning Mirrors

The three beam-turning mirrors used to direct the beam are coated for high reflectivity at the 325 nm wavelength. The first two turning mirrors reflect the beam from the laser to the inlet aperture of the beam expander. The third mirror reflects the laser from the outlet beam expander aperture to the dynamic mirrors.

6.3.4 Dynamic Mirrors

The two reflective coated dynamic mirrors, approximately 6.35 mm square, direct the beam down through the optical window to the process chamber. These mirrors provide the laser movement in the *x-y* plane of the resin. The movements of these mirrors are accomplished via galvanometer motors controlled directly by the control computer.

6.4 PROCESS CHAMBER

The process chamber is accessible through a door coated with special UV absorbing material, to shield the viewer from the laser UV radiation, and to shield the resin from room and sunlight. When the door is open, the interlock circuit causes the safety shutter to close and prevent the laser from entering the process chamber.

The process chamber houses a chamber light, cooling fan, heater, beam profilers, vat and the *z*-stage assembly. Figure 6.3 shows the layout of the process chamber of a SLA-250 machine.

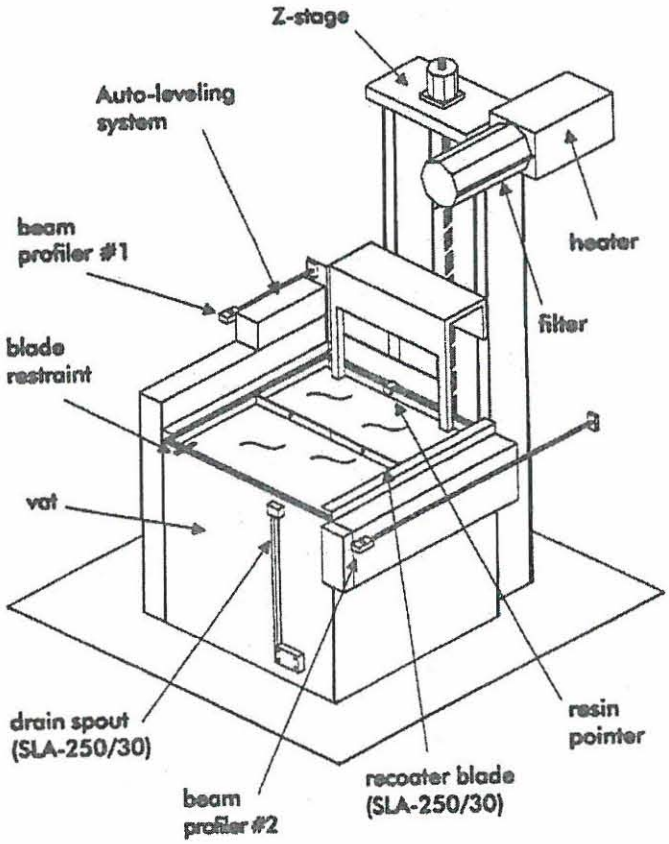

Figure 6.3 Layout of the SLA-250 process chamber

6.4.1 Chamber Light

An overhead light illuminates the resin vat and work surfaces. The fluorescent tube is located behind an UV absorbing acrylic cover.

6.4.2 Cooling Fan

A cooling fan is located on the rear of the SLA cabinet. The fan is equipped with a Polyurethane foam filter.

6.4.3 Heater

Internal temperature of the process chamber, plus or minus one degree Centigrade is controlled through the use of a heater. Air used to heat the chamber is drawn through an activated charcoal filter, heated, and returned to the process chamber.

6.4.4 Z-stage Assembly

The *z*-stage positions the part for building in the *z* or vertical axis by raising and lowering the part through computer controlled operation. The platform, attached to the elevator-cantilevered arms, holds the part while it is being built and is perforated to allow the liquid resin to flow through during a build.

6.4.5 Auto-leveling System

An automatic leveling mechanism using either a Helium Neon (HeNe) laser or diode laser adjusts the liquid level and maintains the correct amount of liquid for drawing each layer. A plunger is used to keep the resin level constant during part building to assure proper layer thickness.

- ***HeNe/Diode Laser- Leveling Assembly***

The Helium Neon (HeNe) and diode leveling assemblies are used as a feedback mechanism to keep the resin at prescribed level. Each consists of a laser, a photosensitive surface called a bi-cell, and the related circuitry for current-to-voltage conversion and signal conditioning. This assembly is shown in Figure 6.4. During normal use, the laser is classified as a Class 1 laser with a maximum power output of 0.95 mW.

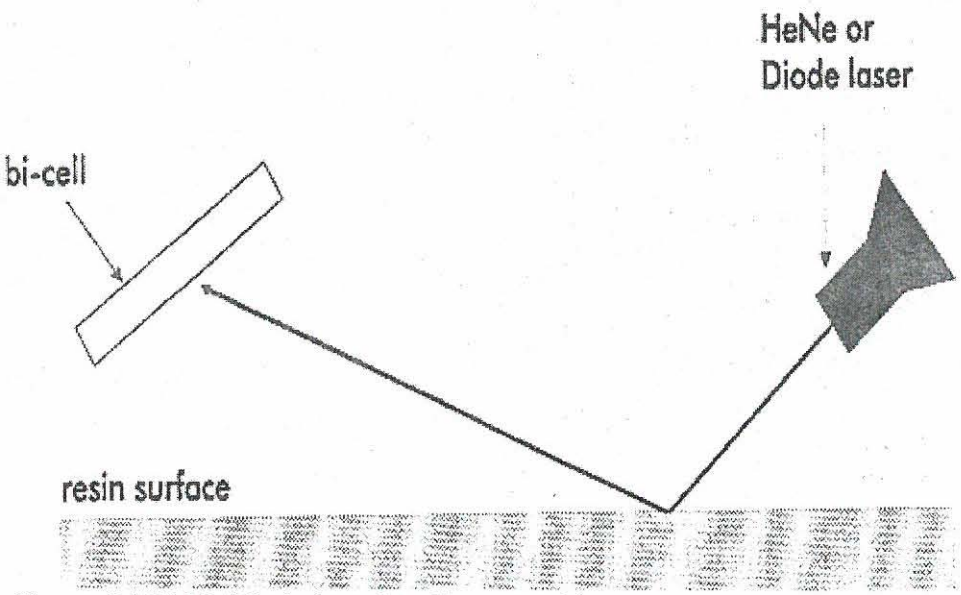

Figure 6.4 HeNe/Diode laser leveling assembly

The beam strikes the resin surface and is reflected up to the bi-cell. The photosensitive surface of the bi-cell is exposed to the laser beam through an open slot. When the beam strikes the surface it produces an electrical signal. Based on the electrical signal, the control computer determines where the beam is striking the cell, and thus determines the resin level. If the beam does not strike the bi-cell, the control computer interprets this lack of signal as a very low resin condition. When the laser moves from the positive cell to the negative cell, as illustrated in Figure 6.5, the output signal changes as it moves through the different resin level stages. A tolerance is established by setting upper and lower limits to adjust resin level sensitivity. Whenever the resin height is between those two limits, the system is considered level and no fine adjustment is necessary. If the resin level state is S0 or S1, resin must be removed from the vat. If the resin level is S5 or S6, resin must be added to the vat. If the resin level is S2, S3 or S4, there is no need to add or remove resin. The system is then between the tolerance [14].

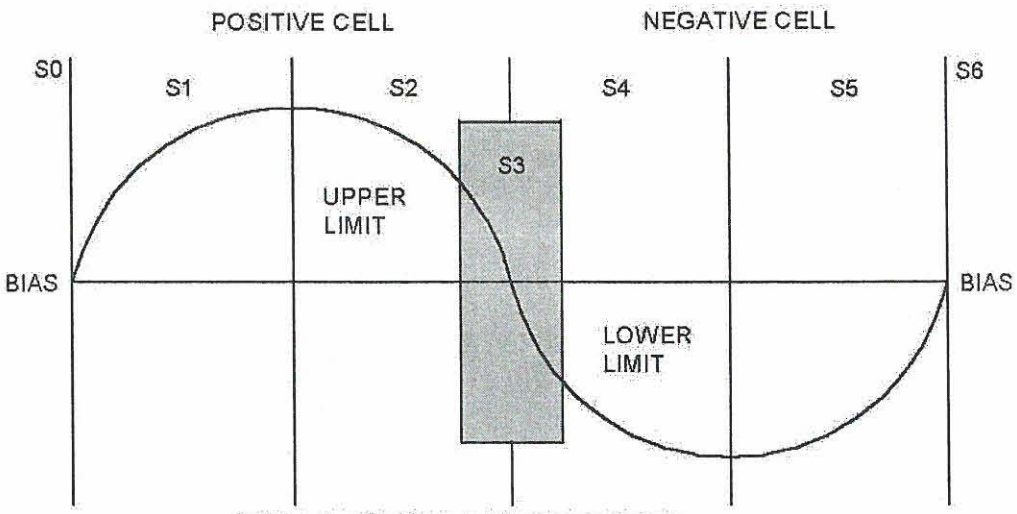

Figure 6.5 Bi-cell sensor output for different resin levels

6.4.6 Beam Profilers

Two beam profilers, consisting of UV sensitive detectors mounted beneath precision apertures, are mounted in the process chamber on two corners of the process chamber. The beam profilers measure the laser beam profile and power. This information is used by the control computer to calculate draw speeds and to compensate for drift of the dynamic mirrors.

The beam profiler sensors are suspended by process chamber attachments. Sensor #1 is in the right rear and sensor #2 in the left front. The profilers provide the scanning system with a position reference for drift correction and power readings. Thermal expansion and

variations in the other portions of the optical system cause drift. The power readings are taken between each layer of drawing and are used by the control computer to calculate laser-scanning speeds. The sensors are also used to check the beam diameter and *x*-*y* ratio.

6.4.7 Vat

The SLA-250 resin vat allows for a part to be built up to 250 mm x 250 mm x 250 mm. The vat rests in the chamber on three ball feet, which align it with the elevator and platform.

6.4.8 Re-coating Blade

The re-coating blade is mounted on the vat assembly and uses wait time to establish a smooth resin surface, prior to drawing the new layer. The re-coating blade establishes the correct thickness of liquid resin above the last solidified layer, prior to drawing the new layer. The drive assemblies consist of stepper motors connected by shafts to toothed belts.

CHAPTER 7

BENCHMARK SOFTWARE

7.1 MAGICS RP VERIFICATION

As explained in Chapter 1, only a completed 3D drawing or an .STL file can be used to calculate an exact build time of a part. The .STL file is imported into Magics RP and it can give build time estimation based on certain parameters, which are supplied by the operator. Because Magics RP is used as one of the benchmarks for the build time calculation process, its operation must be understood as well as certain parameters. Its accuracy must also be verified with experiments.

7.2 MAGICS RP OPERATION

The purpose of this program is to offer a user-friendly solution to all common and uncommon Rapid Prototyping problems. The following functions are offered:

- Visualisation, Measuring and Manipulation of .STL Files.
- Fixing .STL files, Uniting Shells.
- Cutting .STL files, Punching holes.
- Boolean Operations.
- Quotation Making, Build time estimation.
- Collisions detection.

7.2.1 Support Generation

Magics RP is equipped with a module for support generation. Support generation is mainly used for Stereolithography. The generated supports are directly compatible with 3D Systems SLA machines using the .STL or .SLC format.

The support generator allows the generation of supports for a whole platform, as well as editing of supports on each individual surface. This Support Generation Work Routine allows easy adaption of supports after the part has been repositioned on the building platform. The Support Generation Parameters are crucial during the initial automatic support generation, but can also be modified for each individual support.

Normally supports are generated in 5 steps:

- Definition of the support generation parameters in the machine setup.
- Automatic support generation.
- Modifying support types and support parameters.
- 2D and 3D editing of supports.
- Saving and exporting supports.

Magics RP allows the operator to change between the RP mode, where .STL files can be edited, and the Support Generation Mode. In this way one can easily adapt supports once they have been generated. If a part is translated or rotated, the support structure for the part will automatically be updated [16].

7.3 VERIFICATION OF MAGICS RP'S PARAMETERS

Whilst preparing a prototype file with Magics RP, information with respect to *x, y, z* co-ordinates, volume, surface and build time estimation is generated. Re-coating time estimation is also given. Variables that influence the variation between the actual and estimated build times are:

- Surface of the parts and their supports.
- Volume of the parts and their supports.
- Re-coating time.
- Number of parts during a build.
- Boundary locations (*x, y*) in which the laser has to operate during the build.
- Total height of the build.
- Laser power during the build.

7.3.1 Verification of Variables

- ***Surface and Volume***

  To determine how Magics RP calculates the surface and volume of a prototype, five different solid model shapes were drawn. The dimensions of the shapes are given in Table 7.1.

Table 7.1 Dimensions of the modeled shapes

Shape	Base Ø (mm)	Height (mm)	Width (mm)	Depth (mm)
Cylinder	20	30		
Rectangular prism		30	20	10
Hollow rectangular prism:				
Outer rectangular prism		45	20	10
Inner rectangular prism		45	12	4
Non-symmetric hollow rectangular prism				
Outer rectangular prism		45	20	10
Inner rectangular prism		45	12	4
Cone	9	5		

These shapes were exported into the .STL file format to be used by Magics RP. Volumes and surface areas were calculated by using standard formulas.

For the non-symmetric hollow rectangular prism, the hole was placed off-center to generate a non-symmetric wall-thickness. This was done to determine if it would have any influence on the volumetric calculation of the part. These values would be compared with those of the symmetric hollow rectangular prism.

- ***Re-coating Time Estimation***

The total re-coating time estimation, which is dependent on the *z*-height of the model, was obtained from Magics RP. This estimated time consisted of a combined value of the time taken by the sweeper while building the support structure and the part.

The re-coating time per layer for a part and its supports was obtained from the parameters of the SLA machine control software. This time is dependent on the re-coating time per layer and the number of layers in the *z*-direction. The re-coating times for the part and its supports were added to obtain the total re-coating time.

- ***Number of Parts***

For each platform, the number of parts on that platform is obtained. This can be obtained by using Magics RP to view the properties of the generated platform.

- ***Boundary Locations***

The maximum *x* and *y* distances of a platform is obtained by viewing the properties of a generated platform in Magics RP.

- ***Total Height***

To obtain the maximum *z*-height of a platform, the *z*-dimension of the highest part on the platform was used.

- ***Laser Power***

The laser power prior to the building of a platform was obtained from the SLA machine control software.

- ***Experimental Results for Surface, Volume and Re-coating Parameters***

Table 7.2 presents the results of Magics RP's values compared to the calculated values.

Table 7.2 Comparison between Magics RP's values and the calculated values

Shape	**Magics RP**			**Calculated**		
	Volume mm^3	**Surface mm^2**	**Re-coating time**	**Volume mm^3**	**Surface mm^2**	**Re-coating time**
Cylinder	9425	2513	156 min	9425	2513	155 min
Rectangular prism	6000	2200	156 min	6000	2200	155 min
Hollow rectangular prism	6840	4444	230 min	6840	4444	235 min
Non-symmetrical hollow rectangular prism	6840	4444	230 min	6840	4444	235 min
Cone	59	93	75 min	58.905	92.748	60 min

During this experiment it was found that Magics RP calculates the outer surface area of a part and its supports. Also, from Table 7.2 it can be seen that Magics RP uses standard formulas to calculate the volume and the outer surface areas.

From the volumetric and outer surface area calculations of the symmetric hollow rectangular prism and the non-symmetrical hollow rectangular prism, it can be seen that a non-symmetrical wall thickness does not influence the calculations.

7.4 SUMMARY

Table 7.3a and 7.3b show information of platforms that have been built for commercial purposes in the Centre for Rapid Prototyping and Manufacturing. The table lists the variables that can influence the build time estimation process of Magics RP. It also lists Magics RP's estimated build time against the actual build time obtained from the 'build.log' file from the SLA Build Station. The percentage error of the estimated build time against the actual build time is also listed.

Table 7.3a Build time estimation variables with Magics RP's estimation versus actual build time

Platform	NR. of Parts	Total Surface		Total Volume		Delta X (mm)	Delta Y (mm)	Delta Z (mm)
		Parts (mm^2)	Support (mm^2)	Part (mm^3)	Support (mm^3)			
BG04	7	103555	36778	53735	0	238.48	120	54
BG05	5	59146	53952	46278	0	181.7	161.53	45.5
BG06	6	119403	72369	108336	0	222.052	150.1	43.453
BG08	11	64314	45025	54704	0	229.99	92.948	105
BG10	2	148222	171169	201781	0	217	176	156
BG11	4	38404	16110	24234	0	174.93	122.2	45.908
BG13	8	15775	56754	197288	0	233.063	230.67	132
BG14	3	28912	418.77	66315	0	103.345	114.83	92.86
BG15	2	154948	327500	245256	0	234.02	233.76	78
BH01	10	107580	86060	100030	0	169.35	131.73	105
BH03	3	41916	42007	40697	0	109.97	77.5	98.97

Table 7.3b Build time estimation variables with Magisc RP's estimation versus actual build time

Platform	NR. of parts	Laser Power (mW)	Estimate time (sec)				Actual time (sec)	Percentage error
			Part	Support	Re-coating	Total		
BG04	7	20	489	140	203	832	839	0.8
BG05	5	20	365	154	170	689	733	6.0
BG06	6	19	915	147	162	1224	1200	-2.0
BG08	11	19	468	163	385	1016	1230	17.4
BG10	2	19	1525	738	584	2847	2718	-4.7
BG11	4	18	225	87	171	483	453	-6.6
BG13	8	16	1838	326	506	2670	2435	-9.7
BG14	3	21	451	72	338	861	1008	14.6
BG15	2	21	1701	820	280	2801	2697	-3.9
BH01	10	20	805	252	385	1442	1540	6.4
BH03	3	20	329	78	362	769	1004	23.4

The average percentage error of Magics RP for the platforms, which have been investigated, is 3.8 %. This experiment shows that Magics RP has a small average percentage error for its build time estimation. Thus, Magics RP can be used as a benchmark to verify time estimates calculated from the 2D sketches.

CHAPTER 8

DEVELOPMENT OF A BUILD TIME ESTIMATOR

The actual build time depends not only on the laser power, layer thickness, or over cure values, but is also strongly influenced by part size and geometry, as well as re-coating parameters and the build orientation [14].

8.1 FORMULAE AND OTHER INFLUENCING FACTORS

Three key assumptions were made to derive the formulas used. The three assumptions are:

- The photopolymer resin obeys the Beer-Lambert law of absorption.
- The laser irradiance is Gaussian.
- The resin transitions from the liquid phase to the solid phase at the so-called "gel-point".

8.1.1 Beer-Lambert Law

This law describes the intensity of the light transmitted by an absorbing material. Thus:

$$A = \log (1/T) \tag{8.1}$$

Where:

$T = I / I_0$

A = absorbance

T = transmittance

I_0 = intensity of the light beam with no sample present

I = intensity of the light beam after passing through the sample

The absorbence is directly proportional to the length of the light path through the sample and to the concentration of the absorbing material. Beer-Lambert's law is obeyed strictly only when monochromatic radiation – light of single wavelength – is used. Lasers produce monochromatic radiation at only one wavelength [17].

8.2 FOCUSSED LASER SPOT (Wo)

This is calculated by using equation 3.2 where:

$$M^2 = \pi \times W \times \Phi / (2 \times \lambda)$$

Where:

W = 0.795 mm ($1/e^2$ radius at the exit of the laser head)

Φ = 0.72 mrad (full angle divergence of the laser beam) [15]

λ . = the wavelength of the laser

Thus from equation 3.2:

$$M^2 = \pi \times 0.795 \times 0.72 \times 10^{-3} / (2 \times 325 \times 10^{-6})$$

$$= 2.767$$

For calculating the focused spot radius:

$$Wo = 2 \times \lambda \times M^2 \times L / (\pi \times Dl) \qquad (8.2)$$

$$= 2 \times 325 \times 10^{-9} \times 2.767 \times 0.628 / (4.1 \times 10^{-3} \times \pi)$$

$$= 8.768 \times 10^{-5} \text{ m}$$

$$= 0.1 \text{ mm}$$

Where:

L = the distance from the galvanometer mirror limiting aperture

M = mode purity parameter

Dl = 2W, the diameter of the galvanometer mirror limiting aperture

λ = wavelength of the laser [13]

8.3 LASER SCAN VELOCITY

To determine the scan velocity of the laser on a specific resin surface, equation 8.3 is used:

$$Vs = (2/\pi)^{0.5} * \{Pl/(Wo * Ec)\} * \exp(-Cd/Dp) \quad (8.3)$$

Where: Vs = laser scanning velocity at the liquid photopolymer surface (cm/sec)

Pl = laser power (mW)

Wo = Gaussian half-width of the laser spot on the resin surface (cm)

Ec = critical exposure (mJ/cm^2)

Cd = maximum cure depth (cm)

Dp = Penetration depth (cm)

The following important conclusions can be made from equation 8.3:

- The achievable laser scan velocity is directly proportional to the laser power. Thus the higher the laser power the faster the laser scan velocity for a given resin, laser spot size and cure depth.

  $Vs \propto Pl$ (Wo, Ec, Cd, Dp constant)

- The achievable laser scan velocity is inversely proportional to the laser spot size. Thus, increasing the spot size, demands a decrease in laser scan velocity for a given laser power, resin and cure depth.

  $Vs \propto 1/Wo$ (Pl, Ec, Cd, Dp constant)

- The achievable laser scan velocity is inversely proportional to the critical exposure. Thus, if increased critical exposure is needed, the laser scan velocity has to be decreased (a different Ec value implies a different resin).

  $Vs \propto 1/Ec$ (Pl, Wo, Cd, Dp constant)

- The laser scan velocity decreases in an exponential manner with an increase in the ratio Cd/Dp. Doubling Cd requires slowing down the laser scan velocity by a factor of 2.718, resulting in a drawing speed only 37 % of the original value. For a given resin this is the reason why increased cure depths draw much more slowly than shallow cure depths [12].

8.3.1 Drawing Time per Unit Area

In Stereolithography, most of the laser scan time is spent hatching, to solidify the regions of parts interior to their borders. Consider a rectangle of length L, in the scan direction, and width W, perpendicular to the scan direction. Figure 8.1 shows such a rectangle of which the area is simply $A = L \times W$.

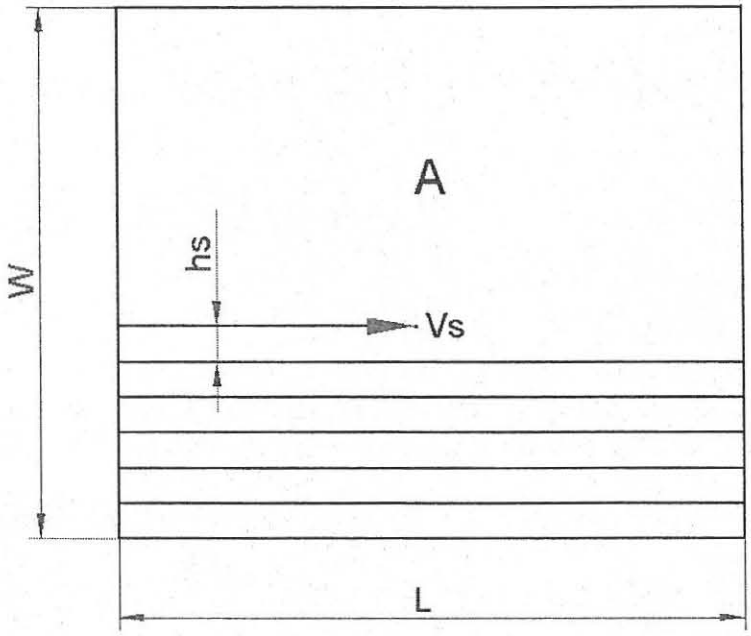

Figure 8.1 Hypothetical scanning rectangle

The time required drawing a single string of length L is:

$$t = L / Vs \tag{8.4}$$

Where: Vs = velocity in scan direction

The number of such vectors in the specific shape is given by:

$$N = W / hs \tag{8.5}$$

Where: hs = hatch spacing.

Thus, the laser drawing time, td, is given by:

$$td = N \times t \tag{8.6}$$

$$= (W / hs) \times (L / Vs)$$

$$= A / (hs \times Vs)$$

From eq. 8.3: $$td = A / (hs \times [(2/\pi)^{0.5} * \{Pl/(Wo * Ec)\} * \exp(-Cd/Dp)]) \tag{8.7}$$

The following important conclusions can be drawn from equation 8.7:

- The drawing time per unit cross-section is directly proportional to the resin critical exposure, Ec. Resins with higher values of Ec will draw more slowly.

  td α Ec (Wo, hs, Pl, Cd and Dp constant)

- The drawing time per unit area is inversely proportional to the laser power, Pl. Higher power lasers will reduce drawing time for a particular resin.

  td α 1/Pl (Wo, hs, Ec, Cd and Dp constant)

- The drawing time per unit area increases exponentially with the increased cure depth to penetration depth ratio. For a given resin with a specific value of Dp, increased cure depths draw much more slowly.

8.3.2 Re-coating Time per Layer

During the build process of a part on the SLA machine, there are intervals when the laser is not scanning a cross-sectional area of a part or support. This non-scan time is also known as the re-coating time for a part or a support. This re-coating time must also be considered when time estimation is performed, because it also has an influence on the total building time. For instance, if a part has a small cross-section, then the re-coating time is more than the scan time for that specific layer of the part. Thus, in some instances the re-coating time can be more than the actual scanning time of a part.

- ***Part Re-coating Time***

During the actual building of test pieces on the SLA machine, it was timed how long it took to scan a single layer of the part. The time is multiplied by the number of layers in the *z*-direction, to obtain the total scan time for the part. The total build time for the supports of the specific part, as well as the total build time (part and its support) was also measured. The build time for the support is subtracted from the total build time to obtain the build time for the part. The difference between the build time and the scan time of the part will be the total non-scan time for the part. Dividing this value by the number of layers provides the non-scan time per layer. Thus:

(scan time per layer) x (number of layers) = total scan time (8.8)

(total build time) – (build time for support) = build time for part (8.9)

(build time for part) – (scan time for part) = total non-scan time (8.10)

(total non-scan time) ÷ (number of layers) = non-scan time per layer (8.11)

This procedure was repeated for all the test pieces of different geometries. The values ranged from 59.28 seconds to 59.46 seconds per layer. An average value of 59.36 seconds was calculated per layer for a part building style.

The re-coating parameters for an ACES part building style are summarised in Table 8.1.

Table 8.1 ACES build style parameters for re-coating of parts (SL5170AP)

Operation	Value
Z-level wait	25 sec
Pre-dip delay	10 sec
Post-dip delay	1 sec
Z-dip distance	6.35 mm

These are the only parameters that the operator can manipulate and are not the only operations that occur during the re-coating process. Other operations include the movement of the sweeper blade across the vat and the waiting time for the resin to settle after the specific operations.

During the building of the test pieces the time taken for the sweeper blade to move over the surface of the vat was measured several times and an average value was calculated. The average value obtained for all the test pieces was 4.74 seconds. The rest of the time (18.62 seconds) is when the machine waits for the resin to settle after each operation as well as the time it takes to analyse the laser beam before it starts to scan the next layer.

- ***Support Re-coating Time***

The re-coating parameters of the ACES build style for building supports are summarised in Table 8.2.

Table 8.2 ACES build style parameters for re-coating of supports (SL5170AS)

Operation	Value
Z-level wait	15 sec
Pre-dip delay	10 sec
Post-dip delay	1 sec
Z-dip distance	6.35 mm

The only difference between the part re-coating time and that for a support is that during the support building process the sweeper blade does not move across the vat after a layer has been completed. The sweeper blade only starts its movement when the part is being built. Thus, for calculating the support re-coating time, the same time as that of the part is used except that the time for the sweeper blade movement and the time difference in the machine parameters is being subtracted. The total time for the re-coating process is:

59.36 – 4.74 (time of sweeper blade movement) = 54.62 sec

54.62 – 10 (time difference in machine parameters) = 44.62 sec

Thus the re-coating time per layer for a support is 44.62 sec.

8.3.3 Volumetric Calculation of a Shape

To calculate the volume of a shape from a 2-Dimensional sketch that must be built on the SLA machine, formulas for basic volumetric shapes are used. Different volumetric shapes are put together to build up a shape similar to that of the 2-Dimensional sketch. The basic volumetric shapes and formulas are summarised in Table 8.3 [11].

Table 8.3 Basic shapes and their volumetric formulas

Shape	Formula
Cube	B^3
Rectangular prism	H x b x th
Triangular prism	½ x b x h x th
Cylinder	$\pi \times r^2 \times l$
Sphere	$4/3 \times \pi \times r^3$
Semi-sphere	$½ \times 4/3 \times \pi \times r^3$
Cone	$1/3 \times \pi \times r^2 \times h$

Where:

h = height

b = width

th = thickness

r = radius

l = length

These formulas are used to calculate the cross-sectional area of the shape per layer. This cross-sectional layer is then used in TK Solver™ to calculate the total build time for the shape.

8.3.4 Build Time Calculation of Support Files

Because support structures consist only of single lines joined together to form a certain support structure (e.g. block, line etc.), the drawing time for the supports is calculated in the following way:

$$t = S/V \tag{8.12}$$

Where:

t = Scan time per layer of the support structure

S = Linear distance which the laser must scan per layer of support structure

V = Specific velocity that the laser beam moves over the resin for a given laser power (in mW) value.

The scan time per layer is then multiplied by the number of layers in the *z*-direction of the specific support file to give the total scan time for the support structure. Table 8.4 represents the scan distance per layer for a certain support structure.

Table 8.4 Scan distance for a certain block support structure

Area to support (mm^2)	Scan distance per layer (cm)
100 x 100	278.32
90 x 90	232.44
80 x 80	190.56
70 x 70	152.68
60 x 60	106.92
50 x 50	79.04
40 x 40	63.04
30 x 30	41.16
20 x 20	19.4
10 x 10	5.64

8.4 BUILD TIME ESTIMATOR

A few important factors must always be kept in mind when orientating a part to be built on a Rapid Prototyping machine. These factors have a big influence on the desired effect/shape of the prototype that has to be built. These factors are as follows:

8.4.1 Choosing a Preferred Direction of Build

The selection of the build orientation is the crucial factor that affects the quality of the surface finish. The preferred build orientation determines other important aspects, such as the build time and the amount of support structure needed. For choosing an orientation, the following factors should therefore be kept in mind.

- ***Surface Finish***

The importance of surface finish depends on the specific use of a part. Surface finish is most important when these prototypes are used as masters for various casting techniques. In this case, an imperfection on the part's surface is transferred to the mould and then to all the downstream parts.

It is important to orient the part in such a way as to minimise the stair stepping effect, as shown in Figure 8.2, which all current Rapid Prototyping systems have. The undesirable stair stepping feature is most often apparent on sloping or curved surfaces. Although it may be impossible to eliminate stair stepping, choosing a preferred orientation allows the user to select the most important surfaces so that these will have the best finish.

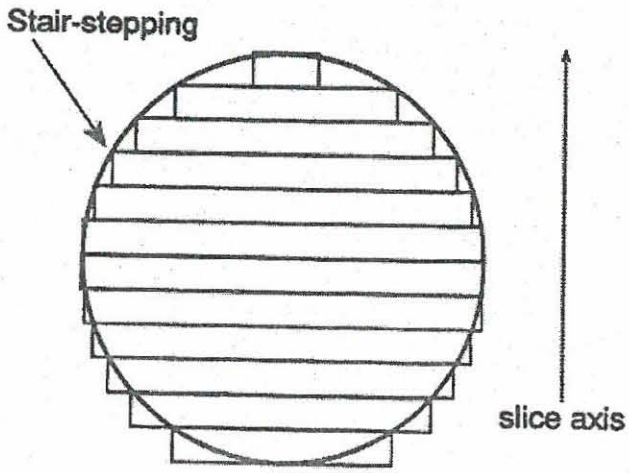

Figure 8.2 Stair stepping effect of Rapid Prototyping systems

- ***Build Time***

  The time required to build a part is affected by the orientation of the part in the vat. Part geometries with a large value in the *z*-axis could take longer to built. Because of the larger *z*-value, more layers need to be built to complete the part. This results in more time spent during the re-coating process, thus increasing the built time. Depending upon the part geometry, parts with a large *z*-value could also be time consuming to slice. This will increase the time before the part can be built on a Stereolithography machine. A part with a large *z*-value could also need more support structures to support it inside the vat, resulting in an increase in the build time. This could add the post processing time of the part (e.g. removal of the support structures). Thus, if surface finish is unimportant the *z*-height should be kept as small as possible.

- ***Support Structure***

  Overhanging features need a support structure to prevent them from sagging. Support is one of the most important factors when deciding how to orient a part since its size directly affects the build time. If the support structure is too large, the part needs time consuming finishing to remove all the support by hand.

8.4.2 Definition of Orientating Rules for Surface Finish

In most parts the requirements on the surface finish of the entire part are not as critical as the surface finish of a few specific geometric features. A preferred orientation can often be selected by mainly considering the following geometric features. The orientation of these geometric features can be:

- Parallel to the x - y plane (0 or 180°)
- Perpendicular to the x - y plane (90 or 270°)
- Angle (everything else)

- ***Description of Crucial Geometric Features and Definition of their Feature Axis***

  Figure 8.3 shows the three basic geometric features. Their feature axes are defined as follows:

  - A round surface is part of a surface of revolution and can be the edge of the part such as a fillet or a major area. Therefore intersection points of the defined radii create a symmetric line, which is the feature axis of this geometric feature. This feature axis should be preferably oriented in the z-direction.
  - A feature plane is the most often used geometric feature. The feature axis of a plane is the normal to the plane. The normal of the plane can be orientated either parallel or perpendicular to the z-direction.
  - Overhangs are important because they need a support structure to prevent them from sagging under their own weight. Also the support structure has to be removed after the building process, which influences the quality of the finished surface. The feature axis of an overhang is directed away from the connecting part. The goal is to minimise the extent of support structure. Therefore the best orientation is with the feature axis in the z-direction, if the overhang can be supported on one of its sides [8].

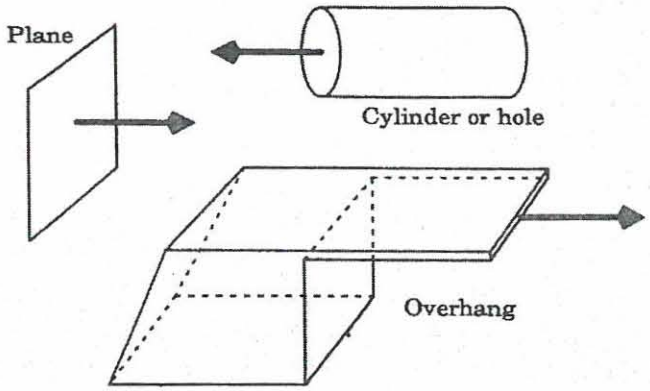

Figure 8.3 Feature axis of various geometrical entities

8.5 WORKFLOW FOR THE BUILD TIME ESTIMATOR PROCESS

If the build time must be calculated from a 2D sketch such as Figure 8.4, the process will be as follows:

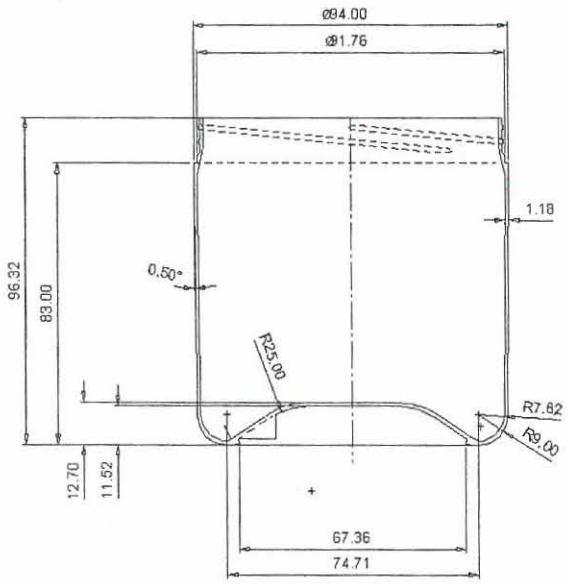

Figure 8.4. Two-dimensional sketch of a product to be built

- Replace features from the 2D sketch with volumetric shapes that represent the same feature as in the 2D sketch, such as cylinders, squares etc. Figure 8.5 shows the first step in the replacement process. By subtracting the cylinders from each other, the outer shell is created.

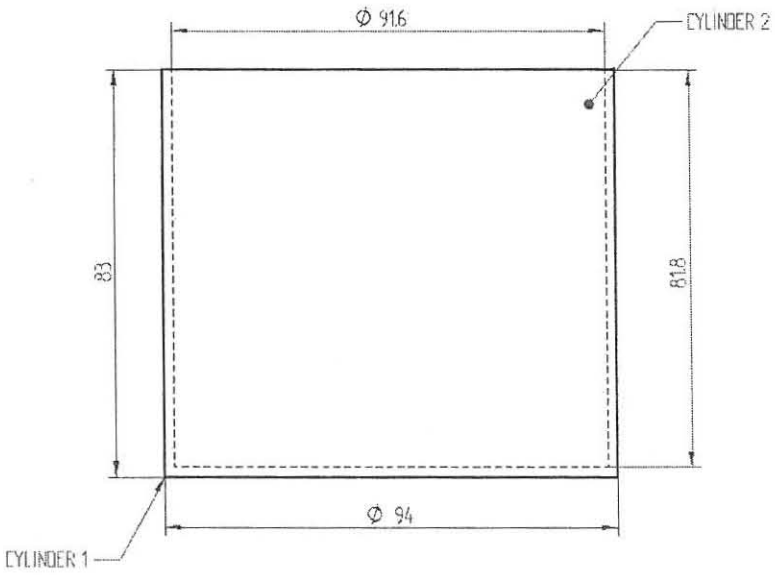

Figure 8.5 First replacements of volumetric shapes from the dimensions of the 2D sketch

- The neck of the product is created by also subtracting two cylinders from each other. Figure 8.6 shows how the neck of the product is created.

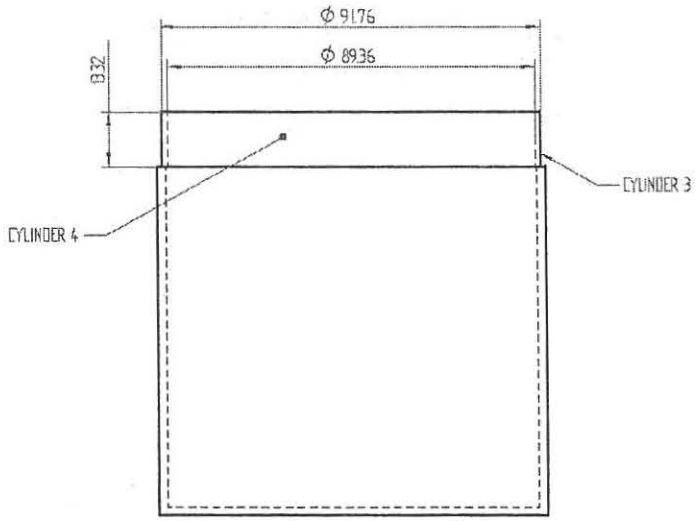

Figure 8.6 Creation of the neck feature

- Inserting two cones creates the taper at the bottom of the product. To obtain the specified wall thickness, cone 2 is subtracted from cone 1. The subtraction of the top part of each individual cone creates the shortened cone. Figure 8.7 illustrates this step.

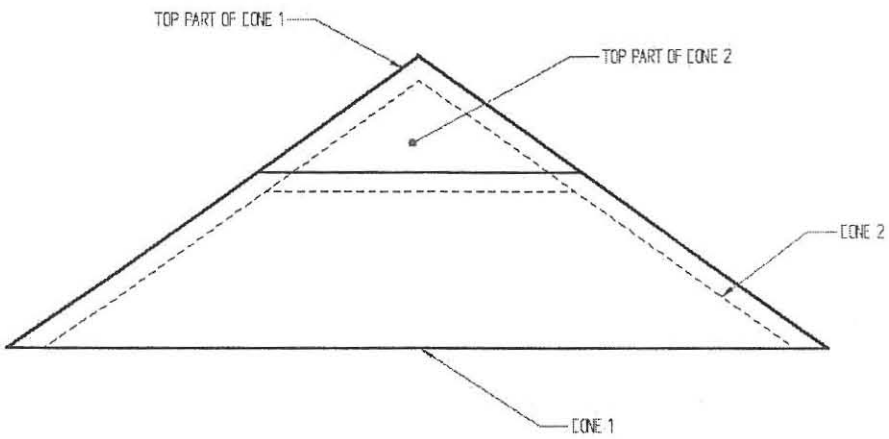

Figure 8.7 Creation of the taper at the bottom of the product

- The closest approximation of volumetric shapes to that of the 2D sketch will result in more accurate build time estimations for the given model. Fig. 8.8 represents the final approximate volumetric model for the 2D sketch.

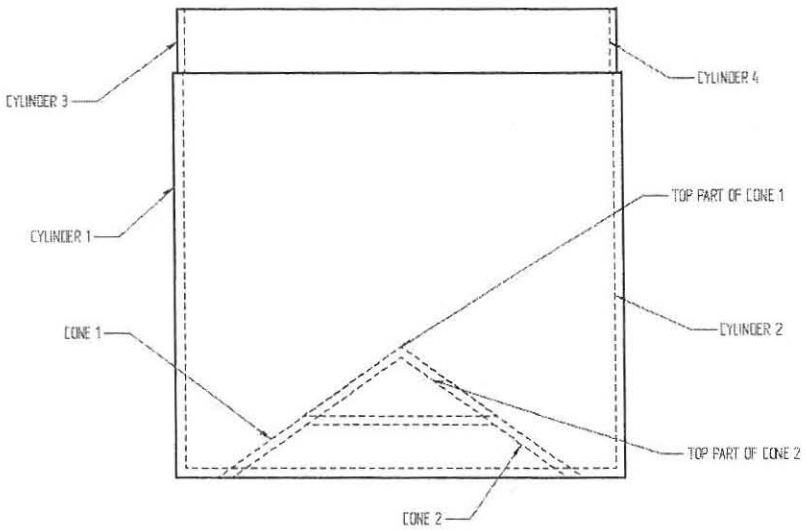

Figure 8.8 Final approximate volumetric model of the 2D sketch

- Calculate the average cross-section of each of the shapes. Models in TK Solver have been written to calculate the average cross-sections of certain volumetric shapes. These shapes are as follows: square, rectangular prism, cylinder, sphere etc (see Appendix A).
- To achieve a hollow feature, two shapes can be subtracted from each other. The average cross-sectional area of the model will be calculated as follows:

The cross-sectional area of cylinder 2 will be subtracted from that of cylinder 1;

The cross-sectional area of cylinder 4 will be subtracted from that of cylinder 3;

The top part of cone 1 will be subtracted from cone 1;

The top part of cone 2 will be subtracted from cone 2;

Finally cone 2 will be subtracted from cone 1.

All the relevant formulas and data are programmed into TK Solver to generate a mathematical calculation process for calculating the total building time of a volumetric shape (see Appendix A) [9]; [18]; [28].

The build time for each volumetric shape is calculated with the TK Solver models. The build times of all the volumetric shapes are added together to obtain the total build time for the part.

If the platform has more than one part, the same procedure as above is applied to each individual part to calculate its build time. The build time for the platform will be the sum of the build times for all the parts. The re-coating time for the platform is calculated by using the layers from a part, which has the largest dimension in the *z*-direction.

TK Solver needs certain input values from the user to calculate the total build time. These values consist of part geometry information, resin dependent values as well as build style and laser parameters. Resin dependant values such, as Ec, Dp and Cd will stay constant if the same resin type is used every time. The build style parameter (hs) is a constant value. The value of the laser beam radius (Wo), will stay constant for a specified laser. The laser power value (Pl) will vary with each build. The user must supply this value before build time estimation is conducted. Part related information such as the average cross-sectional area and height must be supplied.

Values that the user can obtain as output values from TK Solver is the scan speed of the laser (Vs), the drawing time per layer (td), the total number of layers in the *z*-direction (z) and, most importantly, the total scan time of the part (TOT_t). Figure 8.9 shows the basic screen layout of TK solver.

Variables

Sta	Input	Name	Output	Unit	Comment
		Vs	31.722849	cm/sec	Scan Speed per centimeter
	.01	hs		cm	Hatch spacing
	35	Pl		mW	Laser Power
	.01	Wo		cm	Raduis of laser beam
	13.5	Ec		mJ/cm^2	Critical exposure
	9	Cd		cm	Cure depth
	4.8	Dp		cm	Penetration depth
		td	11.1150168	sec	Scan time per layer (single pass)
	3.526	A		cm^2	Cross sectional area
	16.5	H		mm	Height of part
		z	110	mm	Total layers in z direction
		re_coat	6529.6	sec	
		TOT_tp	2445.3037	sec	Total scan time
		TOT_t	8974.9037	sec	Total build time for part

Rules

St	Rule
	Vs = (2/pi())^0.5 *(Pl /(Wo * Ec))* (EXP (-Cd/Dp))
	td = A /(hs * Vs)
	TOT_tp =(td*2) * z
	TOT_t =(td*2+59.36) * z

Figure 8.9 Basic screen layout of TK Solver

- Because a support structure consists of a stack of single cured lines, its building time is calculated by t = S/V. The block type support structure is used for supports. If the size of the support needed has been decided on, the total length to be scanned is calculated. These, as well as the number of layers in the z direction and the laser power, are entered in the specified fields of the TK Solver model: support.tkw. This TK Solver model will calculate the build time of the support structure for a specified height.
- For the total build time of the platform, the times of the parts and the support structure are added together.

CHAPTER 9

TESTING OF BUILD TIME ESTIMATOR

9.1 SUPPORT STRUCTURES

The block support structure was used during the study because it is the most frequently used support structure. Support structure files with different dimensions were tested and the actual build time was compared to the estimated build times of Magics RP and the 2D-build time estimator.

9.1.1 Support file: s_100sup.stl

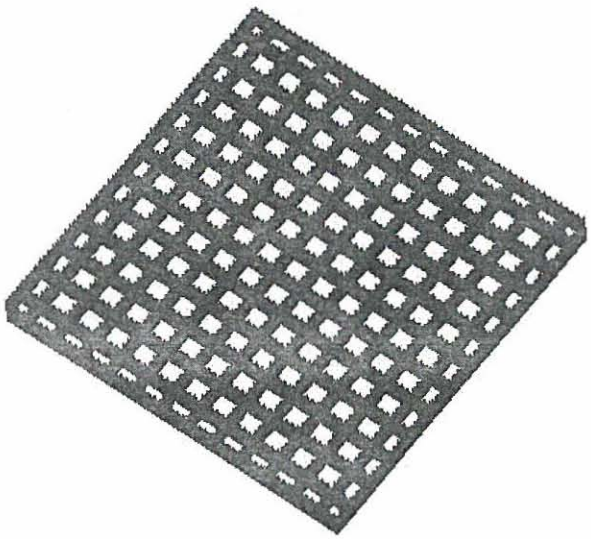

Figure 9.1 Illustration of the support file s_100sup.stl

Figure 9.1 illustrates the support file s_100sup.stl, and the properties of the file are as follows:

- Laser power: 23 mW
- Dimensions: Height: 10.25 mm
  Length: 99.4 mm
  Width: 99.4 mm
- Distance to scan = 278.32 cm
- Scan speed = 38.9 cm/s

The results of the actual build time and the estimated build times for the support file are summarised in Table 9.1.

Table 9.1 Build time results of support file s_100sup.stl

	Actual time (sec)	**Magics RP's time (sec)**	**Magics RP's percentage error**	**2D Estimator's time (sec)**	**2D Estimator's percentage error**
Scan time		1860		912	
Re-coating time		3360		3049	
Total	4260	5220	22.5 %	3961	-7 %

9.1.2 Support file: s_90sup.stl

Figure 9.2 Illustration of the support file s_90sup.stl

Figure 9.2 illustrates the support file s_90sup.stl, and the properties of the file are as follows:

- Laser power: 23 mW
- Dimensions: Height: 10.25 mm
  Length: 89.4 mm
  Width: 89.4 mm
- Distance to scan = 232.44 cm
- Scan speed = 38.9 cm/s

The results of the actual build time and the estimated build times for the support file are summarised in Table 9.2.

Table 9.2 Build time results of support file s_90sup.stl

	Actual time (sec)	**Magics RP's time (sec)**	**Magics RP's percentage error**	**2D Estimator's time (sec)**	**2D Estimator's percentage error**
Scan time		1500		762	
Re-coating time		3360		3049	
Total	3480	4860	39.7 %	3811	9.5 %

9.1.3 Support file: s_80sup.stl

Figure 9.3 Illustration of the support file s_80sup.stl

Figure 9.3 illustrates the support file s_80sup.stl, and the properties of the file are as follows:

- Laser power: 22 mW
- Dimensions: Height: 10.25 mm
  Length: 79.4 mm
  Width: 79.4 mm
- Distance to scan = 190.56 cm
- Scan speed = 37.3 cm/s

The results of the actual build time and the estimated build times for the support file are summarised in Table 9.3.

Table 9.3 Build time results of support file s_80sup.stl

	Actual time (sec)	**Magics RP's time (sec)**	**Magics RP's percentage error**	**2D Estimator's time (sec)**	**2D Estimator's percentage error**
Scan time		1320		653	
Re-coating time		3360		3049	
Total	3600	4680	30 %	3702	2.8 %

9.1.4 Support file: s_70sup.stl

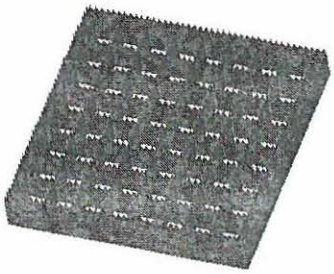

Figure 9.4 Illustration of the support file s_70sup.stl

Figure 9.4 illustrates the support file s_70sup.stl, and the properties of the file are as follows:

- Laser power: 22 mW
- Dimensions: Height: 10.25 mm
  Length: 69.4 mm
  Width: 69.4 mm
- Distance to scan = 152.68 cm
- Scan speed = 37.3 cm/s

The results of the actual build time and the estimated build times for the support file are summarised in Table 9.4.

Table 9.4 Build time results of support file s_70sup.stl

	Actual time (sec)	**Magics RP's time (sec)**	**Magics RP's percentage error**	**2D Estimator's time (sec)**	**2D Estimator's percentage error**
Scan time		1020		523	
Re-coating time		3360		3049	
Total	3540	4380	23.73 %	3572	0.9 %

9.1.5 Support file: s_60sup.stl

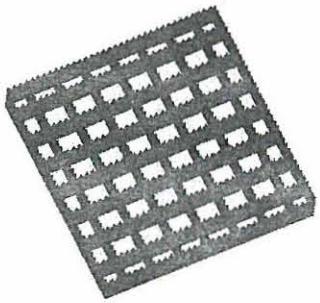

Figure 9.5 Illustration of the support file s_60sup.stl

Figure 9.5 illustrates the support file s_60sup.stl, and the properties of the file are as follows:

- Laser power: 23 mW
- Dimensions: Height: 10.25 mm
  Length: 59.4 mm
  Width: 59.4 mm
- Distance to scan = 106.92 cm
- Scan speed = 38.9 cm/s

The results of the actual build time and the estimated build times for the support file are summarised in Table 9.5.

Table 9.5 Build time results of support file s_60sup.stl

	Actual time (sec)	**Magics RP's time (sec)**	**Magics RP's percentage error**	**2D Estimator's time (sec)**	**2D Estimator's percentage error**
Scan time		660		351	
Re-coating time		3360		3049	
Total	3180	4020	26.4 %	3400	6.9 %

9.1.6 Support file: s_50sup.stl

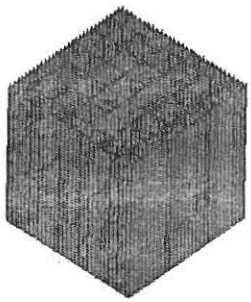

Figure 9.6 Illustration of the support file s_50sup.stl

Figure 9.6 illustrates the support file s_50sup.stl, and the properties of the file are as follows:

- Laser power: 22 mW
- Dimensions: Height: 50.25 mm
  Length: 49.4 mm
  Width: 49.4 mm
- Distance to scan = 79.04 cm
- Scan speed = 37.3 cm/s

The results of the actual build time and the estimated build times for the support file are summarised in Table 9.6.

Table 9.6 Build time results of support file s_50sup.stl

	Actual time (sec)	**Magics RP's time (sec)**	**Magics RP's percentage error**	**2D Estimator's time (sec)**	**2D Estimator's percentage error**
Scan time		2940		1328	
Re-coating time		10800		14948	
Total	18600	13740	-26.12 %	16276	-12.5 %

9.2 PART BUILDING

Part building files with different geometrical shapes such as a cylinder, rectangular prism and a cone, were tested. The actual build time of the test file is compared to the estimated build times of Magics RP and the 2D-build time estimator. The test was also repeated with the same geometrical shapes, but with different laser power values.

9.2.1 Part file block.stl with a laser power value of 27 mW

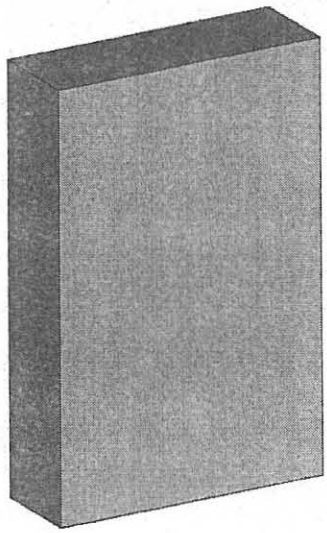

Figure 9.7 Illustration of the part file block.stl

Figure 9.7 illustrates the part file block.stl, and the properties of the file is as follows:

- Laser power: 27 mW
- Dimensions: Height: 45 mm

  Length: 30 mm

  Width: 10 mm

- Volume (part): 13500 mm^3
- Cross-sectional area: 300 mm^2

The results of the actual build time and the estimated build times for the part file are summarised in Table 9.7.

Table 9.7 Build time results of the part file block.stl with Pl = 27 mW

Actual time (sec)	**Magics RP's time (sec)**	**Magics RP's percentage error**	**2D Estimator's time (sec)**	**2D Estimator's percentage error**	**2D Estimator's percentage error from Magics' value**
23280	23280	0.0 %	24817	6.6 %	6.6 %

9.2.2 Part file offset_block.stl with a laser power value of 26 mW

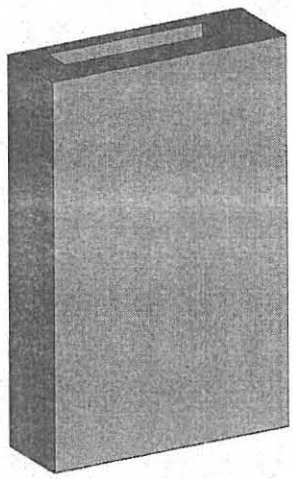

Figure 9.8 Illustration of the part file offset_block.stl

Figure 9.8 illustrates the part file offset_block.stl, and the properties of the file is as follows:

- Laser power: 26 mW
- Dimensions: Outside: Height: 45 mm

  Length: 30 mm

  Width: 10 mm

  Inside: Height: 45 mm

  Length: 20 mm

  Width: 4 mm
- Volume (part): 9900 mm^3
- Cross-sectional area: 220 mm^2

The results of the actual build time and the estimated build times for the part file are summarised in Table 9.8.

Table 9.8 Build time results of the part file offset_block.stl with Pl = 26 mW

Actual time (sec)	**Magics RP's time (sec)**	**Magics RP's percentage error**	**2D Estimator's time (sec)**	**2D Estimator's percentage error**	**2D Estimator's percentage error from Magics' value**
22740	22620	- 0.53 %	23881	5.01 %	5.6 %

9.2.3 Part file cylinder.stl with a laser power value of 26 mW

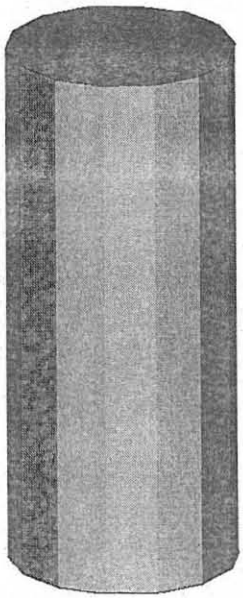

Figure 9.9 Illustration of the part file cylinder.stl

Figure 9.9 illustrates the part file cylinder.stl, and the properties of the file is as follows:

- Laser power: 26 mW
- Dimensions: Base diameter: 20 mm

  Height: 45 mm
- Volume (part): 14137 mm^3
- Cross-sectional area: 314 mm^2

The results of the actual build time and the estimated build times for the part file are summarised in Table 9.9.

Table 9.9 Build time results of the part file cylinder.stl with Pl = 26 mW

Actual time (sec)	**Magics RP's time (sec)**	**Magics RP's percentage error**	**2D Estimator's time (sec)**	**2D Estimator's percentage error**	**2D Estimator's percentage error from Magics' value**
23280	23400	0.52 %	25170	8.12 %	7.56 %

9.2.4 Part file cone.stl with a laser power value of 27 mW

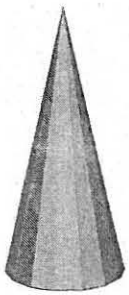

Figure 9.10 Illustration of the part file cone.stl

Figure 9.10 illustrates the part file cone.stl, and the properties of the file is as follows:

- Laser power: 27 mW
- Dimensions: Height: 45 mm

  Base diameter: 20 mm
- Volume (part): 4712 mm^3
- Average cross-sectional area: 108.58 mm^2

The results of the actual build time and the estimated build times for the part file are summarised in Table 9.10.

Table 9.10 Build time results of the part file cone.stl with Pl = 27 mW

Actual time (sec)	**Magics RP's time (sec)**	**Magics RP's percentage error**	**2D Estimator's time (sec)**	**2D Estimator's percentage error**	**2D Estimator's percentage error from Magics' value**
20820	21000	0.86 %	22314	7.16 %	6.26 %

9.2.5 Part file: shrinkage.stl

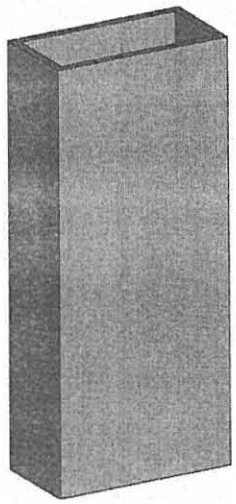

Figure 9.11 Illustration of the part file shrinkage.stl

Figure 9.11 illustrates the part file shrinkage.stl, and the properties of the file are as follows:

- Laser power: 29 mW
- Dimensions: Outer: Height: 135 mm
  Length: 60 mm
  Width: 30 mm
  Inner: Height: 135 mm
  Length: 54 mm
  Width: 24 mm
- Volume (part): 68040 mm^3
- Cross-sectional area: 504 mm^2

The results of the actual build time and the estimated build times for the part file are summarised in Table 9.11.

Table 9.11 Build time results of part file shrinkage.stl with Pl = 29 mW

Actual time (sec)	**Magics RP's time (sec)**	**Magics RP's percentage error**	**2D Estimator's time (sec)**	**2D Estimator's percentage error**	**2D Estimator's percentage error from Magics' value**
72720	73620	1.23 %	75003	3.14 %	1.88 %

9.2.6 Part file block.stl with a laser power value of 49 mW

This part file is the same as the one used in section 9.2.1 (p. 98), but a different laser power value of 49 mW was used during this experiment. The properties of the part file are as follows:

- Laser power: 49 mW
- Dimensions: Height: 45 mm
  Length: 30 mm
  Width: 10 mm
- Volume (part): 13500 mm^3
- Cross-sectional area: 300 mm^2

The results of the actual build time and the estimated build times for the part file are summarised in Table 9.12

Table 9.12 Build time results of part file block.stl with Pl = 49 mW

Actual time (sec)	**Magics RP's time (sec)**	**Magics RP's percentage error**	**2D Estimator's time (sec)**	**2D Estimator's percentage error**	**2D Estimator's percentage error from Magics' value**
22740	21600	- 5.01 %	23038	1.3 %	6.66 %

9.2.7 Part file offset_block.stl with a laser power value of 47 mW

This part file is the same as the one used in section 9.2.2 (p. 100), but a different laser power value of 47 mW was used during this experiment. The properties of the part file are as follows:

- Laser power: 47 mW
- Dimensions: Outside: Height: 45 mm
  Length: 30 mm
  Width: 10 mm
  Inside: Height: 45 mm
  Length: 20 mm
  Width: 4 mm
- Volume (part): 9900 mm^3
- Cross-sectional area: 220 mm^2

The results of the actual build time and the estimated build times for the part file are summarised in Table 9.13.

Table 9.13 Build time results of part file offset_block.stl with Pl = 47 mW

Actual time (sec)	Magics RP's time (sec)	Magics RP's percentage error	2D Estimator's time (sec)	2D Estimator's percentage error	2D Estimator's percentage error from Magics' value
20640	21240	2.91 %	22529	9.15 %	6.07 %

9.2.8 Part file cylinder.stl with a laser power value of 46 mW

This part file is the same as the one used in section 9.2.3 (p. 102), but a different laser power value of 46 mW was used during this experiment. The properties of the part file are as follows:

- Laser power: 46 mW
- Dimensions: Base diameter: 20 mm
  Height: 45 mm
- Volume (part): 14137 mm^3
- Cross-sectional area: 314 mm^2

The results of the actual build time and the estimated build times for the part file are summarised in Table 9.14.

Table 9.14 Build time results of part file cylinder.stl with Pl = 46 mW

Actual time (sec)	**Magics RP's time (sec)**	**Magics RP's percentage error**	**2D Estimator's time (sec)**	**2D Estimator's percentage error**	**2D Estimator's percentage error from Magics' value**
21600	21720	0.55 %	23294	7.84 %	7.25 %

9.2.9 Part file cone.stl with a laser power value of 50 mW

This part file is the same as the one used in section 9.2.4 (p. 104), but a different laser power value of 50 mW was used during this experiment. The properties of the part file are as follows:

- Laser power: 50 mW
- Dimensions: Height: 45 mm

  Base diameter: 20 mm
- Volume (part): 4712 mm^3
- Average cross-sectional area: 108.58 mm^2

The results of the actual build time and the estimated build times for the part file are summarised in Table 9.15.

Table 9.15 Build time results of part file cone.stl with Pl = 50 mW

Actual time (sec)	**Magics RP's time (sec)**	**Magics RP's percentage error**	**2D Estimator's time (sec)**	**2D Estimator's percentage error**	**2D Estimator's percentage error from Magics' value**
19800	20340	2.73 %	21643	9.31 %	6.41 %

9.3 CASE STUDIES

Platform files with different laser power values, number of parts, resin type and part geometries were tested. Each platform also had a different *z* height value. The actual build time of the platform was compared to the estimated build times of Magics RP and the 2D-build time estimator.

9.3.1 Platform file: saam

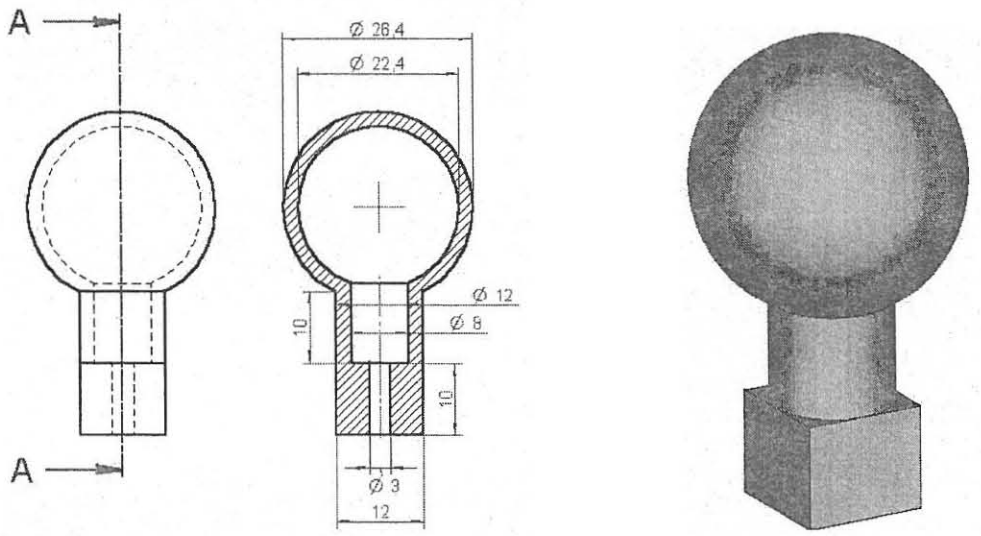

Figure 9.12 Illustration of platform saam

Figure 9.12 illustrates the platform file saam, and the properties of the platform are as follows:

- Laser power: 48 mW
- Volume (part): 5620 mm^3
- Resin used: SL 5170
- Maximum *z* height: 45 mm

The results of the actual build time and the estimated build times for the platform are summarised in Table 9.16.

Table 9.16 Build time results of platform saam

Actual time (sec)	Magics RP's time (sec)	Magics RP's percentage error	2D Estimator's time (sec)	2D Estimator's percentage error	2D Estimator's percentage error from Magics' value
23520	20640	-12.24 %	21798	-7.32 %	5.6 %

9.3.2 Platform file: cl06

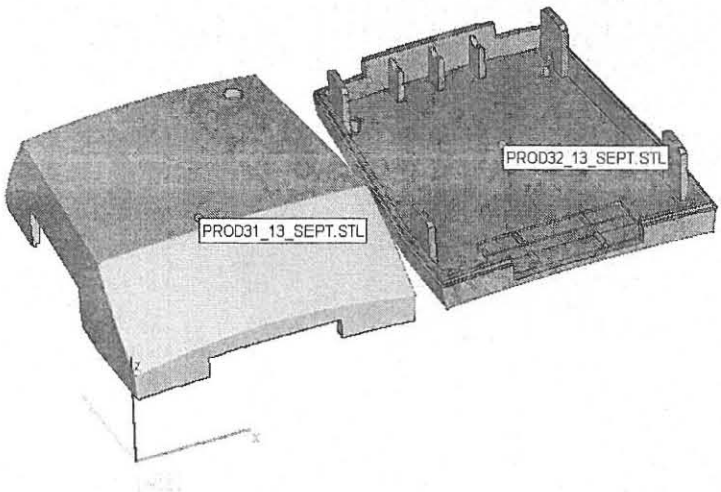

Figure 9.13 Illustration of platform cl06

Figure 9.13 illustrates the platform file cl06, and the properties of the platform are as follows:

- Part files on platform: prod31_13_sept.stl , prod32_13_sept.stl
- Laser power: 48 mW
- Total volume (parts): 10127 mm^3
- Resin used: SL 5170
- Maximum *z* height: 16.1 mm

The results of the actual build time and the estimated build times for the platform are summarised in Table 9.17.

Table 9.17 Build time results of platform cl06

Actual time (sec)	**Magics RP's time (sec)**	**Magics RP's percentage error**	**2D Estimator's time (sec)**	**2D Estimator's percentage error**	**2D Estimator's percentage error from Magics' value**
10920	10863	-0.52 %	11610	6.32 %	6.88 %

9.3.3 Platform file: df01

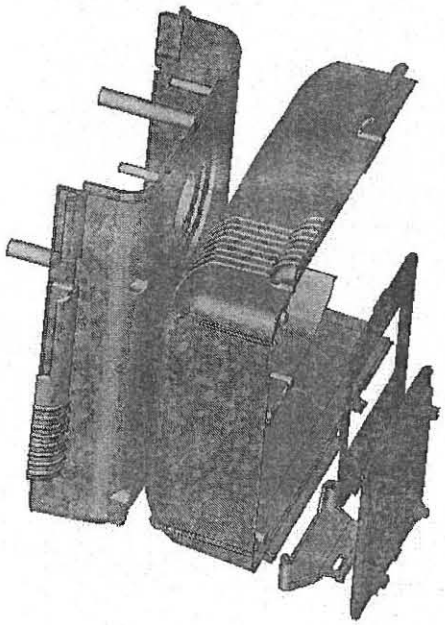

Figure 9.14 Illustration of platform df01

Figure 9.14 illustrates the platform file df01, and the properties of the platform are as follows:

- Part files on platform: free1.stl, free2.stl, free3.stl, free4.stl and free5.stl
- Laser power: 13 mW
- Total volume: 227713.5 mm^3
- Resin used: Somos 9110
- Maximum *z* height: 220 mm

The results of the actual build time and the estimated build times for the platform are summarised in Table 9.18.

Table 9.18 Build time results of platform df01

Actual time (sec)	**Magics RP's time (sec)**	**Magics RP's percentage error**	**2D Estimator's time (sec)**	**2D Estimator's percentage error**	**2D Estimator's percentage error from Magics' value**
250920	365640	45.72 %	238558	-4.93 %	- 34.76 %

9.3.4 Platform file: df02

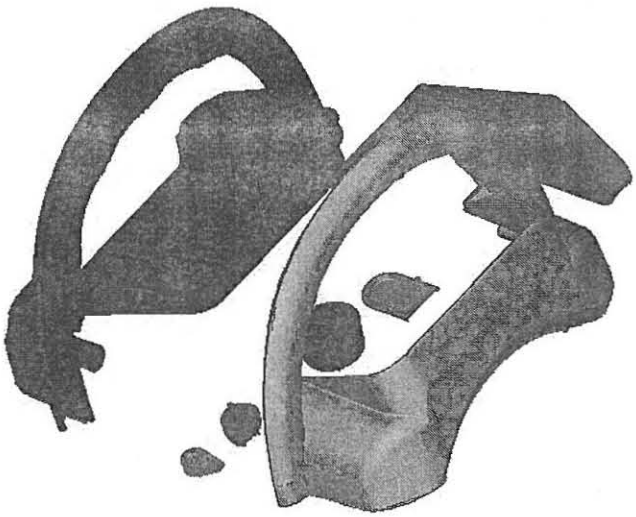

Figure 9.15 Illustration of platform df02

Figure 9.15 illustrates the platform file df02, and the properties of the platform are as follows:

- Part files on platform: free1.stl, free2.stl, free3.stl, free4.stl, free5.stl, free6.stl, free7.stl and free8.stl
- Laser power: 13 mW
- Total volume: 112531.6 mm^3
- Resin used: Somos 9110
- Maximum *z* height: 120.97 mm

The results of the actual build time and the estimated build times for the platform are summarised in Table 9.19.

Table 9.19 Build time results of platform df02

Actual time (sec)	**Magics RP's time (sec)**	**Magics RP's percentage error**	**2D Estimator's time (sec)**	**2D Estimator's percentage error**	**2D Estimator's percentage error from Magics' value**
117780	138900	17.93 %	102761	-12.75 %	- 26.02 %

9.3.5 Platform file: dg03

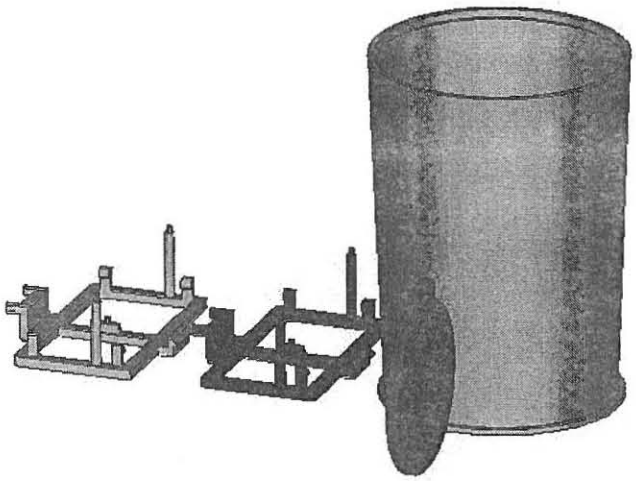

Figure 9.16 Illustration of platform dg03

Figure 9.16 illustrates the platform file dg03, and the properties of the platform are as follows:

- Part files on platform: 1psitek.stl, 2psitek.stl, grow_miss.stl, and spice.stl
- Laser power: 13 mW
- Total volume: 73258.3 mm^3
- Resin: Somos 9110
- Maximum z height: 120 mm

The results of the actual build time and the estimated build times for the platform are summarised in Table 9.20.

Table 9.20 Build time results of platform dg03

Actual time (sec)	**Magics RP's time (sec)**	**Magics RP's percentage error**	**2D Estimator's time (sec)**	**2D Estimator's percentage error**	**2D Estimator's percentage error from Magics' value**
78900	69360	- 12.09 %	75882	-3.83 %	9.4 %

9.3.6 Platform file: dg04

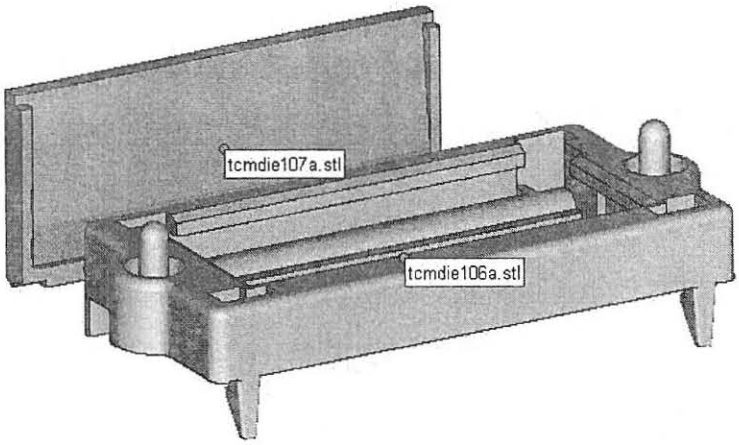

Figure 9.17 Illustration of platform dg04

Figure 9.17 illustrates the platform file dg04, and the properties of the platform are as follows:

- Part file on platform: tcndie107a.stl, tcmdie106a.stl
- Laser power: 12 mW
- Total volume (parts): 6523 mm^3
- Resin used: Somos 9110
- Maximum *z* height: 18.6 mm

The results of the actual build time and the estimated build times for the platform are summarised in Table 9.21.

Table 9.21 Build time results of platform dg04

Actual time (sec)	**Magics RP's time (sec)**	**Magics RP's percentage error**	**2D Estimator's time (sec)**	**2D Estimator's percentage error**	**2D Estimator's percentage error from Magics' value**
12300	15420	25.37 %	11411	-7.23 %	-26 %

9.3.7 Platform file: slatest1

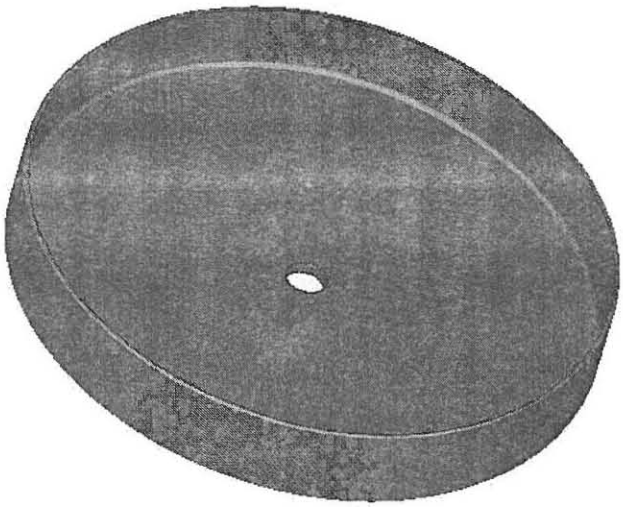

Figure 9.18 Illustration of platform slatest1

Figure 9.18 illustrates the platform file slatest1, and the properties of the platform are as follows:

- Part file on platform : slatest1.stl
- Laser power: 33 mW
- Total volume: 30015.98 mm^3
- Resin: Somos 9110
- Maximum *z* height: 16.5 mm

The results of the actual build time and the estimated build times for the platform are summarised in Table 9.22.

Table 9.22 Build time results of platform slatest1

Actual time (sec)	Magics RP's time (sec)	Magics RP's percentage error	2D Estimator's time (sec)	2D Estimator's percentage error	2D Estimator's percentage error from Magics' value
19860	20580	3.63 %	18120	-8.76 %	- 11.95 %

9.3.8 Platform file: dk09_ger

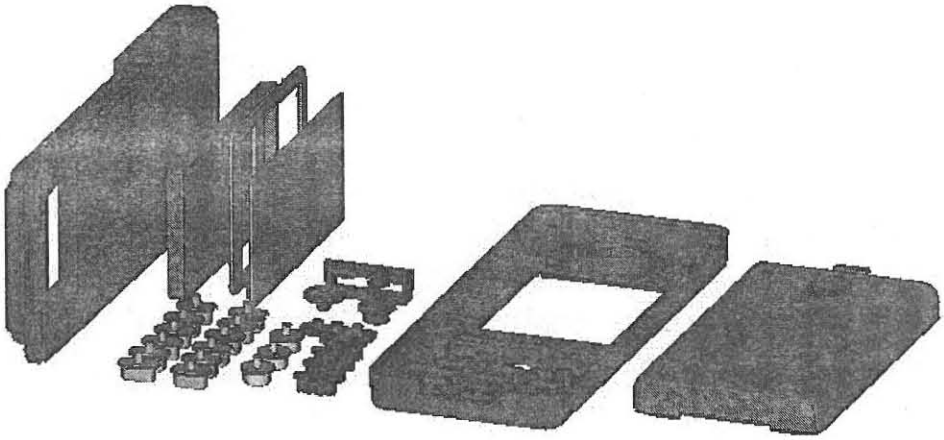

Figure 9.19 Illustration of platform dk09_ger

Figure 9.19 illustrates the platform file dk09_ger, and the properties of the platform are as follows:

- Part files on platform: flutter1.stl, flutter2.stl, flutter3.stl, flutter4.stl, flutter5.stl, flutter6.stl, flutter7.stl, and flutter8.stl.
- Laser power: 33 mW
- Total volume: 35869.98 mm^3
- Resin used: Somos 9110
- Maximum *z* height: 49 mm

The results of the actual build time and the estimated build times for the platform are summarised in Table 9.23.

Table 9.23 Build time results of platform dk09_ger

Actual time (sec)	**Magics RP's time (sec)**	**Magics RP's percentage error**	**2D Estimator's time (sec)**	**2D Estimator's percentage error**	**2D Estimator's percentage error from Magics' value**
36840	32640	-11.4 %	35946	-2.43 %	10.13 %

9.3.9 Platform file: dk12_mst

Figure 9.20 Illustration of platform dk12_mst

Figure 9.20 illustrates the platform file dk12_mst, and the properties of the platform are as follows:

- Part file on platform: p1.stl
- Laser power: 31 mW
- Total volume: 31797 mm^3
- Resin used: Somos 9110
- Maximum *z* height: 7 mm

The results of the actual build time and the estimated build times for the platform are summarised in Table 9.24.

Table 9.24 Build time results of platform dk12_mst

Actual time (sec)	**Magics RP's time (sec)**	**Magics RP's percentage error**	**2D Estimator's time (sec)**	**2D Estimator's percentage error**	**2D Estimator's percentage error from Magics' value**
19200	21420	11.56 %	17036	- 11.27 %	-20.47 %

9.3.10 Platform file: dk13_ger

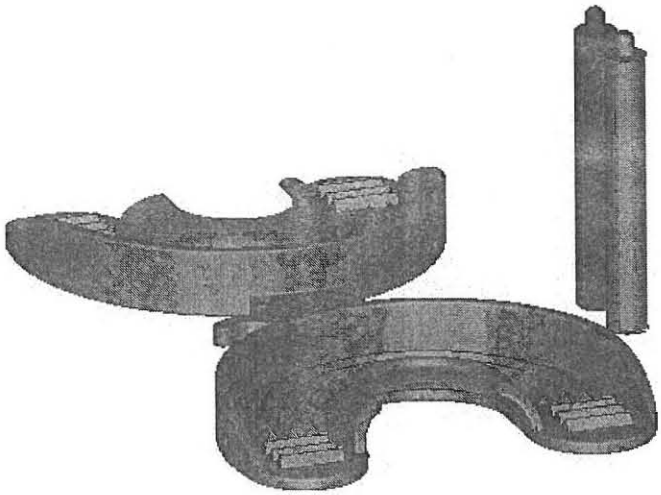

Figure 9.21 Illustration of platform dk13_ger

Figure 9.21 illustrates the platform file dk13_ger, and the properties of the platform are as follows:

- Part files on platform: strelit1.stl, strelit2.stl and gum.stl.
- Laser power: 32 mW
- Total volume: 16242.622 mm^3
- Resin used: Somos 9110
- Maximum *z* height: 44.8 mm

The results of the actual build time and the estimated build times for the platform are summarised in Table 9.25.

Table 9.25 Build time results of platform dk13_ger

Actual time (sec)	**Magics RP's time (sec)**	**Magics RP's percentage error**	**2D Estimator's time (sec)**	**2D Estimator's percentage error**	**2D Estimator's percentage error from Magics' value**
27120	20880	-23 %	28960	6.78 %	38.7 %

CHAPTER 10

BUILDING COST CALCULATION

To implement the 2D-build time estimator as a useful tool, it should be used in conjunction with other formulas for the accurate calculation of the costs involved to build a prototype.

To calculate the total cost to manufacture a part, the following formulas will be used:

Total part cost = Pre-processing cost + post processing cost + build cost + material cost + maintenance cost (10.1)

- The pre-processing operation of a part consists of placing the part on the platform. The cost is calculated as follows:

  Pre-processing cost = pre-processing time x (hourly rate of computer equipment + hourly rate of personnel) (10.2)

- In the post processing operation the part must be broken off from the platform and the support structure must be broken off the part, before it can be cleaned and placed into the post curing apparatus.

  Post processing cost = post processing time x hourly rate of personnel (10.3)

- Build cost = build time (calculated by the build time estimator) x hourly rate of the prototyping equipment (10.4)

- Material cost of part = cost of resin used + cost of consumables used (10.5)

- Maintenance costs include the costs of the maintenance of the prototyping system, as well as the cost of upgrading the software (Magics RP). The cost of replacing the laser is also included under the maintenance cost.

Finally, the price to build a prototype consists of the total part cost + the profit.

CHAPTER 11

ANALYSIS AND DISCUSSION OF RESULTS

11.1 BUILD TIME RESULTS

The following conclusions can be made from the data obtained during the growing of test pieces for support structures, part files and case studies:

11.1.1 Support Structures

The time estimation results of the 2D-build time estimator varies from accurate (0.9%) to inaccurate results between –12.5% and 9.5%. The average percentage error of the results is 0.1%. If the benchmark's (Magics RP) results are analysed, a similar phenomenon is observed. The results of Magics RP vary between –26.12% and 39.7% with an average percentage error of 19.37%. A probable explanation for the large percentage errors of Magics' build time prediction could be its interpretation of support structures. Last mentioned are interpreted as files with bad edges and bad contours, which could have an influence during Magics' build time estimation calculations.

11.1.2 Part Files

- *Test Pieces*

  The time estimation results of the benchmark (Magics RP) for the test pieces varies from –5.01% to 2.91% with an average percentage error of 0.36 %. The percentage

error for the 2D-build time estimator varies between –3.14% and 9.31%. The average percentage error for the 2D-build time estimator is 5.69%.

The time-estimation values obtained from the experimental results for supports are more accurate than the benchmark's time predictions for the same volumes. A large percentage of the results are within the 10% deviation limit, proving the use of the 2D-build time estimator for support build time calculations for support structures. The 2D-build time estimator's predicted build time for the test pieces is inside the 10% deviation limit for parts without complex geometries or surfaces. The results show that accurate build time calculations can be made by substituting part geometries with standard volumetric shapes.

- ***Case Studies***

  The parts grown on the platforms during the case studies were supplied to the service bureau in the .STL file format. The dimensions of the parts were measured with the measuring and section functions of Magics RP. These dimensions were used in the volumetric substitution process. The procedure followed for the volumetric substitution of the .STL files is the same as for the volumetric substitution of 2D-sketches.

  The platforms tested in the case study had the following differences:

  - Some of the platforms were built with the Ciba-Geigy SL5170 resin and others with the Somos 9110 resin.

- The laser power value varied.
- The number of parts on the platforms.
- The parts had different geometries.
- The total build height of the platforms was different, it varied from z = 7 mm to z = 220 mm.

The percentage error of the 2D-build time estimator for the platforms tested, varied from –12.75 % to 6.78 %. Of tests performed on full platforms, 80 % were within the 10 % deviation limit. The percentage error of Magics RP varies from –23 % to 45.72 %, with 20 % of the platforms inside the 10 % deviation limit. The average percentage error of Magics RP is 6.94 % and the average percentage error of the 2D-build time estimator is –4.54 %.

A probable explanation for the build time prediction outside the 10% deviation limit (such as section 9.3.4 Platform file: df02, p117) is that the complex geometries of the platforms were not represented accurately enough by volumetric shapes. A more accurate representation would be time consuming, resulting in a more time-consuming quotation process.

From the results of platform file: dk09_ger (section 9.3.8, p125), it may be concluded that the 2D-build time estimator can achieve an accurate build time estimation of platforms with a large number of parts, when geometries are not complex. Platforms with a large value in the z-direction (Platform file: dg03, p 119 and Platform file: df01,

p115) were also predicted within the 10% deviation limit. The 2D-build time estimator also successfully estimated the build time for parts grown in different resins and laser power values.

Taking above-mentioned build time estimation results for parts, supports and platforms into account, it compare well against that of the benchmark's time estimations. In some cases, it even exceeded that of the benchmark. When cost and time estimates need to be done for project planning, budgeting and management purposes, the 2D-build time estimator's results should be sufficient for parts (or platforms of parts) without complex geometries or surfaces, as it falls within a 10% deviation limit for platforms that have to be built on the SLA machine. Some complex platforms however, have been identified out of the case studies. Complex platforms can be defined as platforms with parts that are difficult or time-consuming to substitute with basic volumetric shapes. Examples of such platforms are Df01, Df02 and Dk09_ger, where percentage errors of - 4.93 %, - 12.75 % and - 2.43 % respectively, have been calculated, resulting in an average percentage error of - 6.7 %. Should the latter be used as an adjustment factor to incorporate complexity, calculated results can be adjusted by 7%, not to under-estimate the predicted time.

CHAPTER 12

CONCLUSIONS AND RECOMMENDATIONS

12.1 INPUT PARAMETERS

For successful use of the 2D-build time estimator, the following input parameters will be needed:

- A detailed 2-Dimensional drawing or sketch of the product/s to be built on the SLA machine is needed to make accurate part-substitutions.
- The build orientation of the part – the operator needs to know which surfaces are important, to minimise the stair step effect through build-orientation. As support structures are also a function of build-orientation, and hence, impact on the build time, the operator must strive to place the parts in such a way that the build time is kept as small as possible. If possible, the parts must be placed in such a way that the minimum support structures are needed. This will save build time as well as impact on the time-consuming process to remove these structures. It can also affect the part-quality.
- The number of parts that have to be placed on the platform.
- The base cross-sections of the parts to be placed on the platform. This is needed to determine the position of the parts on the platform in the build envelope of the SLA machine (250 x 250 mm for the SLA-250 machine).
- Volumetric substitution of the product. The substituting volumetric shapes can then be used in the TK Solver models to calculate the build time.
- The latest laser power value of the laser in the SLA machine.
- The cross-sectional areas of the parts that will need a support structure.

- The scanning distance of the support structures. These values, together with the latest laser power value are used in a TK Solver model (total_supp_time_5170 or total_supp_time_9110) to calculate the build time of the supports.
- The latest running costs of the SLA build station. These include the cost of the resin, replacement of the laser, the annual license fee for the software and the hourly labour costs.

12.2 APPLICATIONS

Applications of the 2D-build time estimator:

- It gives a future client an idea what the cost would be to grow a prototype without having a solid model or .STL-file of the product.
- If the cost to grow the prototype is too high, the inventor can make changes to the design before a solid model is created. If a solid model had already been created, the inventor would have to incur further costs for design iterations.
- It could save time with regards to quoting on projects and impact on the project's planning budgets. This is due to the fact that it is not necessary to compile a solid model of the part for the quotation process.
- It could also enable a Rapid Prototyping service bureau to quote on design sketches. Quotes based on inaccurate estimates could lead to opportunity losses for both the bureau and the company, should it be too expensive. Similarly, quotes that are too low could have negative financial implications for both the service bureau and the company.

12.3 COST EFFECTIVENESS

In some companies, management is responsible for quoting. Because the manager has many duties to attend to, the quotation process must be a fast and accurate process. The difference between the quoting procedure using Magics RP and the 2D-build time estimator is as follows:

For Magics RP:

1. Convert files to the .STL file format
2. Placement of parts on the platform according to the client's specifications.
3. Obtain a build time estimation and material volume from Magics RP.
4. Processing the quote, using the above-mentioned time and material volume.

For the 2D-build time estimator:

1. Substitution of volumetric shapes and calculation of material volume.
2. Calculate the scan distance needed for the support structures.
3. Process data in the TK Solver models.
4. Obtain build time estimation from the TK Solver results.
5. Processing the quote, using the calculated time and material volume.

Currently, the 2D-build time estimator's quoting procedure can be time-consuming - especially when a large number of parts have to be built, such as platform df01 (section 9.3.3, p115) and platform df02 (section 9.3.4, p117). To quote on these platforms with Magics RP, it requires approximately 30 minutes, using .STL files. With the 2D-build time

estimator, at least two hours will be needed. If however, solid models and hence, .STL files are not available, it may take much more than two hours to create the files needed to generate a quote with Magics RP. It is therefore clear that the 2D-build time estimator offers time-saving benefits if it is used in the initial phase of a project, where only design sketches are available. It would generally take less time to do the geometrical substitution, than necessary for developing a solid model. Also, geometrical substitution requires less skill than solid modeling, and does not need the specialised and expensive 3D CAD software. The results showed that it is very applicable on stand-alone projects, and can be a very cost-effective tool during the quotation process, achieving accurate results fast.

12.4 RECOMMENDATIONS

Although this method works effectively, there is still room for improvements such as:

- Specialised software can be developed to make the quotation process increasingly user-friendly, faster and efficient. It will reduce time spent and increase the efficiency of the process. Once done, it can also be offered as a web-based tool for clients to access.
- Build time estimation models can be made easier by grouping TK Solver models into one (e.g. one model to calculate the volume, composed of different volumetric shapes).
- A database for orientation and placement of support files can be created to assist the operator in selecting these parameters.
- A more accurate and faster process must be found for large platforms with complicated part geometries. It is suggested that a factor of between 7% and 10% be incorporated for extra time needed for platforms containing parts with complex geometries. Last mentioned will be a function of the user's expertise.

APPENDIX A

TK SOLVER METHODS CREATED

The following models were created in TK Solver to assist in the build time estimation process, as well as the quoting process of a part to be built on the SLA machine.

A.1 TK Solver Model: square.tkw

This model assists in calculating the average cross-section of a square shape for a given height. Input variables consist of the width of one of the sides. The output variable represents the average cross-sectional area of this shape per layer. The basic screen layout, with the formulas used in this model, is illustrated in Figure A.1.

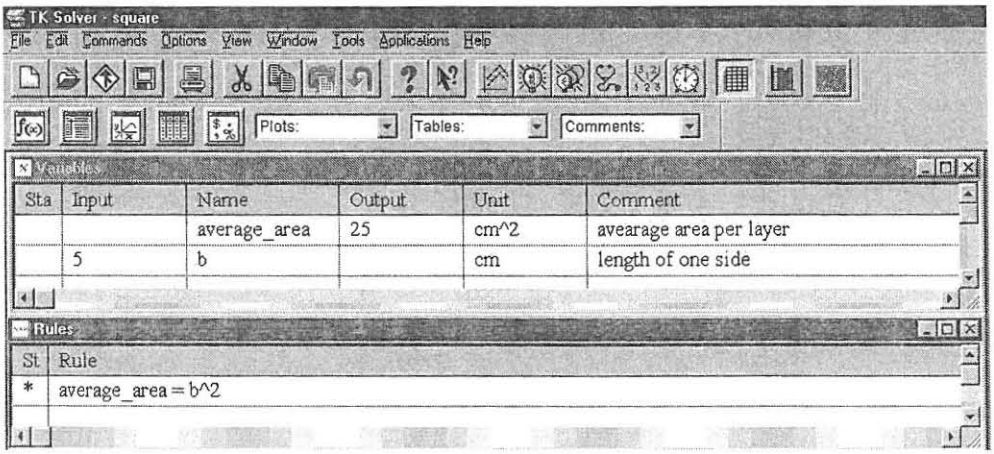

Figure A.1 Basic screen layout of the square.tkw model

A.2 TK Solver Model: rectangle.tkw

This model assists in calculating the average cross-section of a rectangular prism for a given height. Input variables consist of the length and width of the sides. The output variable represents the average cross-sectional area of this shape per layer. The basic screen layout, with the formulas used in this model, is illustrated in Figure A.2.

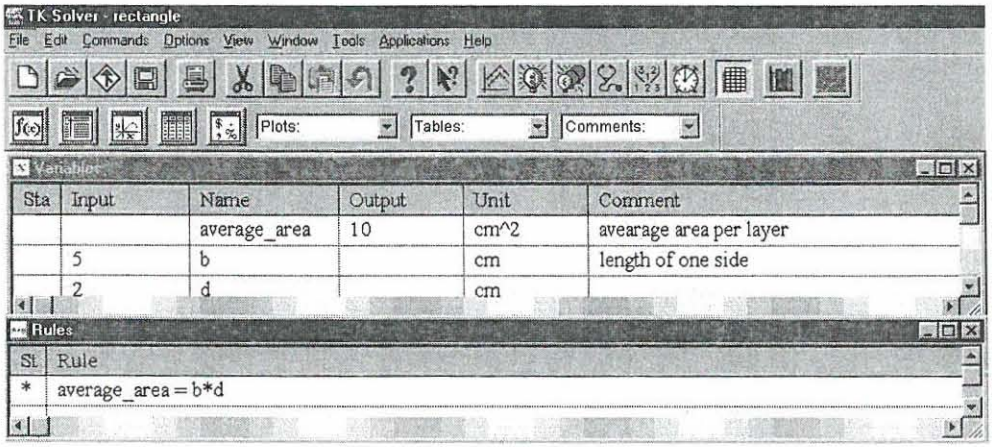

Figure A.2 Basic screen layout of the rectangle.tkw model

A.3 TK Solver Model: cylinder.tkw

This model assists in calculating the average cross-section of a cylindrical shape for a given height. The input variable consists of the radius of the cylinder. The output variable represents the average cross-sectional area of this shape per layer. The basic screen layout, with the formulas used in this model, is illustrated in Figure A.3.

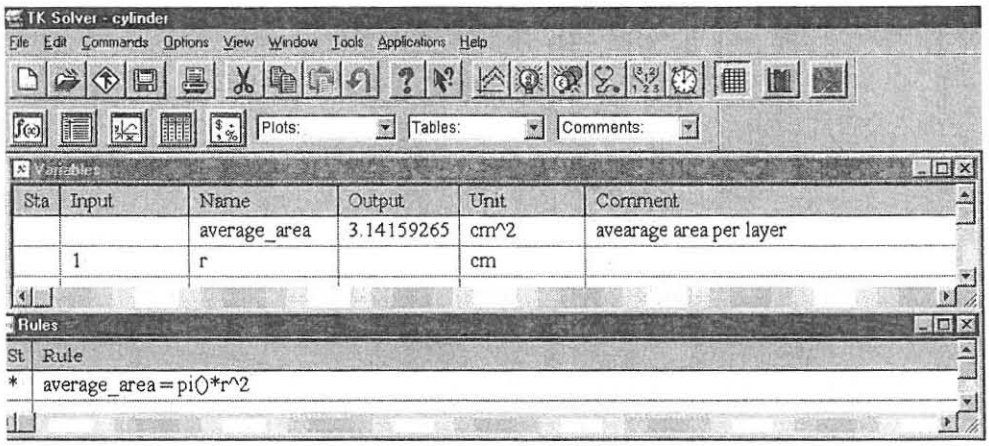

Figure A.3 basic screen layout of the cylinder.tkw model

A.4 TK Solver Model: tri_area.tkw

This model assists in calculating the average cross-section of a triangular prism for a given height with the triangle in the position as shown in Figure A.4. Input variables consist of the height of the shape, length of the base and height of the triangle. Output variables such as the average cross-sectional area for the total height of the part can be obtained. The basic screen layout, with the formulas used in this model, is illustrated in Figure A.5.

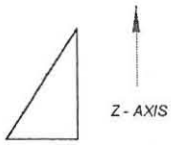

Figure A.4 Preferred direction of the triangular prism

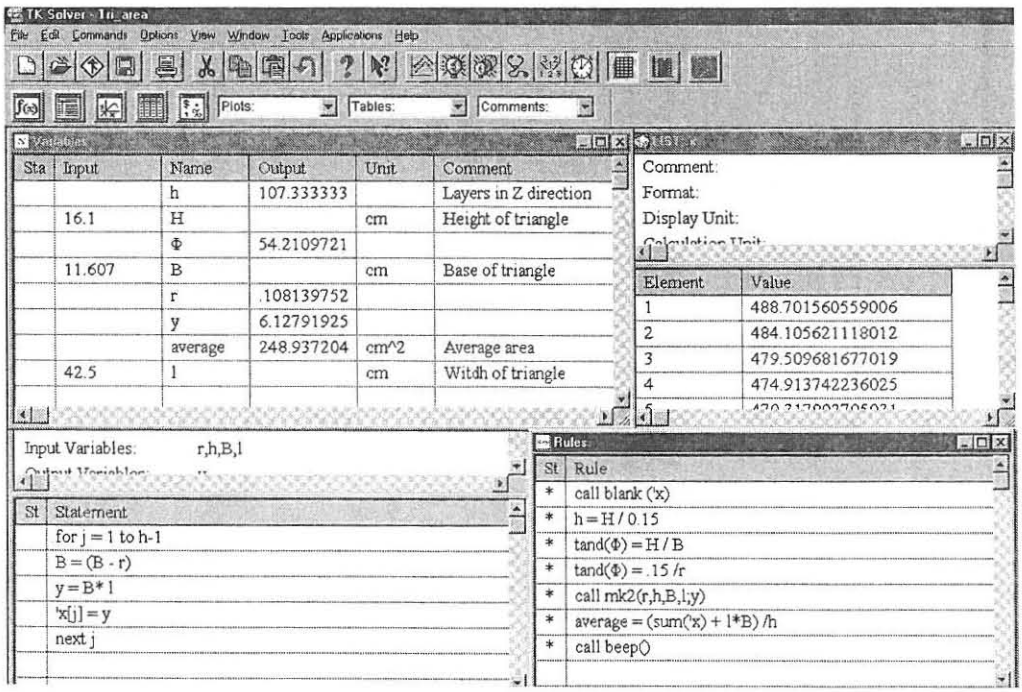

Figure A.5 Basic screen layout of the tri_area.tkw model

A.5 TK Solver Model: cone_area.tkw

This model assists in calculating the average cross-section of a cone shape for a given height. Input variables consist of the height of the shape and the base radius of the cone. Output variables such as the average cross-sectional area for the total height of this shape per layer can be obtained. The basic screen layout, with the formulas used in this model, is illustrated in Figure A.6.

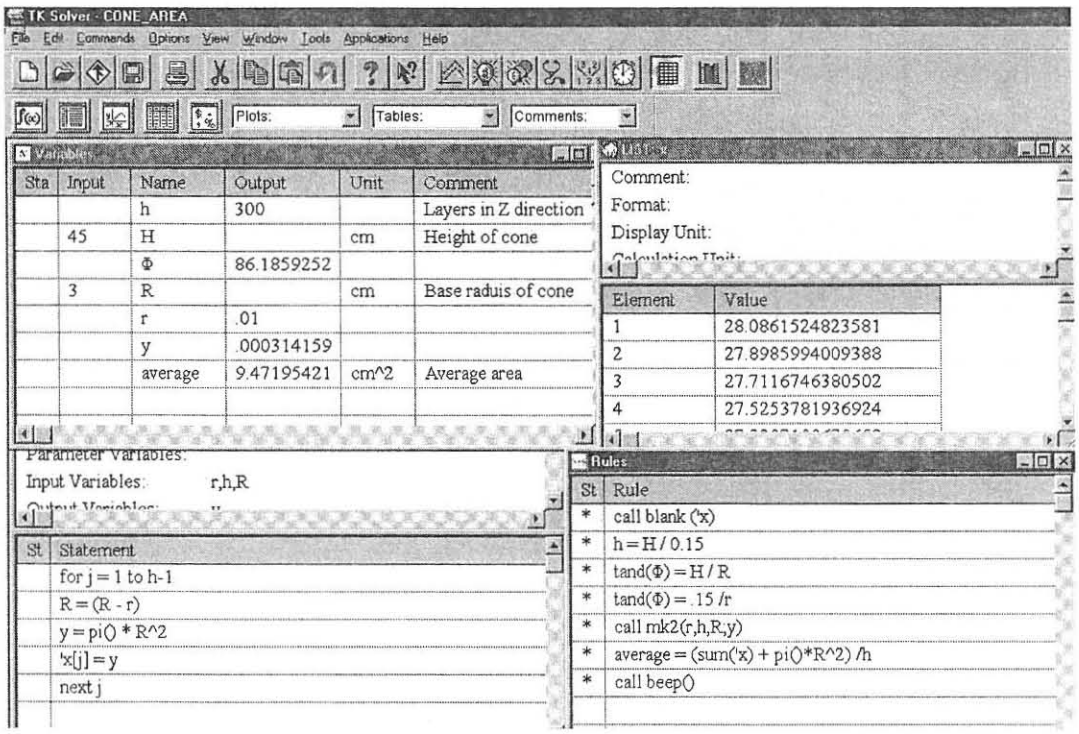

Figure A.6 Basic screen layout of the cone_area.tkw model

A.6 TK Solver Model: sphere_area.tkw

This model assists in calculating the average cross-sectional area of a sphere. Input variables consist of the radius of the shape. Output variables such as the average cross-sectional area of this shape per layer can be obtained. The basic screen layout, with the formulas used in this model, is illustrated in Figure A.7.

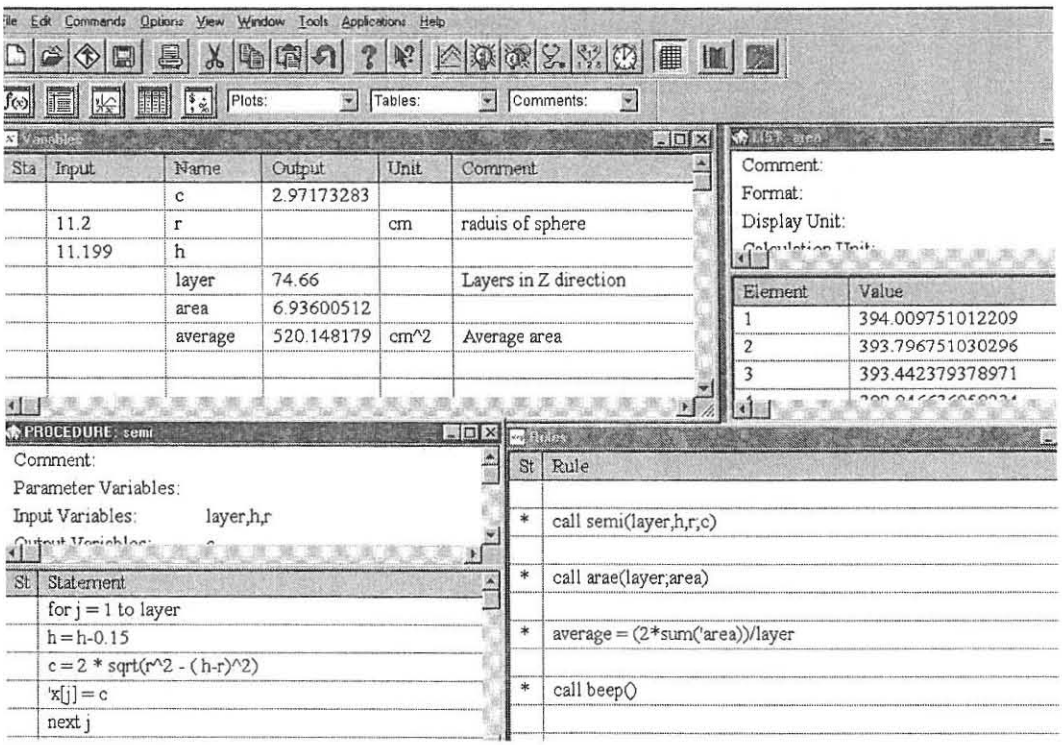

Figure A.7 basic screen layout of the model sphere_area.tkw

A.7 TK Solver Model: semi_sphere_area.tkw

This model assists in calculating the average cross-sectional area of a semi-sphere. Input variables consist of the height of the shape and the base radius. Output variables such as the average cross-sectional area of this shape per layer can be obtained. The basic screen layout, with the formulas used in this model, is illustrated in Figure A.8.

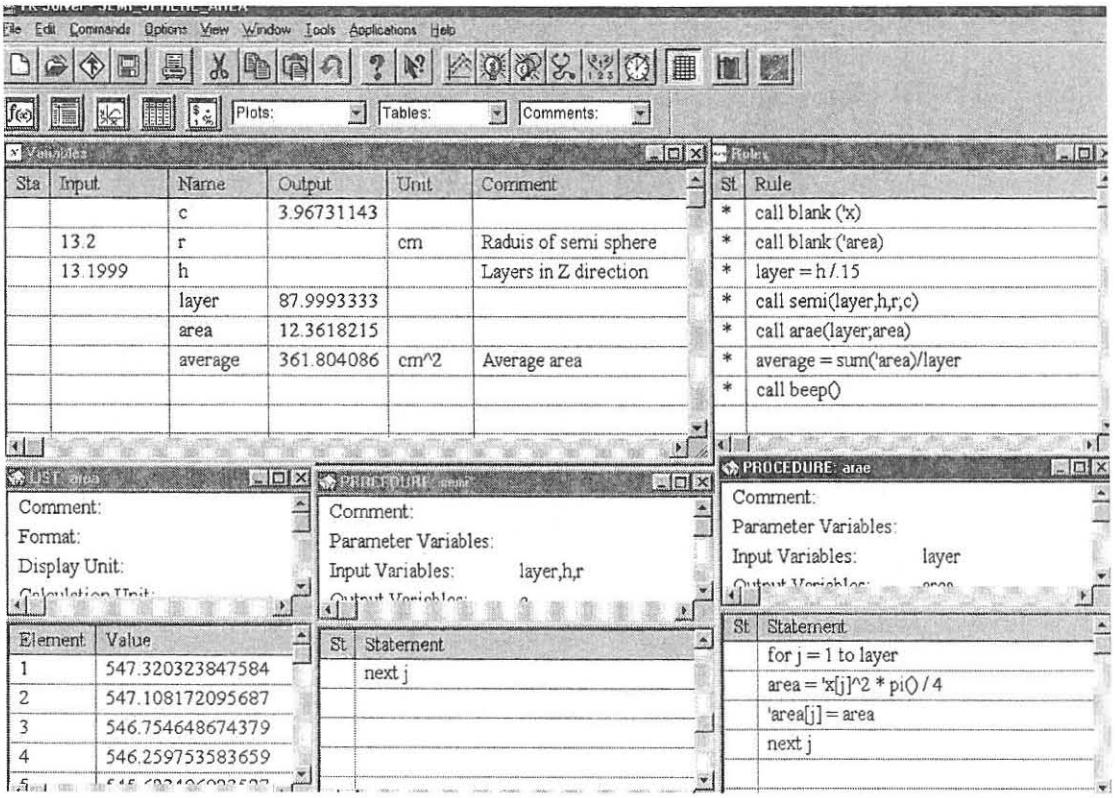

Figure A.8 Basic screen layout of the model semi_sphere_area.tkw

A.8 TK Solver Model: disk.tkw

This model assists in calculating the average cross-section of a disk for a given diameter with the disk in the position as shown if Figure A.9. Input variables consist of the diameter of the shape and the width of the disk. Output variables such as the average cross-sectional area for the total height of the part can be obtained. The basic screen layout, with the formulas used in this model, is illustrated in Figure A.10.

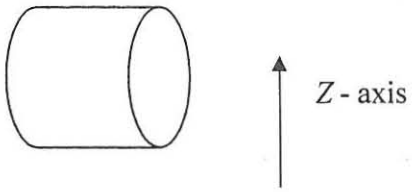

Figure A.9 Orientation of the disk geometry

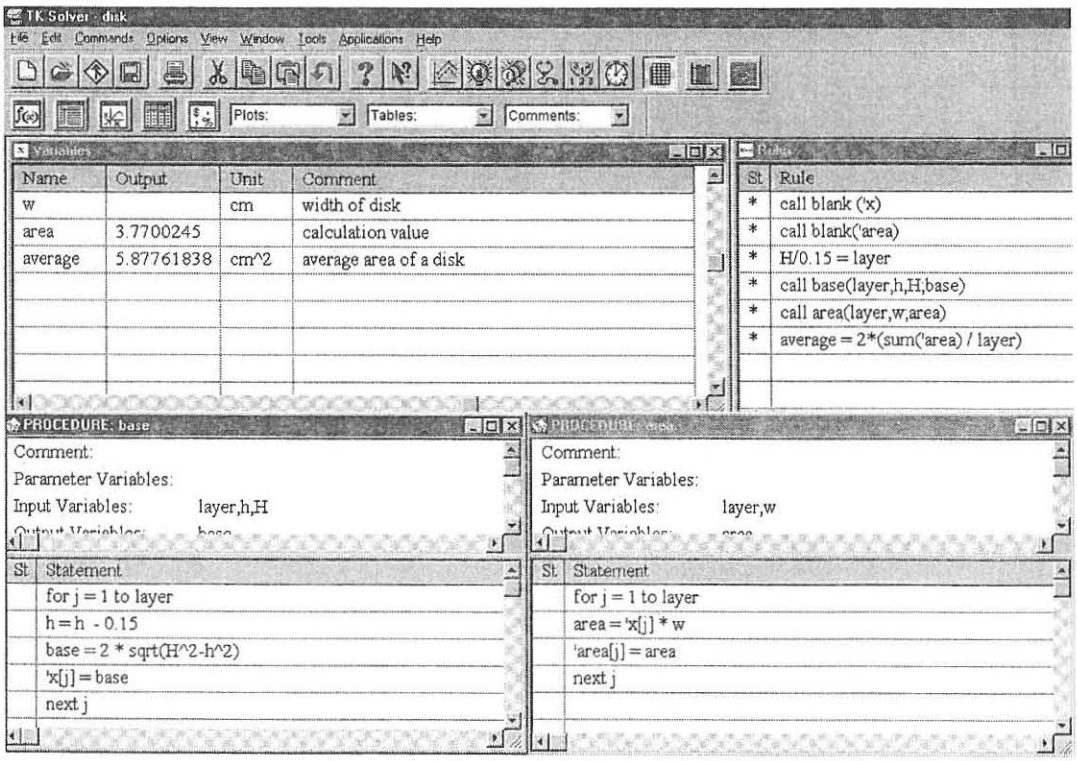

Figure A.10 Basic screen layout of the model disk.tkw

A.9 TK Solver Model: total_supp_time_SL5170.tkw

This model assists in the build time calculation for a support structure built with the Ciba-Geigy SL 5170 resin. Input variables such as Pl, Wo, Ec, Cd, Dp, height of part and distance to scan are needed. Output variables such as Vs and the total scan time for a given support can be obtained from this model. The basic screen layout, with the formulas used in this model, is illustrated in Figure A.11.

File Edit Commands Options View Window Tools Applications Help

Plots: Tables: Comments:

Variables

Sta	Input	Name	Output	Unit	Comment
		Vs	31.722849	cm/sec	Scan Speed per centimeter
	35	Pl		mW	Laser Power
	.01	Wo		cm	Raduis of laser beam
	13.5	Ec		mJ/cm^2	Critical exposure
	9	Cd		cm	Cure depth
	4.8	Dp		cm	Penetration depth
		z	68.3333333		Total layers in z direction
	10.25	H		mm	Height of support
		distance	278.32		length to be scanned per layer os support file
	278.32	s		cm	
		Tsupp	8.7734869	sec	scantime per layer of support structure
		Tsupp_tot	3648.55494	sec	Total scan time of support for a given height

Rules

St	Rule
*	Vs = (2/pi())^0.5 *(Pl /(Wo * Ec))* (EXP (-Cd/Dp))
*	z=H/.15
*	distance = s
*	Tsupp = s / Vs
*	Tsupp_tot = (Tsupp + 44.62)*z
*	tsuppa = Tsupp * z

Figure A.11 Basic screen layout of the total_supp_time_SL5170.tkw model

A.10 TK Solver Model: total_build_time_SL5170.tkw

This model assists in the build time calculation for a part built with the Ciba-Geigy SL5170 resin. Input variables such as Pl, Wo, Ec, Cd, Dp, hs, height of the part and the average cross-sectional area of part are needed. Output variables such as the total scan time for a certain part can be obtained from this model. The basic screen layout, with the formulas used in this model, is illustrated in Figure A.12.

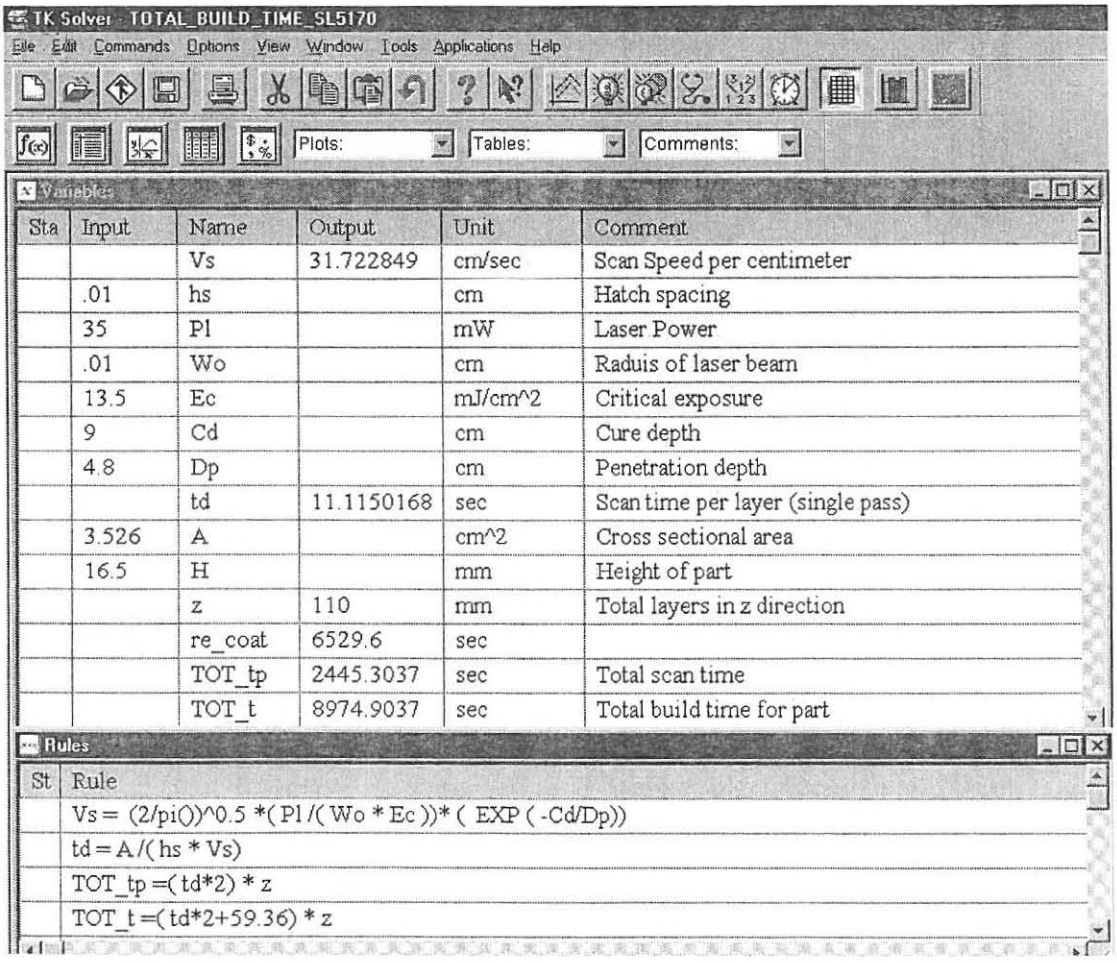

Figure A.12 basic screen layout of the total_build_ time_SL5170.tkw model

A.11 TK Solver Model: total_supp_time_9110.tkw

This model assists in the build time calculation for a support structure built with the Somos 9110 resin. Input variables such as Pl, Wo, Ec, Cd, Dp, height of part and distance to scan are needed. Output variables such as Vs and the total scan time for a given support can be obtained from this model. The basic screen layout, with the formulas used in this model, is illustrated in Figure A.13.

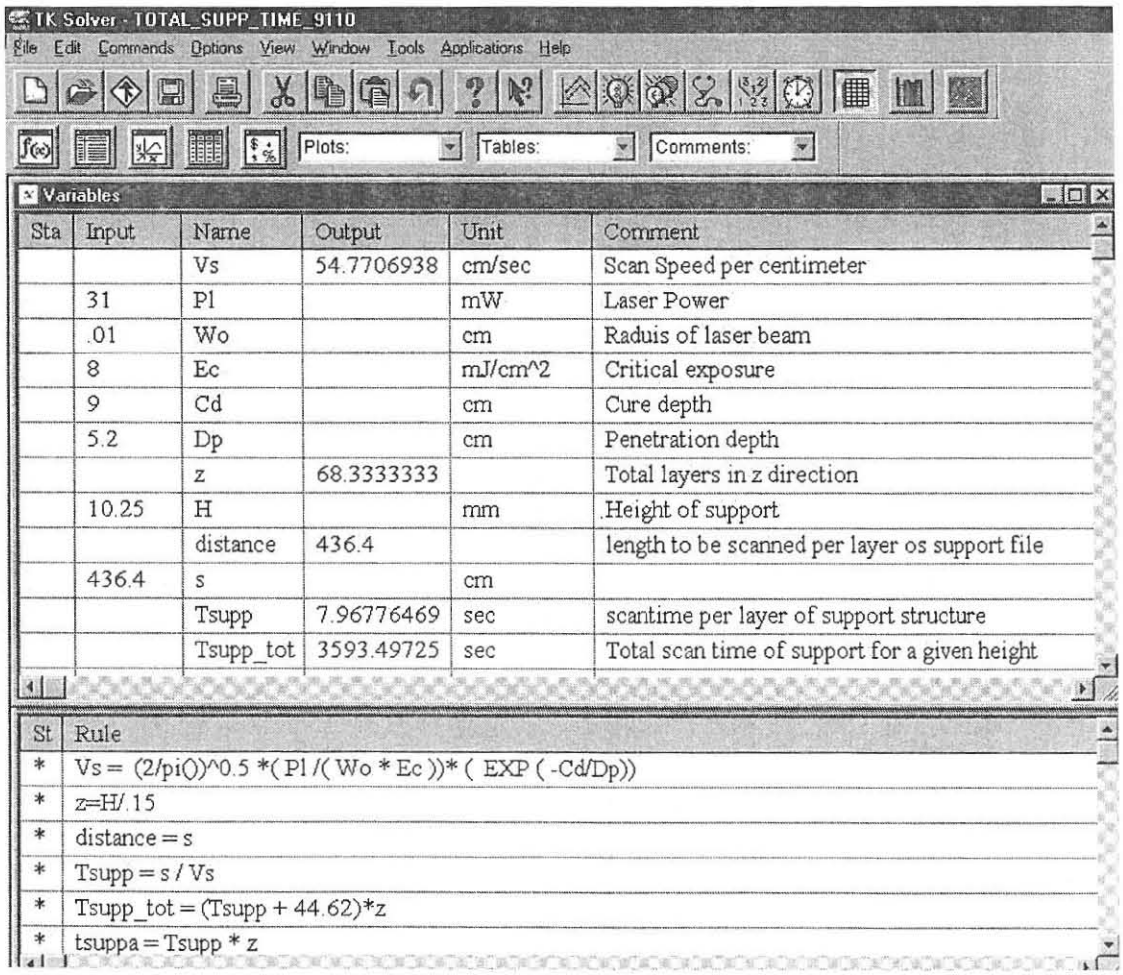

Figure A.13 Basic screen layout of the total_supp_time_9110.tkw model

A.12 TK Solver Model: total_build_time_9110.tkw

This model assists in the build time calculation for a part built with the Somos 9110 resin. Input variables such as Pl, Wo, Ec, Cd, Dp, hs, height of the part and the average cross-sectional area of part are needed. Output variables such as the total scan time for a certain part can be obtained from this model. The basic screen layout, with the formulas used in this model, is illustrated in Figure A.14.

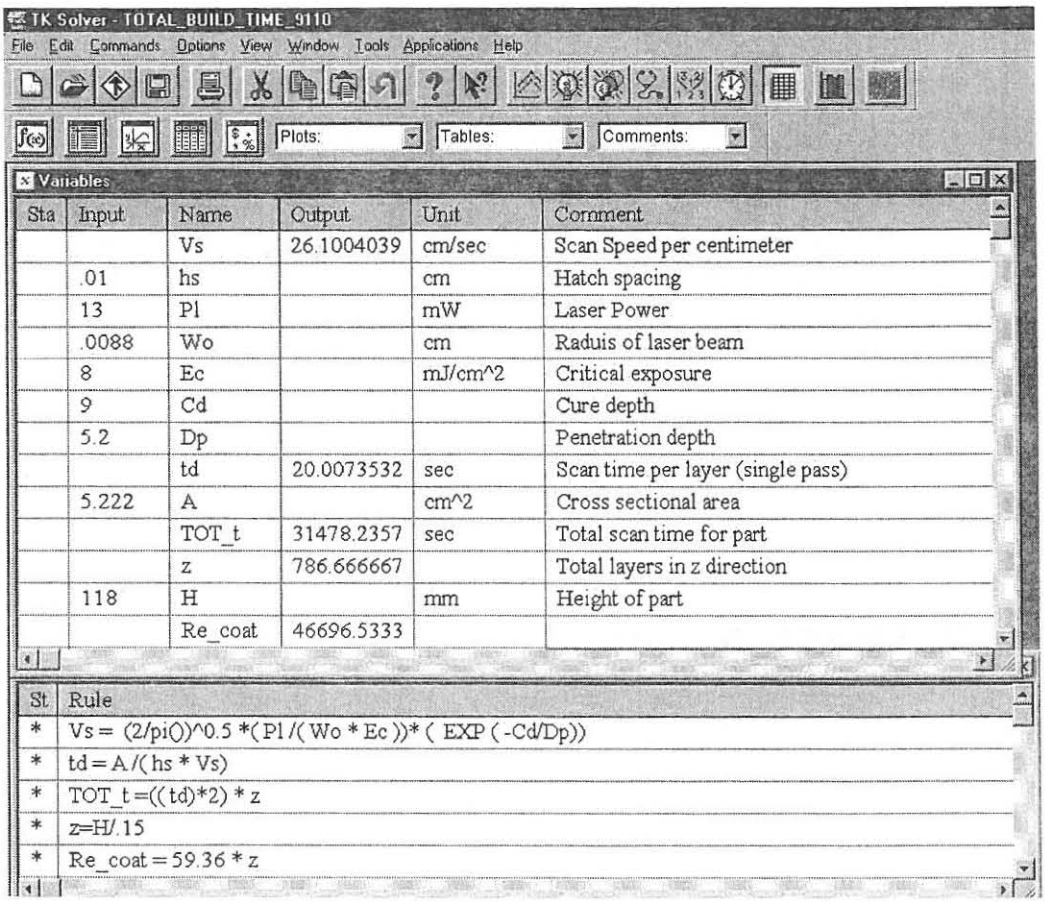

Sta	Input	Name	Output	Unit	Comment
		Vs	26.1004039	cm/sec	Scan Speed per centimeter
	.01	hs		cm	Hatch spacing
	13	Pl		mW	Laser Power
	.0088	Wo		cm	Raduis of laser beam
	8	Ec		mJ/cm^2	Critical exposure
	9	Cd			Cure depth
	5.2	Dp			Penetration depth
		td	20.0073532	sec	Scan time per layer (single pass)
	5.222	A		cm^2	Cross sectional area
		TOT_t	31478.2357	sec	Total scan time for part
		z	786.666667		Total layers in z direction
	118	H		mm	Height of part
		Re_coat	46696.5333		

St	Rule
*	Vs = (2/pi())^0.5 *(Pl /(Wo * Ec))* (EXP (-Cd/Dp))
*	td = A /(hs * Vs)
*	TOT_t =((td)*2) * z
*	z=H/.15
*	Re_coat = 59.36 * z

Figure A.14 Basic screen layout of the total_build_time_9110.tkw model

A.13 TK Solver Model: final_cost.tkw

This model assists in the quotation process. As input variables, the cost for the pre processing and post processing processes are included. Also included are the building, maintenance and material costs. The profit margin can also be included in this model. Output variables such as the final price to quote the customer can be obtained from this model. The basic screen layout of this model is illustrated in Figure A.15.

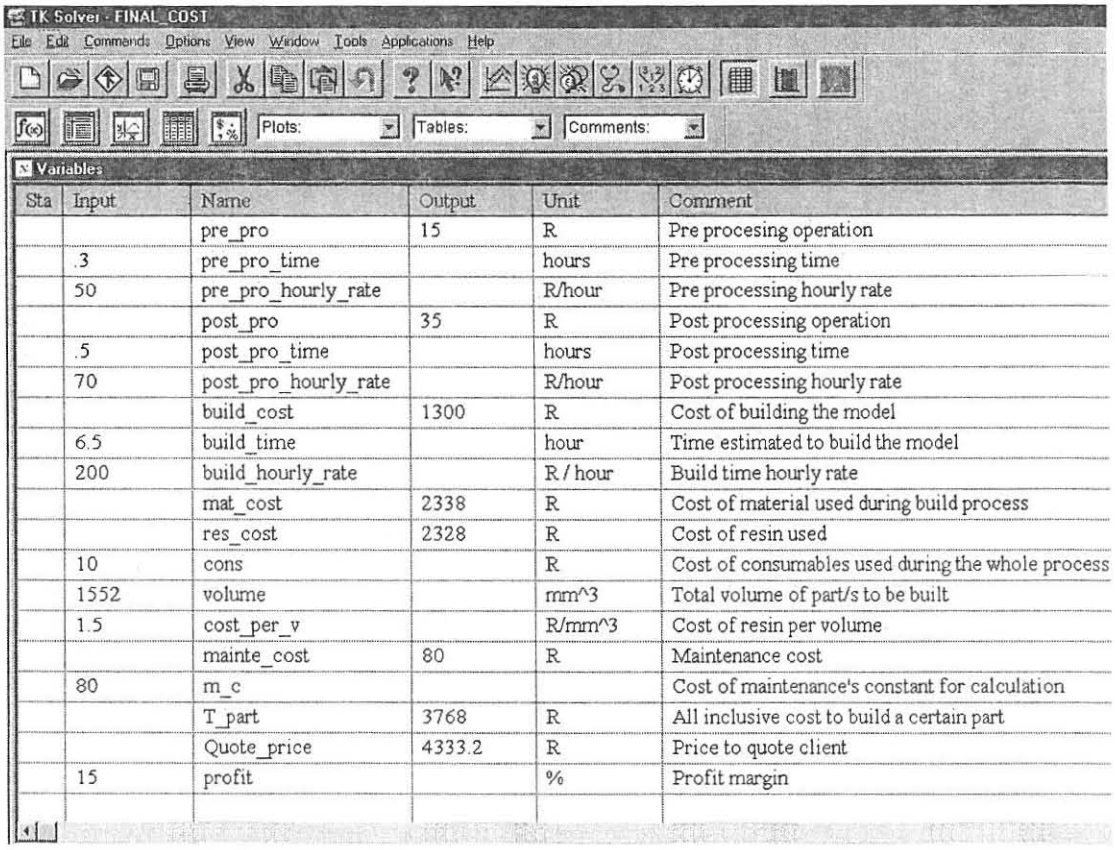

Sta	Input	Name	Output	Unit	Comment
		pre_pro	15	R	Pre procesing operation
	.3	pre_pro_time		hours	Pre processing time
	50	pre_pro_hourly_rate		R/hour	Pre processing hourly rate
		post_pro	35	R	Post processing operation
	.5	post_pro_time		hours	Post processing time
	70	post_pro_hourly_rate		R/hour	Post processing hourly rate
		build_cost	1300	R	Cost of building the model
	6.5	build_time		hour	Time estimated to build the model
	200	build_hourly_rate		R / hour	Build time hourly rate
		mat_cost	2338	R	Cost of material used during build process
		res_cost	2328	R	Cost of resin used
	10	cons		R	Cost of consumables used during the whole process
	1552	volume		mm^3	Total volume of part/s to be built
	1.5	cost_per_v		R/mm^3	Cost of resin per volume
		mainte_cost	80	R	Maintenance cost
	80	m_c			Cost of maintenance's constant for calculation
		T_part	3768	R	All inclusive cost to build a certain part
		Quote_price	4333.2	R	Price to quote client
	15	profit		%	Profit margin

Figure A.15 Basic screen layout of the final_cost.tkw model

APPENDIX B

VOLUMETRIC MODEL REPRESENTATION OF THE CASE STUDIES

The following shows how the parts of the platforms used in the case studies (section 9.3 p111), were represented by different volumetric shapes. These volumetric shapes were used to calculate the estimated build times of the platforms.

B.1 Volumetric Representation of Platform cl06

Figure B.1 shows how volumetric models were used to represent the parts (prod32_13_sept and prod31_13_sept), of platform cl06. These shapes were used in the build time calculation process of the 2D-build time estimator.

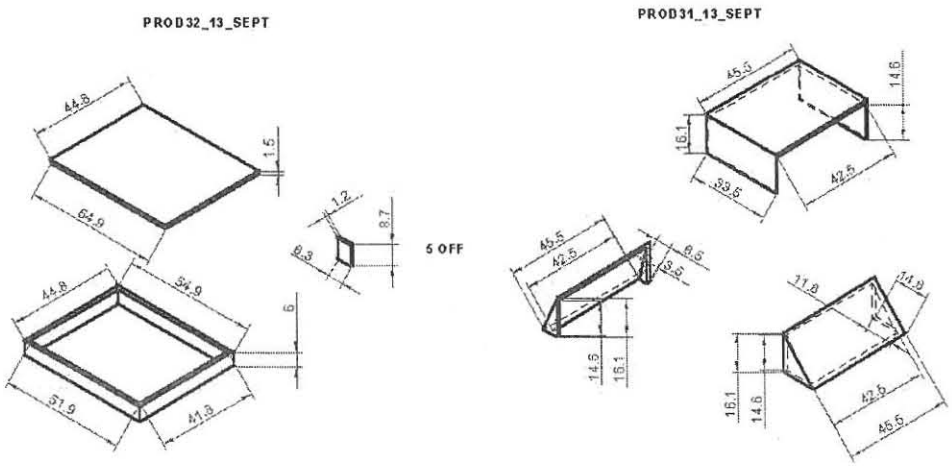

Figure B.1 Volumetric representation of platform cl06

An approximate area of 2652 mm^2 needed support. For the calculation processes the scan distance of two 50 x 50 mm support structure were used (scan distance per layer: 158.08 cm).

B.2 Volumetric Representation of Platform df01

Figure B.2 and B.3 show how volumetric models were used to represent the parts (free1, free2, free3, free 4 and free5), of platform df01. These shapes were used in the build time calculation process of the 2D-build time estimator. A total scan distance of 1083.12 cm per layer was used for the calculation of the support build time.

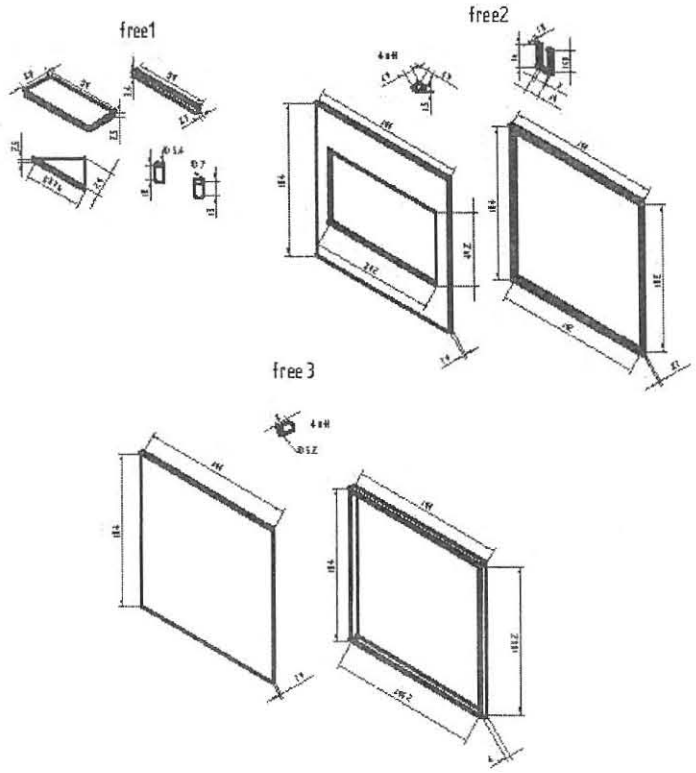

Figure B.2 Volumetric representation of parts free1, free2 and free3 of platform df01

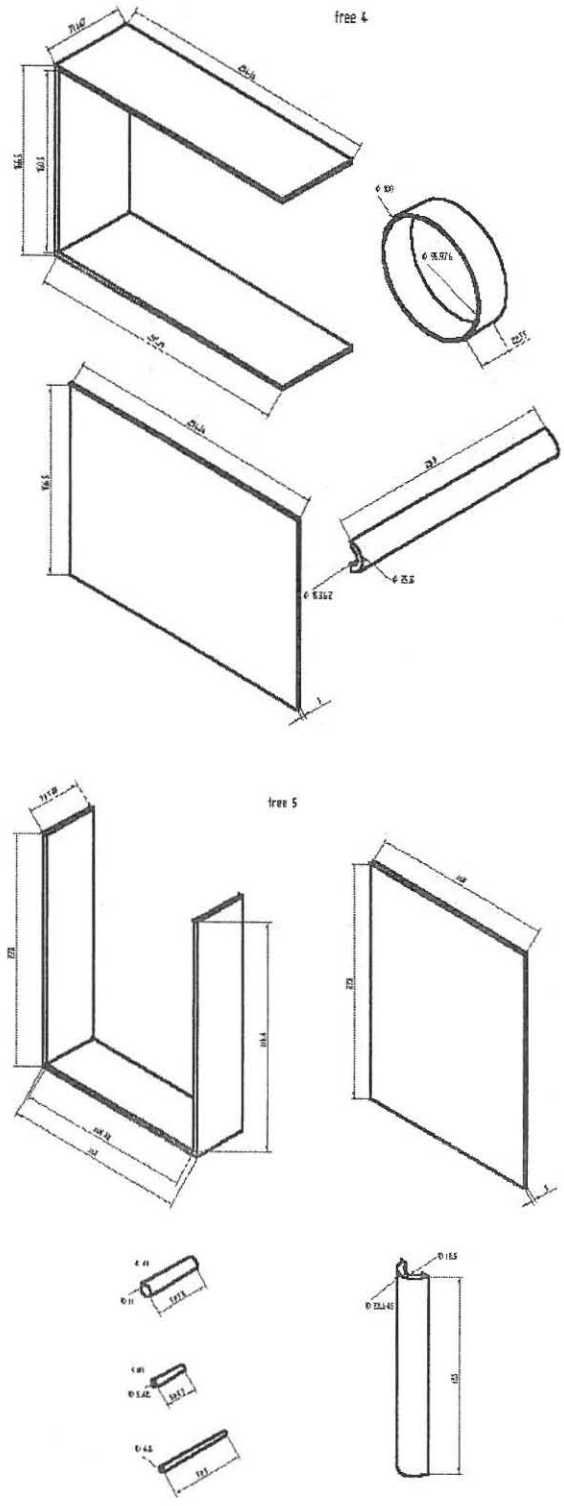

Figure B.3 Volumetric representation of parts free4 and free5 of platform df01

B.3 Volumetric Representation of Platform df02

Figure B.4, B.5 and B.6 show how volumetric models were used to represent the parts (free1, free2, free3, free4, free5, free6, free7 and free8), of platform df02. These shapes were used in the build time calculation process of the 2D-build time estimator. A total scan distance of 1295.2 cm per layer was used for the calculation of the support build time.

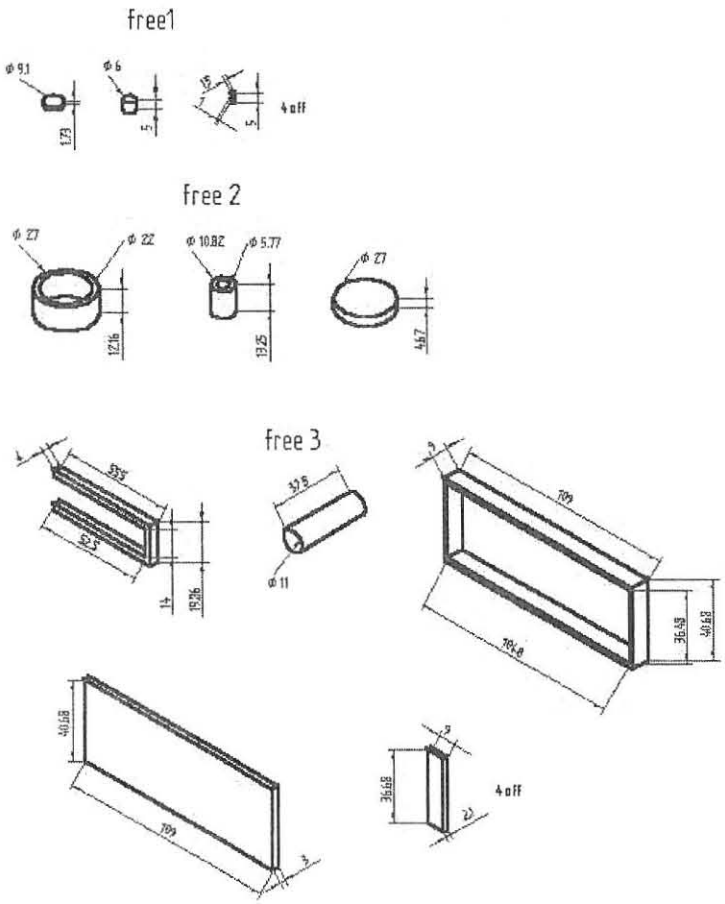

Figure B.4 Volumetric representation of parts free1, free2 and free3 of platform df02

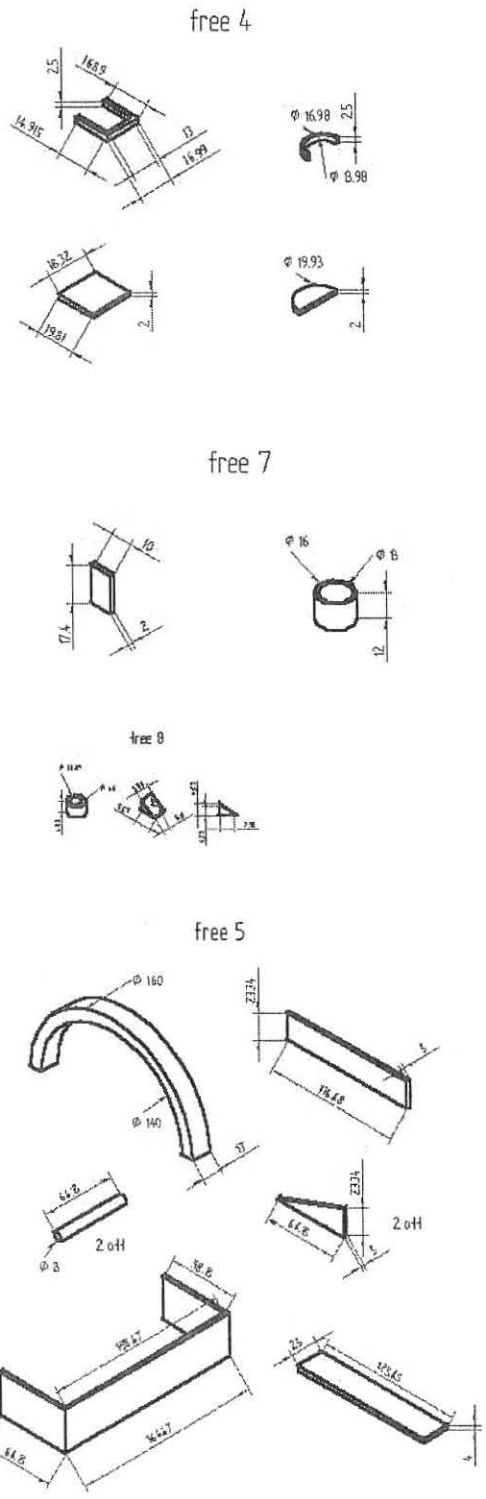

Figure B.5 Volumetric representation of parts free4, free5, free7 and free8 of platform df02

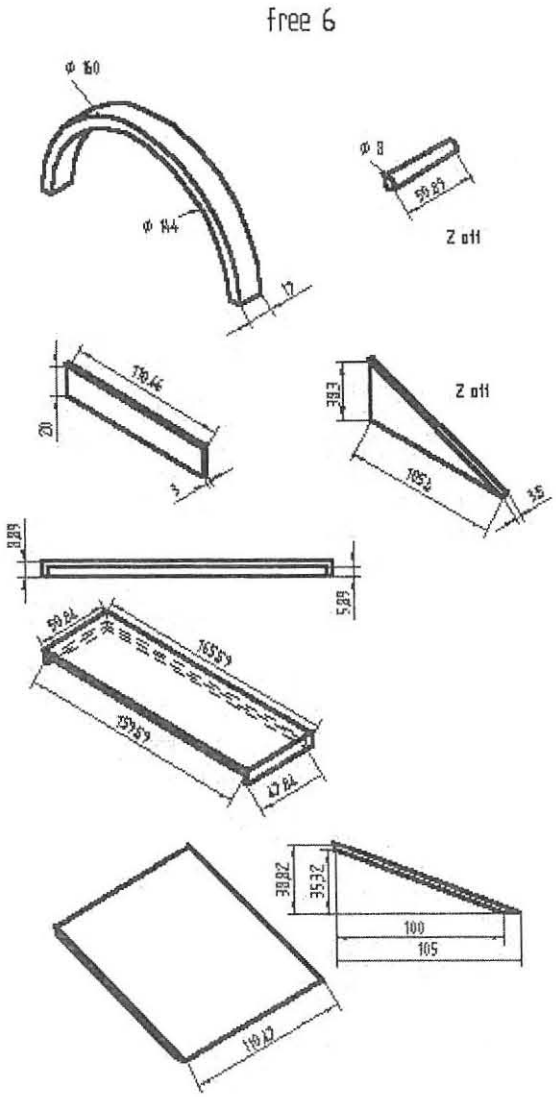

Figure B.6 Volumetric representation of part free6 of platform df02

B.4 Volumetric Representation of Platform dg03

Figure B.7 shows how volumetric models were used to represent the parts (psitek, spice and miss care), of platform dg03. These shapes were used in the build time calculation process of the 2D-build time estimator. A total scan distance of 450.43 cm per layer was used for the calculation of the support build time.

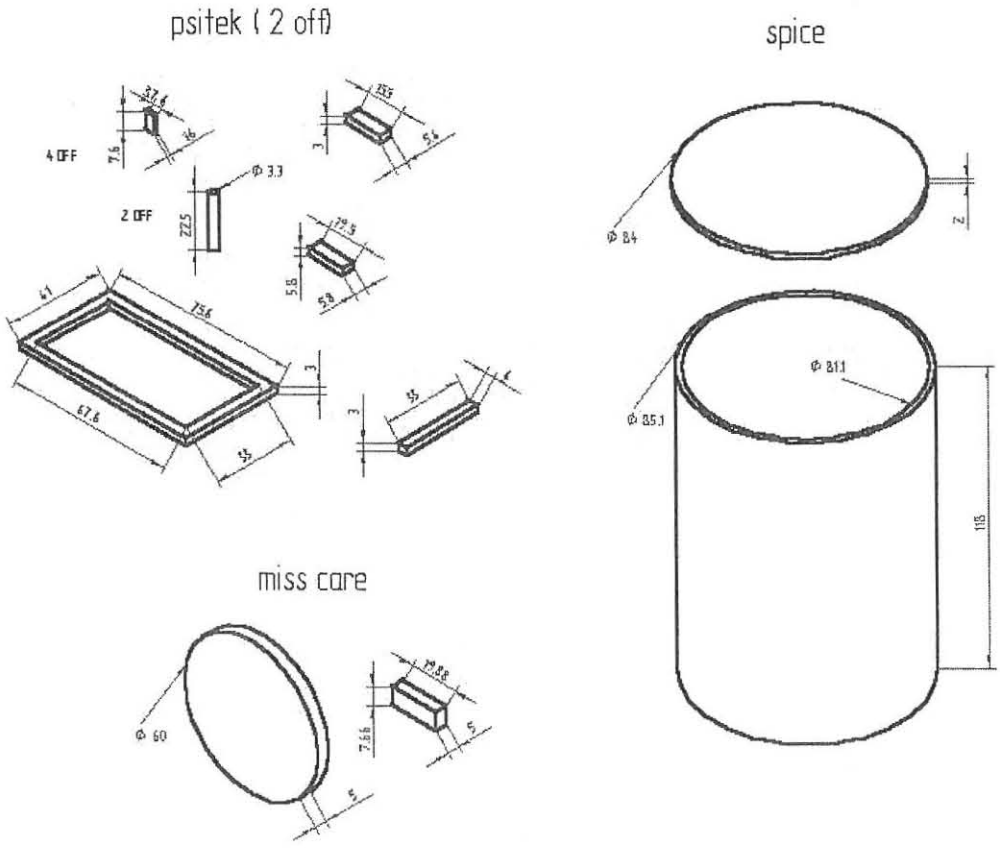

Figure B.7 Volumetric representation of platform dg03

B.5 Volumetric Representation of Platform dg04

Figure B.8 shows how volumetric models were used to represent the parts (tcmdie107a and tcmdie106a), of platform dg04. These shapes were used in the build time calculation process of the 2D-build time estimator.

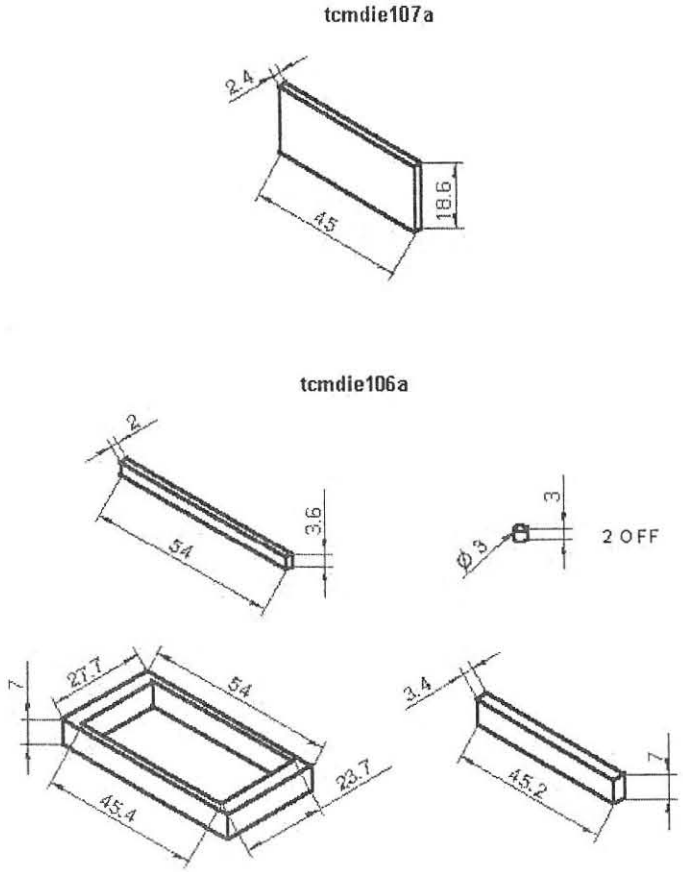

Figure B.8 Volumetric representation of platform dg04

An approximate area of 693 mm^2 needed support. For the calculation processes the scan distance of a 20 x 20 mm and three 10 x 10-mm support structures are used (scan distance per layer: 36.32 cm).

B.6 Volumetric Representation of Platform slatest1

Figure B.9 shows how volumetric models were used to represent the part (slatest1), of platform slatest1. These shapes were used in the build time calculation process of the 2D-build time estimator. A total scan distance of 327.96 cm per layer was used for the calculation of the support build time.

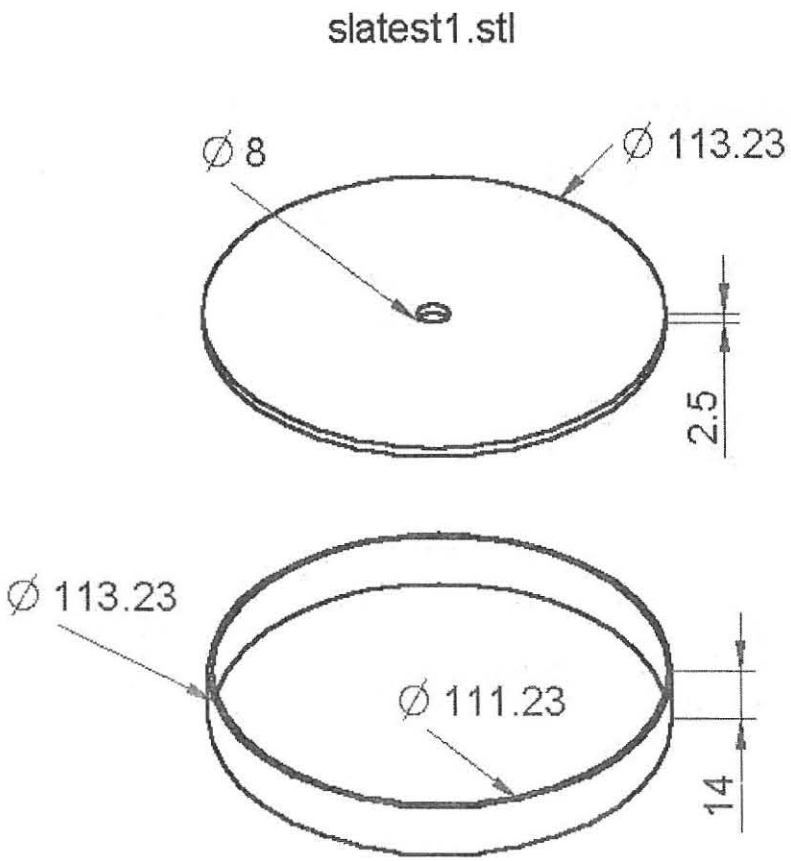

Figure B.9 Volumetric representation of platform slatest1

B.7 Volumetric Representation of Platform dk09

Figure B.10 and B.11 show how volumetric models were used to represent the parts (flutter1, flutter2, flutter3, flutter4, flutter5, flutter6, flutter7 and flutter8), of platform dk09. These shapes were used in the build time calculation process of the 2D-build time estimator. A total scan distance of 617.7 cm per layer was used for the calculation of the support build time.

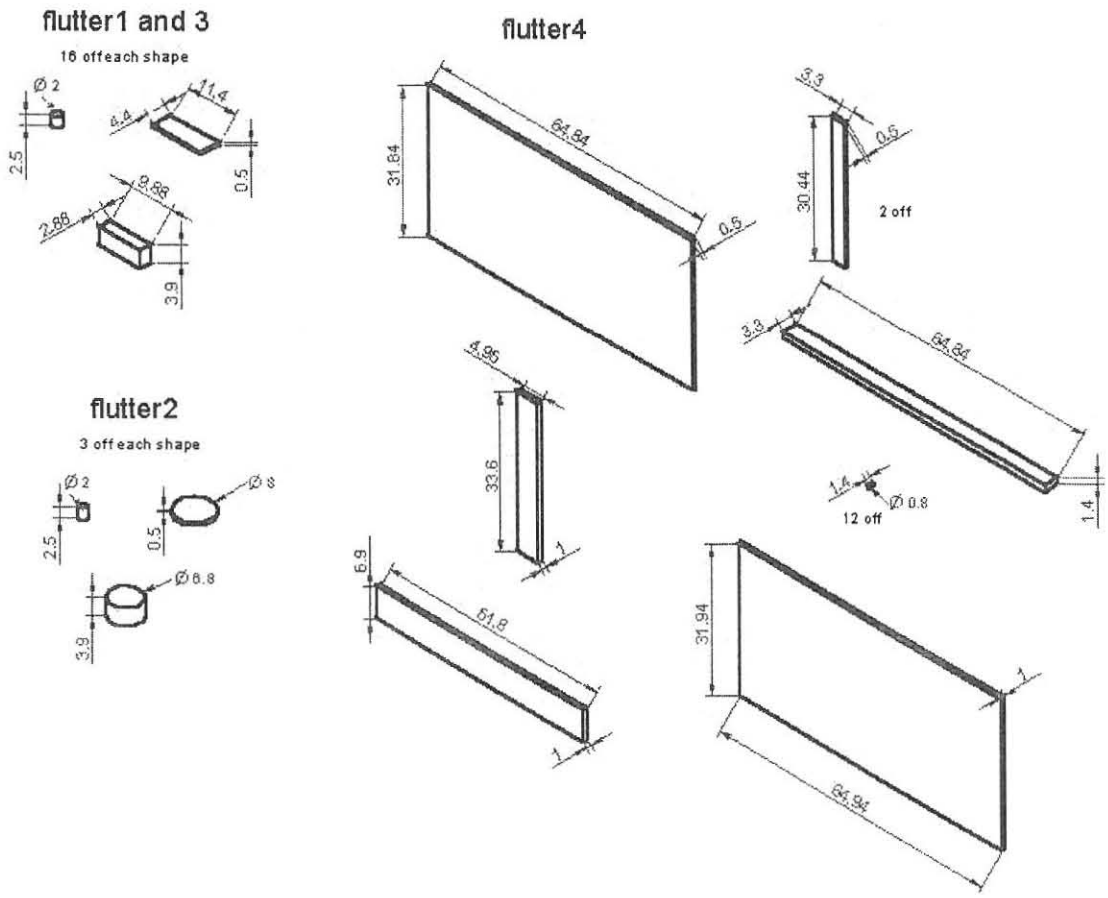

Figure B.10 Volumetric representation of parts flutter1, flutter2, flutter3 and flutter4 of platform dk09

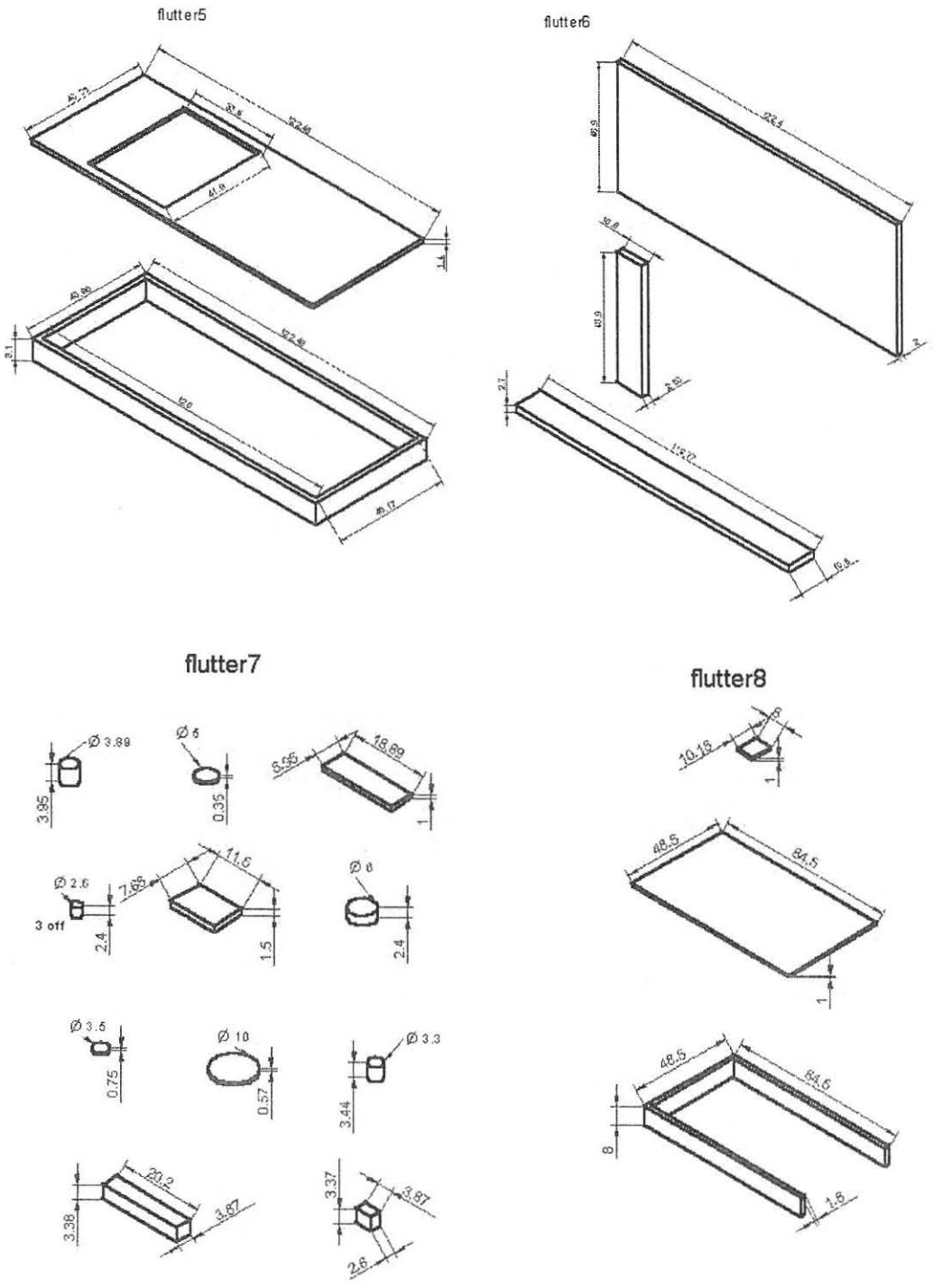

Figure B.11 Volumetric representation of parts flutter5, flutter6, flutter7 and flutter8 of platform dk09

B.8 Volumetric Representation of Platform dk12

Figure B.12 shows how volumetric models were used to represent the part (p1), of platform dk12. These shapes were used in the build time calculation process of the 2D-build time estimator. A total scan distance of 431 cm per layer was used for the calculation of the support build time.

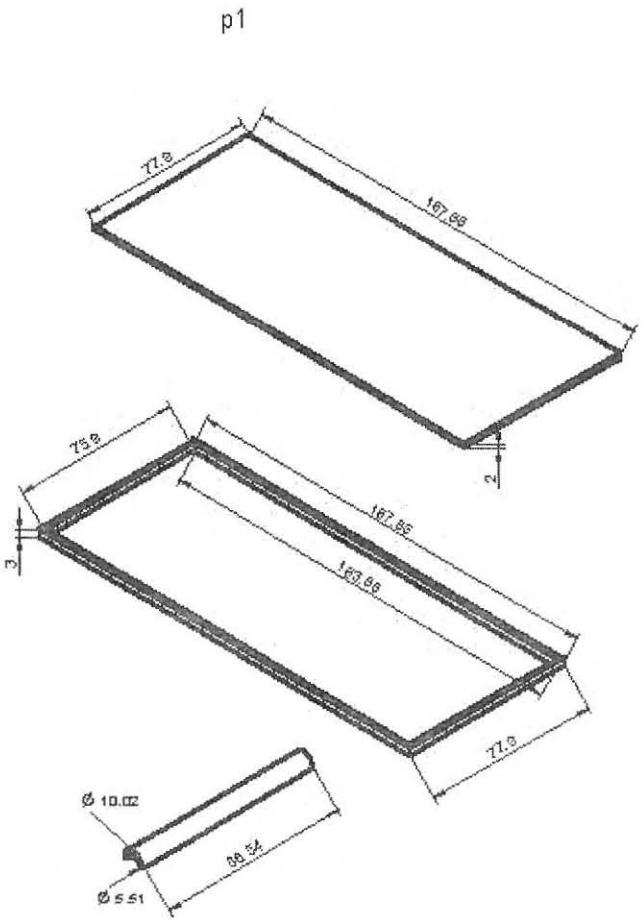

Figure B.12 Volumetric representation of platform dk12

B.9 Volumetric Representation of Platform dk13

Figure B.13 shows how volumetric models were used to represent the parts (sterlit1, sterlit2 and gum), of platform dk13. These shapes were used in the build time calculation process of the 2D-build time estimator. A total scan distance of 410 cm per layer was used for the calculation of the support build time.

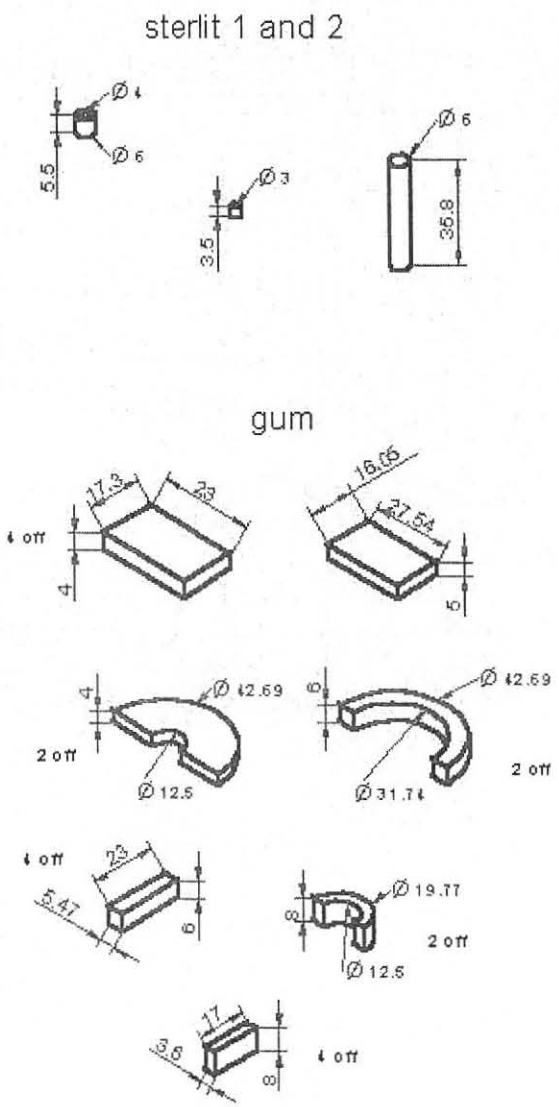

Figure B.13 Volumetric representation of platform dk13

REFERENCES

1. **BEACH, D.P., SHOTWELL, A. and ESSUE, P.** Applications of laser and laser systems, 1st edition New Jersey, PTR Prentice Hall, 1993.
2. **CHASSAPIS, C., GERDES, V. and WEBB, D.** Computer aided support structure design for Stereolithography models, The Fifth International Conference on Rapid Prototyping, 1994, pp. 221-228.
3. **CHRYSSOLOURIS, G.** Laser machining theory and practice, 1st edition. New York, 1991.
4. **CIBA-GEIGY CORPORATION**, Cibatool® SL 5170 Property sheet.
5. **DSM,** Somos® 9110 Epoxy Photopolymer Product data, 2001/02.
6. **DTM,** The Sinterstation System 2000 user's guide, April 1998.
7. **ELLIS, K., GORNET, T., OSBORNE, T. and REGADE, R.** An object-oriented knowledge based simulation estimation of the DTM rapid prototyping costs, The Fifth International Conference on Rapid Prototyping, 1994, pp. 211-220.
8. **FADEL, G. and FRANK, D.** Preferred direction of build for rapid prototyping processes, The Fifth International Conference on Rapid Prototyping, 1994, pp.191-200.
9. **FERGUSON, R.J.** TK Solver for Windows – Student Manual ,1997.
10. **HECH, J.** The laser guidebook, 2end edition ,McGraw-Hill , 1992.
11. **HOFFMAN, E.D.** Student's Shop Reference Handbook, Industrial Press Inc. New York, 1986.
12. **JACOBS, P.F.** Fundamentals of Stereolithography, Proceedings of the first European Conference , 1992.

13. **JACOBS, P.F.** Rapid Prototyping & Manufacturing – Fundamentals of Stereolithography , Society of Manufacturing Engineers, 1992.

14. **JACOBS, P.F.** Stereolithography and other RP&M Technologies, Society of Manufacturing Engineers, 1996.

15. **KIMMON ELECTRIC Co.Ltd.** Laser head test data, December 2000.

16. **MATERIALISE SOFTWARE**, Magics RP 6.3, 2001/02.

17. **McGRAW-HILL,** Encyclopedia of Science & Technology , Book number 17, 1997, pp.198-200.

18. **SALMON, W.I.** Structures and Abstractions – An Introduction to Computer Science with Turbo Pascal, Irwin, 1992.

19. **SCHMIDT, L.** A benchmarking comparison of commercial techniques in rapid prototyping, The Fifth International Conference on Rapid Prototyping, 1994, pp. 211-220.

20. **SILVAST, W.T.** Laser Fundamentals, Cambridge University Press, 1996.

21. **SPAVEN, D.A.** Integration of CAD Modeling and Selective Laser Sintering (SLS) to achieve rapid product development , First Asia/Pacific Conference on Rapid Product Development, 1995, Section 17.

22. **STEEN, W.M.** Laser Material Processing, 2^{end} edition , 1998.

23. **TAIT, D.** Rapid prototyping cost analysis , The Fifth International Conference on Rapid Prototyping, 1994, pp. 327-332.

24. **VENUVOID, P.K. and MA, W.** Rapid Prototyping – Laser Based and Other Technologies. Kluwer Academic Publishers, 2004.

25. **VENUVOID, P.K and SUN, H.** Corporate cultures in the eras of productivity, quality and innovation: A perspective from Hong Kong. Proc. Asian Academy Seminar, Hyderabad, India.

26. **WOHLERS, T.** Wohlers Report 2000 – Rapid Prototyping and Tooling state of the Industry. Wohlers Associates Inc. Fort Collins, Colorado, 2000.

27. **WOHLERS, T.** Wohlers Report 2002 – Rapid Prototyping and Tooling state of the Industry. Wohlers Associates Inc. Fort Collins, Colorado, 2002.

28. **TK SOLVER 3 FOR WINDOWS,** User's Guide, 1997.

29. **3D SYSTEMS USER GUIDE,** SLA-250 Buildstation user guide.

30. **3D SYSTEMS USER GUIDE,** Workstation user guide.

LIST OF ABBREVIATIONS AND ACRONYMS

2D	Two-dimensional
3D	Three-dimensional
ACES	Accurate clear epoxy solid
CAD	Computer aided design
CAM	Computer aided manufacturing
CAE	Computer aided engineering
Laser	Light amplification by stimulated emission of radiation
RMS	Root-mean-square
RP	Rapid Prototyping
RTV	Room temperature vulcanizing
.STL	Stereolithography file format
SLA	Stereolithography process
SLS	Selective laser sintering
TEM	Transverse electromagnetic mode
UV	Ultra violet light